

Development of lab-simulated slow pyrolysis and generation of pyrolysis profiles of common hydrocarbon polymers for fire debris analysis



Submitted in the fulfilment of the requirements of the degree of

MSc. (By Research)

By

YuanTing Low

Supervised by: Dr. Eádaoin Tyrrell

Dr. Cormac Quigley

Dr. Eoin Gillespie


Submitted to the Atlantic Technological University

July 2023

Declaration of Originality

I, YuanTing Low, hereby certify that the content presented in this thesis is my own.

I certify that, to the best of my knowledge, my project does not breach any copyright or infringe upon any proprietary rights and that any ideas, techniques, quotations, or any other material from the work of other people included in my project are fully acknowledged in accordance with the standard referencing practices. I am aware of and understand the University's policy on plagiarism and certify that this report is my own work, except where indicated by referencing.

Signed: 

Date: 13th July 2023

Acknowledgements

I would like to thank Atlantic Technological University for granting me the Research & Innovation Strategic Endowment (RISE) Scholarship for their funding to this research project.

I would like to sincerely thank the chemistry and physics technicians for their assistance and for being so accommodating throughout the two years. I would like to thank my supervisors Cormac Quigley, Eádaoin Tyrrell, and Eoin Gillespie for their support and guidance during my research.

Lastly, I would like to thank my family and friends for their support and encouragement throughout this journey.

Table of Contents

List of Abbreviations.....	4
List of Tables.....	7
List of Figures.....	8
Abstract.....	10
Chapter 1: Introduction.....	11
Aims & Objectives.....	14
Chapter 2: Literature Review.....	16
2.1 Fire.....	16
2.2 Combustion and Pyrolysis.....	17
2.2.1 Pyrolysis Mechanisms.....	17
2.3 Fire Investigation.....	22
2.4 Current Methods for Fire Debris Analysis.....	22
2.5 Recent Advancement in Fire Debris Analysis.....	23
2.5.1 Fire Debris Sampling.....	23
2.5.2 Sample Collection and Storage.....	28
2.5.3 Extraction.....	29
2.5.4 Instrumental Analysis and Data Interpretation.....	32
2.5.5 Chromatographic Analysis.....	33
2.5.6 Statistical Analysis and Machine Learning.....	35
2.5.7 Summary.....	37
2.5.8 Limitations.....	38
Chapter 3: Materials & Methods.....	47
3.1 Standards.....	47
3.2 Optimisation.....	52
3.2.1 Pyrolysis Compartment & Tilting Platform.....	52
3.2.2 Furnace Calibration.....	53

3.2.3	Sample Preparation.....	54
3.2.4	Extraction.....	55
3.2.5	GCMS.....	57
3.3	Validation of Pyrolysis.....	58
3.3.1	Experimental Simulation.....	63
3.3.2	Real World Simulation.....	63
3.4	Slow Pyrolysis Profiles.....	64
3.4.1	Preparation of Samples.....	64
3.4.2	Instrumental & Data Analysis.....	64
Chapter 4: Results & Discussion.....		69
4.1	Optimisation.....	69
4.1.1	Furnace Calibration.....	69
4.1.2	Heating Apparatus.....	70
4.1.3	Extraction Time.....	72
4.1.4	GCMS.....	73
4.1.5	Optimised Analysis Method.....	75
4.2	Validation of Pyrolysis.....	76
4.2.1	Time Variation Analysis.....	76
4.2.2	Pyrolysis Temperature Analysis.....	81
4.2.3	Ignitable Liquid Ratio Analysis.....	87
4.2.4	Pyrolysis of Common Polymers.....	89
4.2.5	Pyrolysis of Common Polymer with Acetone.....	91
4.2.6	Pyrolysis of Polypropylene with Common Ignitable Liquids.....	94
4.2.7	Re-evaluation of Importance of Temperature in Pyrolysis of Substrates with Ignitable Liquid.....	97
4.2.8	Real World Simulation.....	101
4.3	Slow Pyrolysis Profiles.....	102

Chapter 5: Conclusion.....	108
Chapter 6: Future Work.....	110
References.....	111
Appendix 1: FTIR of Selected Substrates.....	124
Appendix 2: RStudios Code for PCA.....	126

List of Abbreviations

AAr	alkyne aromatic
AB	alkylbenzene
ABS	Acrylonitrile Butadiene Styrene
ACC	Activated Charcoal Cloth
ACP	Activated Charcoal Pellet
ACS	Activated Charcoal Strip
AI	Artificial Intelligence
AMDIS	Automated Mass Spectral Deconvolution and Identification System
ASTM	American Society for Testing and Materials
CAR	Carboxen
CMV	Capillary Microextraction of Volatile
CTIF	Comité Technique International de Prévention et d'Extinction du Feu (The International Technical Committee for the Prevention and Extinction of Fire)
DART	Direct analysis in real time
DB-1MS	(100%)-dimethylpolysiloxane
DB-5MS	(5%-phenyl)-methylpolysiloxane phase capillary column
DVB	Divinylbenzene
EIP	Extracted ion profile
E-Nose	Electronic nose
EU	European Union
FID	Flame ionisation detection
GC x GC	Two-dimensional gas chromatography
GC-FT-ICR-MS	Gas chromatography-Fourier transform ion cyclotron resonance mass spectrometry
GCMS	Gas chromatography-mass spectrometry
HCA	Hierarchical cluster analysis
HP-5MS	(5%-phenyl)-methylpolysiloxane phase capillary column
HS-MS	Headspace mass spectrometry
IL	Ignitable liquid
IMS	Ion mobility spectrometry
IRMS	Isotope ratio mass spectrometry

LDA	Linear discrimination analysis
LDPE	Low density polyethylene
Mm	Molecular mass
m/z	Mass-to-charge ratio
NAP	naphthalene
NCAI	nitrogen-containing aliphatic
NCAr	nitrogen-containing aromatic
NCC	nitrogen-containing cyclic
NCH	nitrogen-containing heterocyclic
NCHAR	nitrogen-containing heterocyclic aromatic
NFPA	National Fire Protection Association
NIST	National Institute of Standards and Technology
Ny	Nylon
OAI	oxygenated aliphatic
OAr	oxygenated aromatic
OC	oxygenated cyclic
OCAI	oxygenated cyclic aliphatic
ONCA	oxygenated nitrogen-containing
ONCAI	oxygenated nitrogen-containing aliphatic
ONCAr	oxygenated nitrogen-containing aromatic
ONCC	oxygenated nitrogen-containing cyclic
ONCHAR	oxygenated nitrogen-containing heterocyclic aromatic
PAH	Polycyclic aromatic hydrocarbons
PB	Polybutadiene
PCA	Principal component analysis
PDMS	Polydimethylsiloxane
PE	Polyethylene
PEG	Polyethylene glycol
PER	Polyester
PET	Polyethylene terephthalate
PID	Photoionization detector
PLS-DA	Partial least square discriminant analysis
PP	Polypropylene

PPA	Polypropylene with acetone
ppb	Parts per billion
PS	Polystyrene
PVC	Polyvinyl chloride
Py-GCMS	Pyrolysis gas chromatography mass spectrometry
R_{AB}	Resolution between two neighbouring components
RS	Random scission
SBR	Styrene-butadiene rubber
SBS	Styrene-butadiene-styrene
SGC	Side group scission
SPME	Solid phase microextraction
TIC	Total ion chromatogram
TOFMS	Time-of-flight mass spectrometry
t_r	Retention time
UV	Ultra-violet
VOC	Volatile organic compound
w_A	Base width of peak

List of Tables

Table 1 Fluorescence of ignitable liquids under each light source.....	24
Table 2 Summary of literature review on chemical analysis of fire debris.....	40
Table 3 Chemical information of standard mixture.....	47
Table 4 Polynuclear aromatic hydrocarbons chemical information.....	48
Table 5 GC optimisation conditions.....	56
Table 6 Indicative fragments for ignitable of interest.....	57
Table 7 Chemical information of selected substrates.....	58
Table 8 Chemical information of selected ignitable liquids.....	58
Table 9 Target compounds for the identification of gasoline in fire debris samples provided by ASTM standards E1618.....	60
Table 10 PAHs compounds major m/z and compound group.....	60
Table 11 Chemical information of selected substrates.....	64
Table 12 Chemical information of selected flammable liquids.....	65
Table 7 Furnace calibration.....	67
Table 8 Temperature setting for sample pyrolysis.....	68
Table 8 Temperatures measured with temperature probe and thermocouple in sand bath at different positions.....	69
Table 9 Temperatures measured with temperature probe and thermocouple in sand bath with water at different positions.....	69
Table 10 Temperature measured in an oven.....	70
Table 11 GC optimisation conditions.....	72
Table 12 Peak resolution using standard mixture solution.....	73
Table 13 Peak resolution using PAHs standard.....	73
Table 19 Presence of aromatic product types in samples for 550 °C and 300 °C.....	100
Table 22 List of component groups.....	101

List of Figures

Figure 1 Distribution of globally reported fire, fire death, and fire injuries in 2020.....	13
Figure 2 Distribution of global (a) fossil-based plastic production and (b) application of plastics	14
Figure 3 Fire tetrahedron.....	18
Figure 4 Common polymers and their primary degradation mechanisms.....	19
Figure 5 Random chain scission mechanism.....	20
Figure 6 Side group scission mechanism.....	21
Figure 7 Monomer reversion mechanism.....	22
Figure 8 Image of tilting platform.....	54
Figure 9 Furnace calibration.....	54
Figure 10 Polypropylene chemical structure.....	55
Figure 11 Experimental setup for SPME temperature optimisation.....	57
Figure 12 Graph of furnace calibration.....	69
Figure 13 Temperature differences between temperature probe and thermocouple.....	72
Figure 14 The effect of time on the extraction of volatile compounds.....	73
Figure 15 Reference standard separation under condition 7.....	75
Figure 16 Heatmap comparison of pyrolysis results for time variation.....	78
Figure 17 Chromatograms from time variation analysis on PP only.....	79
Figure 18 Chromatograms from time variation analysis on PP with the presence of acetone.....	80
Figure 19 Chromatograms from time variation analysis on acetone.....	81
Figure 20 Heatmap comparison of pyrolysis results for temperature variation.....	84
Figure 21 Chromatograms from temperature variation analysis on PP.....	85
Figure 22 Chromatograms from temperature variation analysis on PP with the presence of acetone.....	86
Figure 23 Chromatograms from temperature variation analysis on acetone.....	87
Figure 24 Heatmap comparison of ratio effect on pyrolysis of PP and acetone.....	88
Figure 25 Chromatograms from ratio variation analysis on PP:acetone.....	89
Figure 26 Chromatograms from pyrolysis of substrates at 550 °C for 30 min.....	91
Figure 27 General pyrolysis mechanisms for the formation of aromatic products.....	92
Figure 28 Chromatograms from pyrolysis of substrates in the presence of acetone at 550 °C for 30 min.....	94

Figure 29 Chromatograms from pyrolysis of PP in the presence of different ignitable liquids at 550 °C for 30 min.....	97
Figure 30 Comparison of carbon number at each category and number of PAHs from pyrolysis of PP with ignitable liquids at 550 °C for 30 min.....	98
Figure 31 Chromatograms from pyrolysis of substrate in the presence of acetone at 300 °C and 550 °C for 30 min to determine the importance of temperature effect.....	99
Figure 32 Chromatograms from pyrolysis of PP in the presence of different ignitable liquid at 300 °C for 30 min to determine the importance of temperature effect.....	100
Figure 33 Chromatograms from pyrolysis of PP in the presence of different ignitable liquids at 550 °C for 30 min to determine the importance of temperature.....	101
Figure 34 Scree plot of the components.....	105
Figure 35 Correlation matrix from the data.....	106
Figure 36 Cos2 plot of the samples.....	107
Figure 37 PCA plot of samples.....	108
Figure 40 FTIR of HDPE sample.....	125
Figure 41 FTIR of LDPE sample.....	125
Figure 42 FTIR of nylon sample.....	125
Figure 43 FTIR of PET sample.....	126
Figure 44 FTIR of PER sample.....	126
Figure 45 FTIR of PP sample.....	126
Figure 46 FTIR of PS sample.....	127

Abstract

This study aimed to investigate the pyrolysis behaviour of substrates and the influence of various factors on the formation of degradation products through experimental and real world simulations. Experimental simulation involved the pyrolysis of substrates in an inert environment constructed of a glass ampoule and steel compartment. Real world simulation involved the pyrolysis of substrates under a thin metal sheet with external heat from a propane torch. Experimental simulation results illustrate the formation of aromatics from common polymers were possible when the temperature exceeded 550 °C for 30 min. The presence of a matrix profile can be masked by ignitable liquids when the ratio was greater than the substrate. Samples subjected to 550 °C pyrolysis produced strong positive correlation between all samples regardless of the substrate types or presence of ignitable liquid. Samples with similar chemical structure, such as PP, HDPE, LDPE had greater correlation between themselves compared to phenyl ring structured PER and PET. Nylon sample had closer correlation with aliphatic PP, HDPE, and LDPE. Aliphatic samples subjected to ≤ 300 °C pyrolysis had negative correlation with both aromatic (PC1) and oxygenated products (PC2). There was no secondary cracking for the cyclisation process to take place.

Keywords: polymers; ignitable liquids; pyrolysis conditions; lab-simulated fire debris

Chapter 1: Introduction

Fires are destructive and life-threatening incidents globally. Figure 1 depicts the reported fire cases in 2020 by 34 countries to the CTIF (The International Technical Committee for the Prevention and Extinction of Fire) database (Brushlinsky *et al.*, 2022). In 2020, there were 2.8 million fires reported across 34 countries, and of that 24.25% of the fires were residential. Residential fires were the main cause of deaths and injuries which accounted for an average of 82.75% of fire deaths in 21 countries and 60.59% of fire injuries in 18 countries (Brushlinsky *et al.*, 2022). Arson is defined as the intentional burning or charring of property (Ahrens *et al.*, 2021). It is a growing concern that individual lives will be taken from the destructive force as well as damage and pollution to the environment. The National Fire Protection Association (NFPA) reported that house fires accounted for 26% of all recorded fires between 2015 and 2019 in the United States (Ahrens *et al.*, 2021). The common causes of house fires include cooking (54.47%), heating equipment (14.73%), faulty electrical distribution and lighting equipment (10.29%), intentional fire setting (9.13%), smoking materials (5.24%), exposure to another fire (3.76%), and candles (2.38%). The true cause of the intentional fire setting is the most difficult to determine. Although it has been reported that 64% of intentional fires were suicides, there is a significant overlap between intentional and arson fires (Ahrens *et al.*, 2021). Therefore, it is important to identify the origin and cause of the fire incidents to draw hypothesis about whether a crime was committed. The general process of fire debris analysis consists of the following steps: (1) sample identification and collection, (2) extraction of volatile compounds from fire debris sample, (3) chemical analyses of the extracted volatile compounds and (4) data analysis and interpretation of the results to identify the compounds and their possible source (Almirall *et al.*, 2004).

The challenge to investigators and analysts of an arson case revolves around the fact that no two fires are identical in terms of their intensity, size, and burning environment (DeHaan *et al.*, 1997). The investigators are responsible for collecting useful and evidential fire debris from the incident, which are brought to the lab for analysts to determine the presence of possible ignitable liquids. However, the fire destruction will not only yield potential ignitable liquid residue, but also the breakdown of material within the fire scene generating interfering patterns. The generated interfering patterns will add another layer of complication to the sample collection and analysis of the ignitable liquids (Nic Daéid, 2005).

Arson investigation requires adequate expertise, skill, and technology to identify the cause of the fire incident. Fuel, oxygen, and heat are the three factors that affect the fire dynamics. If any one of the factors is removed, the fire chain reaction will extinguish and stop the spread of fire (Stauffer *et al.*, 2008, Churchward *et al.*, 2004). The ratio of fuel to oxygen to heat may be established by examining the burning path of fire and suggest the movement of fire within the fire scene. It can also help to generate a hypothesis on whether an external body had entered into the compartment thereby adding oxygen to amplify the combustion (Jackson *et al.*, 2011). The examination of ventilation along with the collection of fire debris from different areas affected, as well as the degree of burning is important for the investigation. The fire debris collected are subjected to lab analysis and comparison to reference samples from the lab to interpret the degradation of the material and the possible presence of an ignitable liquid (ASTM, 2019). The presence of ignitable liquid residue may be masked by the pyrolysis and combustion interference products from combustibles (Almirall *et al.*, 2004).

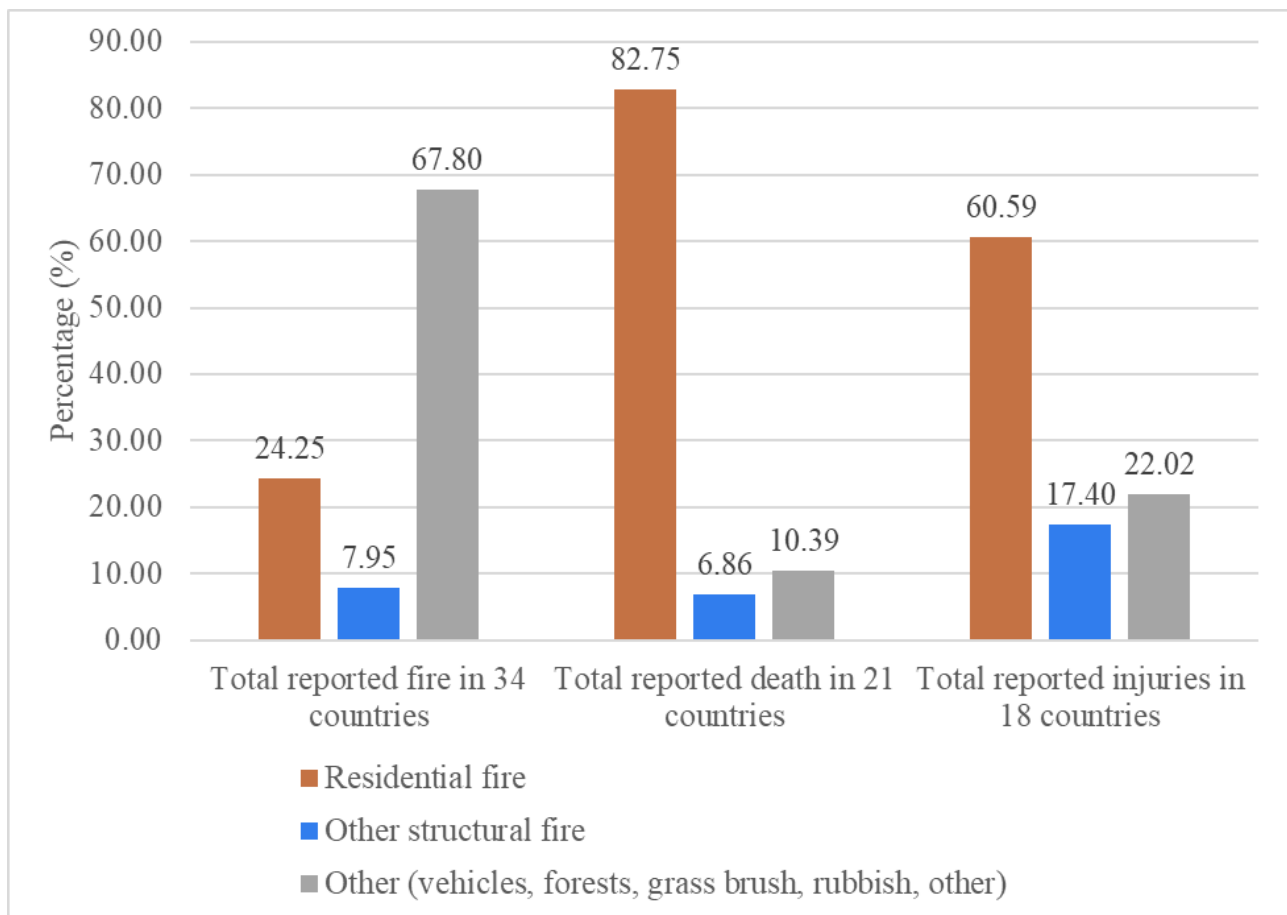


Figure 1 Distribution of globally reported fire, fire death, and fire injuries in 2020 (data source: Brushlinsky *et al.*, 2022)

The literature review (Section 2) demonstrated the primary focus in studying ignitable liquids for arson cases was on gasoline and diesel, as indicated in Table 2. These liquids are commonly chosen due to their accessibility and low cost. They primarily consisted of hydrocarbon structures, with alkanes, cycloalkanes, and aromatics being the main classes. However, the studies used cellulose-based materials, such as paper, Kimwipes™, and wood as substrates. Polymer-based materials commonly found in household products, which decompose into similar ranges of hydrocarbons under pyrolysis conditions were rarely investigated due to the concerns about their potential interference with the detection of ignitable liquids.

In 2021, the global production of fossil-based plastic reached 352.8 million tonnes (EPRO, 2022). Among the various types of plastic, polyethylene (LDPE and HDPE) accounted for the highest proportion, contributing to 30% of the overall production, followed by polypropylene at 21%, Figure 2(a) (EPRO, 2022). The statistic, Figure 2(b), revealed that packaging accounted for 44% of the total plastic production (EPRO, 2022). The extensive use of polymers in packaging suggests a significant likelihood of hydrocarbon fragments originating from these polymers being present in fire debris. However, the investigations into petroleum-based polymers like polypropylene (PP), polyethylene (PE), polyvinyl chloride (PVC), and polyethylene terephthalate (PET) were rarely investigated.

Over half of the studies for the presence of ignitable liquids were conducted either with no burning or with the addition of ignitable liquids after the burning process, Table 2. These results were not sufficient to represent the presence of ignitable liquids in the fire scene.

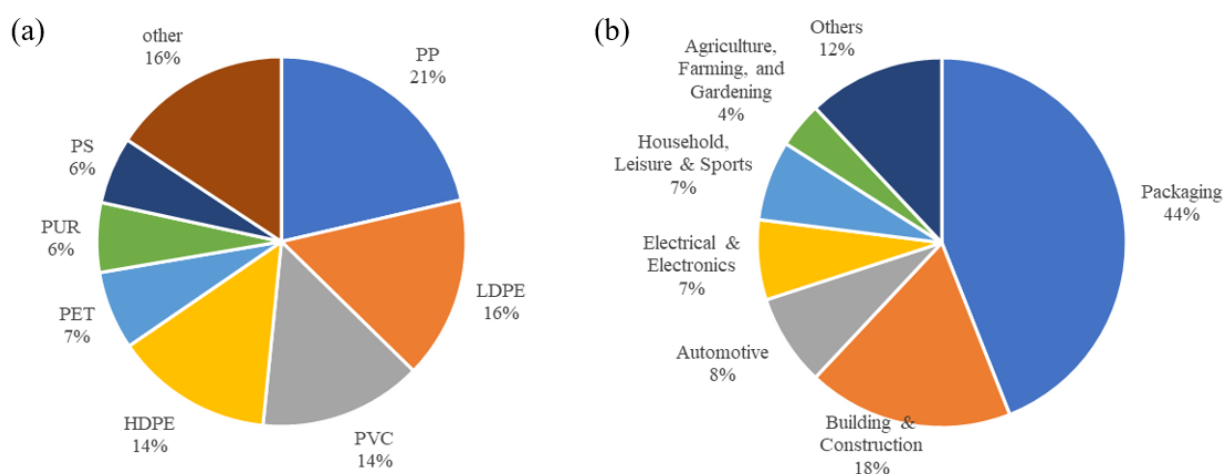


Figure 2 Distribution of global (a) fossil-based plastic production and (b) application of plastics (EPRO, 2022)

Aims & Objectives

Simulation of “real life” fire debris by pyrolysis, analysing, and interpreting materials in the lab is the goal of this research. If a real fire debris scenario can be simulated in a lab, it implies an alternative way of generating reference samples for comparison purposes where unburned reference sample from the fire scene is impossible to collect. Unfortunately, a full-scale duplication of a fire scene is near impossible in the lab. Therefore, focusing on creating testing conditions for lab burns of common household polymers was the main approach to this research.

A database comprising different lab burn techniques and substrates can enhance the investigative understanding of arson scenes. The application of chromatographic analysis can assist in identifying potential ignitable liquids and pyrolysis products. By employing chemometric and contour plot techniques to project simulated lab burn data, analysts can differentiate between burnt materials that may or may not contain ignitable liquids. Such analyses can also help in determining the similarity between lab burn data to casework fire debris and ignitable liquids contained in the reference collection and substrate databases.

For the purposes of this research, organic polymer substrates and their favoured degradation mechanisms were the focus with the investigation on the effect of temperature, duration, ratio, and presence of external ignitable liquids. Specifically, the pyrolysis of polypropylene (PP), polyethylene terephthalate (PET), high-density polyethylene (HDPE), low-density polyethylene (LDPE), polyester (PER), and nylon (Ny) are investigated.

This research investigated the effect of temperature, time, and presence of ignitable liquids on the process of pyrolysis with a view to informing the investigation of scenes of fire. Pyrolysis products, if not correctly identified, can easily be confused as ignitable liquids. Pyrolysis can be categorised according to the temperature range, mild pyrolysis (300-500 °C), typical pyrolysis (500-800 °C), and extreme pyrolysis (>800 °C). Existing literatures has explored products formed at mild pyrolysis temperature 400 °C or below (Vermesi *et al.*, 2016; Sandercock, 2012).

There is no existing research investigation on the effect of ignitable liquids from household materials on the pyrolysis of common polymers. The aim of this research is to study the effect of pyrolysis temperature, duration, and the ratio of materials present on the resulting pyrolysis profiles of selected synthetic polymers (PP, PET, HDPE, LDPE, PER, Ny). The effect of

ignitable liquids (acetone, hexane, butan-2-one, pentan-3-one, ethyl acetate, and isopropanol) present with the polymers are also investigated. This study considered the effect of pyrolysis reaction time and different temperatures on the pyrolysis products of common polymers. This can be a useful insight to the determination of the presence of ignitable liquids from collected fire debris.

Chapter 2: Literature Review

2.1 Fire

Fire is an exothermic chemical reaction involving the interaction of combustible material, oxidiser, and thermal energy. It is a self-sustaining chain reaction known as a combustion reaction (Jackson *et al.*, 2011). Combustible materials can be defined as those that are “capable of burning” under normal atmospheric pressure and temperature (Churchward *et al.*, 2004). It is also known as fuel and generally encountered fuel are organic with carbon-based structures. Some examples of organic fuels include gasoline, natural gas, plastics, wood, etc. The combustibles can exist as solids, liquids, or in gaseous form depending on the environmental factors, temperatures and pressures. The oxidiser provides oxygen to the combustion reaction and normally will consist of oxygen present in air. However, an oxidiser can also be chlorine, fluorine, or chemicals containing oxygen in their structure (Churchward *et al.*, 2004). Thermal energy is the ignition source required to activate the combustion reaction. A self-sustained combustion, known as a fire, occurs when excess heat from an exothermic reaction ignites fuel vapours in the absence of the initial ignition source (Churchward *et al.*, 2004). Figure 3 illustrates the fire tetrahedron and the fire will be extinguished if one of the factors is removed.

Flaming and smouldering are the two mechanisms to combust solids (Churchward *et al.*, 2004; Jackson *et al.*, 2011). Flaming combustion takes place in the gas or vapour phase of a fuel. The flame can be seen above the surface of solid or liquid fuels. A flaming combustion will stop when the oxygen level is <10% (Belcher *et al.*, 2010) but can continue under post-flashover temperature conditions when oxygen level is close to 0% (Churchward *et al.*, 2004). A flashover is known as pyrolysis of combustible surfaces to generate flammable gases (Jackson *et al.*, 2011). Although a flashover does not always happen, it happens when the thermal radiation meets all exposed combustible surfaces to pyrolyze and ignite with adequate ventilation. Smouldering is a surface-burning phenomenon with solid fuels and involves a lower rate of heat release and no visible flame. When the smouldering process generates sufficient energy or when the airflow is increased, the smouldering process can change to flaming combustion (Churchward *et al.*, 2004).

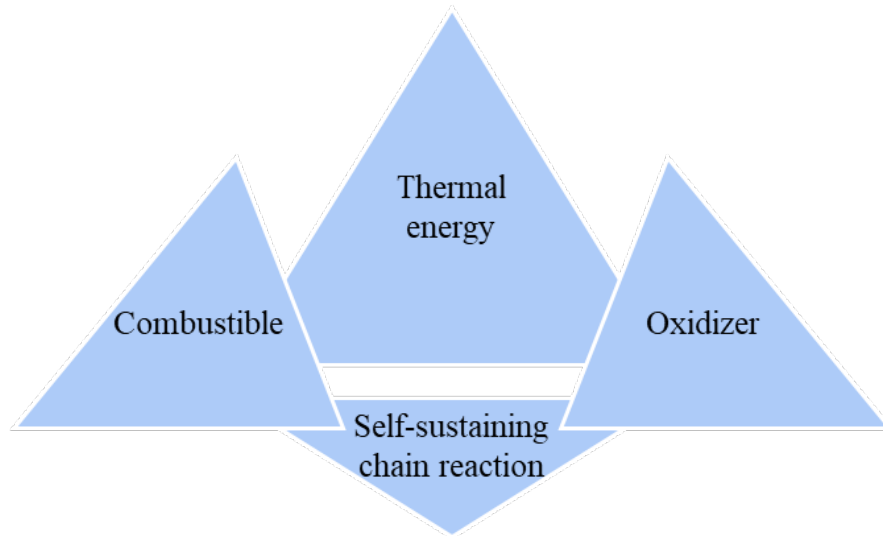


Figure 3 Fire tetrahedron (Churchward *et al.*, 2004)

2.2 Combustion and Pyrolysis

Combustion and pyrolysis are thermal degradation processes that occur in organic materials. Both share similarities but the main differences between combustion and pyrolysis are the oxygen availability, products generated, energy output, and process temperature. Combustion requires oxygen to occur whereas pyrolysis occurs in the absence of oxygen (Stauffer *et al.*, 2008; Churchward *et al.*, 2004). Combustion is also defined as a rapid oxidation of fuel in the presence of oxygen to produce heat, light, and various combustion products. The primary combustion products include carbon dioxide and water vapour as shown in equation 1 (Zhang *et al.*, 2007).

Equation (1)

On the other hand, pyrolysis undergoes other mechanisms to produce smaller volatile and semi-volatile compounds, including hydrocarbons, alcohols, ketones, and acids. These thermal degradation mechanisms include random chain scission, side group scission, rearrangement, cyclisation, and dehydrogenation reactions (Moldoveanu, 1998). Typically, combustion generates higher energy outputs than pyrolysis. The presence of oxygen in a combustion reaction allows the oxidation of fuel to release heat and increase in process temperature. In contrast, pyrolysis occurs at lower temperatures and is less efficient in producing energy outputs (Al-Haj Ibrahim, 2020).

2.2.1 Pyrolysis Mechanisms

Stauffer (2003) identified three distinct degradation mechanisms observed during the pyrolysis of polymeric materials. These commonly observed mechanisms include random scission, side group scission, and monomer reversion. Additionally, less commonly observed mechanisms such as rearrangement of natural and synthetic organic materials, as well as cross-linking leading with char formation can occur (Gebre *et al.*, 2021). It should be noted that pyrolysis of burned material does not always follow a single mechanism but often involves multiple pyrolysis pathways simultaneously (Zeng *et al.*, 2020). The specific pyrolysis pathways observed depends on the strength of the molecular bonds within the substrate being burned and the temperature at which the heat is applied (Gebre *et al.*, 2021). These variations in pyrolysis mechanisms pose challenges for fire debris analysts when interpreting chromatographic profiles. Figure 4 illustrates commonly encountered polymers and the favoured degradation mechanisms associated with them (Stauffer, 2003; Moldoveanu, 1998).

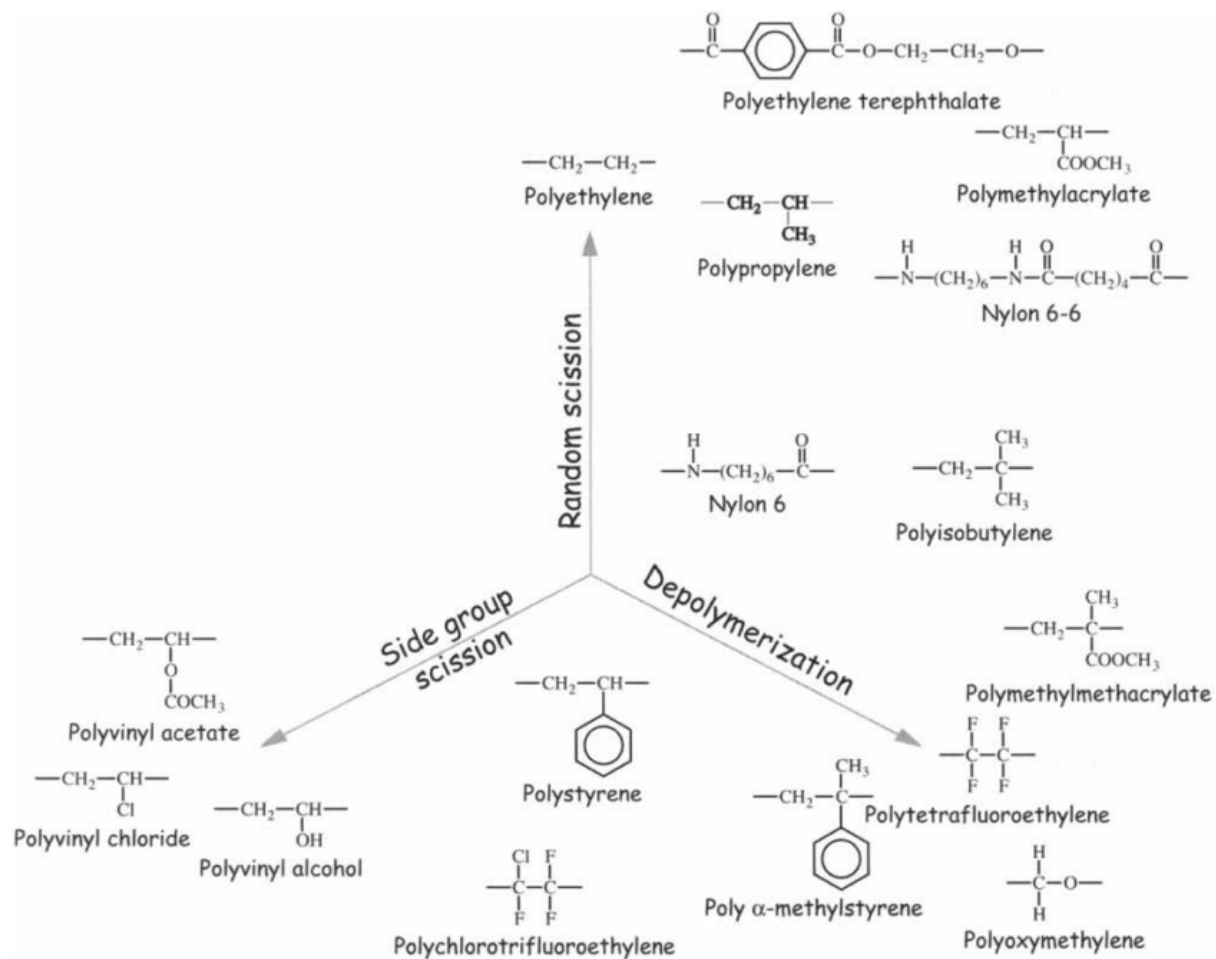


Figure 4 Common polymers and their primary degradation mechanisms (Stauffer, 2003)

Random Chain Scission

Random scission refers to the random breaking of carbon-carbon bonds within a molecule, resulting in the formation of smaller components such as alkanes, alkenes, and alkadienes (Lentini, 1998). This mechanism is commonly observed in polymers that have carbon-carbon bonds of similar strength in their backbone structure (Sánchez-Jiménez *et al.*, 2010). Polyethylene and polypropylene are polymers that often undergo random scission. When polyethylene is burned, the chromatographic profile will exhibit the presence of radical, unsaturated hydrocarbons (alkenes), and saturated hydrocarbons (alkanes) (Stauffer *et al.*, 2008). The mechanism of random chain scission in polyethylene is illustrated in Figure 5. In the case of polypropylene, the scission of carbon chains mainly occurs between tertiary and secondary carbons. This is due to the presence of methyl substituents along the backbone of polypropylene, resulting in every other carbon attached to a methyl group being tertiary (Wampler, 2002).

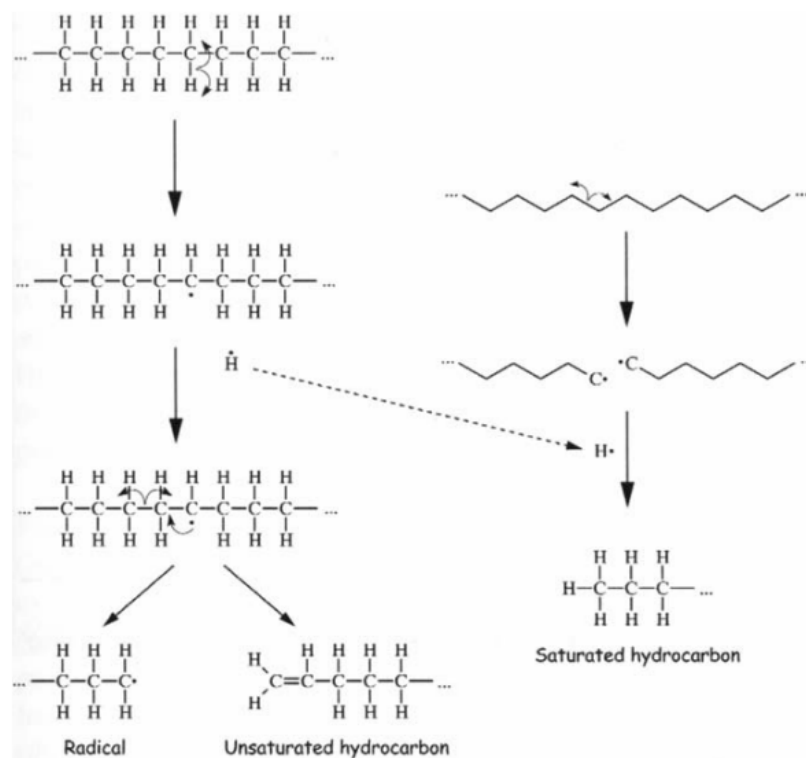


Figure 5 Random chain scission mechanism (Stauffer, 2003)

Side Group Scission

Side group scission refers to the loss of groups attached to the side of the carbon backbone in a polymer, leading to the formation of a linear polyunsaturated structure. This polyunsaturated structure then undergoes further degradation, including scission, aromatisation, and char formation (Beyler *et al.*, 2002). Polyvinyl chloride (PVC) is an example of a polymer that

undergoes side group scission. During this process, PVC loses hydrogen chloride (HCl) and forms a conjugated double bond backbone (Liu *et al.*, 2023). The conjugated double bonds in the backbone undergo additional degradation, resulting in the formation of aromatic components and smaller fragments. Side group scission of the carbon-carbon backbone in PVC yields aromatic components such as benzene, toluene, ethylbenzene, styrene, and naphthalene (Kusch, 2012; Beyler *et al.*, 2002). The mechanism of side group scission in PVC is depicted in Figure 6. Polymers with side group scission as primary mechanisms yield similar aromatic products once the side groups are eliminated.

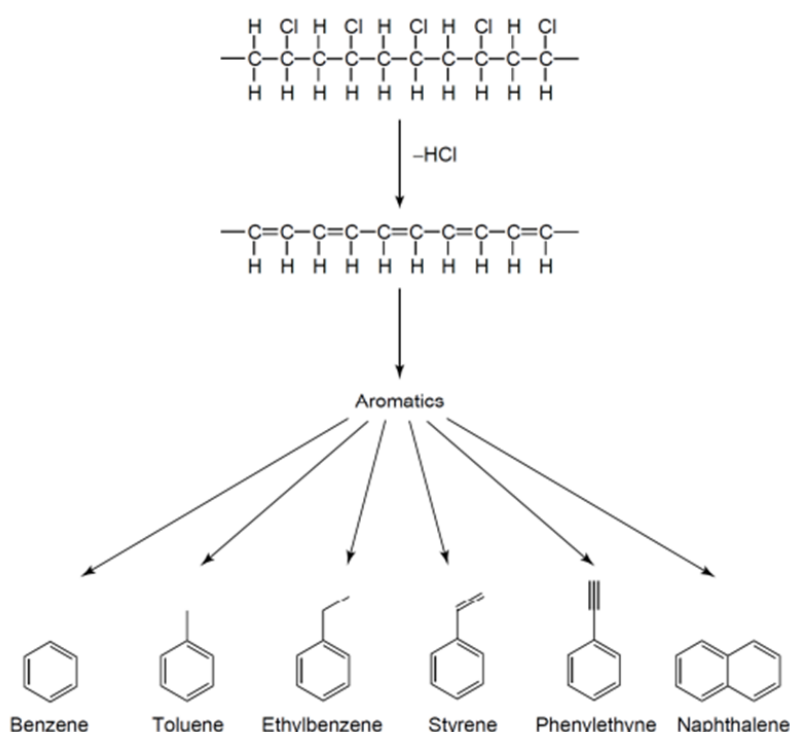


Figure 6 Side group scission mechanism (Stauffer, 2003)

Monomer Reversion

Monomer reversion or depolymerisation occurs when a polymer undergoes a free radical mechanism that reverts it back to the individual monomer or a group of monomers used in its synthesis. This depolymerisation mechanism produces a simple chromatogram characterised by large peaks corresponding to the monomers generated from the degradation of the polymer. Polystyrene and polymethacrylates are examples of polymers that undergo depolymerisation (Wampler, 2007). Specifically, polymethacrylates undergo scission, releasing a smaller unsaturated component and a free radical, Figure 7 (Stauffer, 2003). This process, often referred to as “unzipping”, results in the formation of a major peak within the chromatogram

representing the smaller unsaturated monomer for polymethacrylates (Kusch, 2012). When the polymer undergoes complete depolymerisation, the chromatographic profile will show a single peak corresponding to the monomer. However, it is important to note that the depolymerisation process can occur after the side group scission process leading to additional peaks in the chromatogram (Stauffer, 2003).

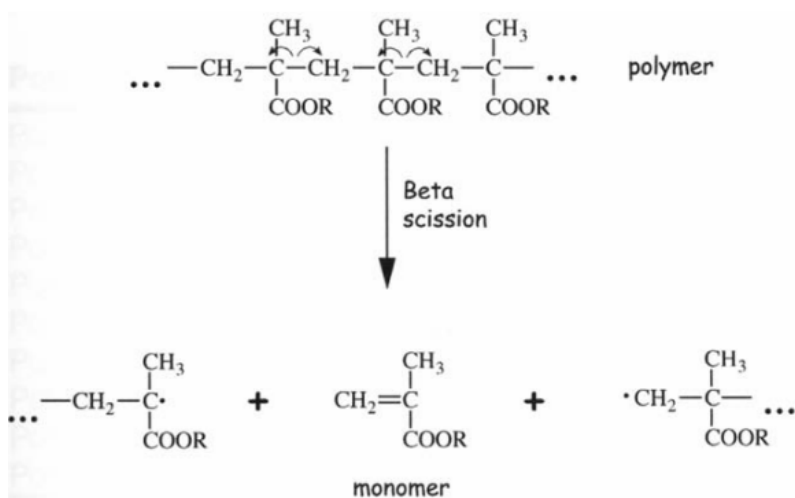


Figure 7 Monomer reversion mechanism (Stauffer, 2003)

Free Radical Mechanisms

Free radical reaction is one of the minor degradation pathways in the pyrolysis of polymers. Free radicals are highly reactive species that have an unpaired electron. They are formed when a molecule or atom undergoes homolytic bond cleavage resulting in the generation of two radicals. In the context of pyrolysis, the high temperatures break the chemical bonds within the polymer chains leading to the formation of free radicals. The free radical mechanisms consist of three main steps: initiation, propagation, and termination. The initiation step occurs when energy from the heat source or from thermal degradation breaks a weak bond in the polymer. This bond cleavage generates two radicals, one located on the polymer chain and the other on the fragment that detached from the original polymer. These radicals are highly reactive and seek to stabilise themselves by either reacting with other radicals or with stable molecules present in the system. The second step is propagation where the original fragment reacts with neighbouring polymer chains or with stable molecules such as small hydrocarbon fragments in the system. This reaction involves the transfer of the unpaired electron from the original fragment to the stable molecule, resulting in the formation of a new radical. The newly formed radical can then initiate a chain reaction by further propagating the decomposition process. The chain reaction continues as the newly formed radical reacts with other polymer chains or stable

molecules creating a cascade of reactions. This leads to the production of various smaller fragments, such as hydrocarbons, aldehydes, ketones, and aromatic compounds, depending on the specific polymer being pyrolyzed. The reaction proceeds until the radicals are consumed or until termination reactions occur. The final step in the free radical reaction is termination. This involves the combination of two radicals, resulting in the formation of stable molecules without any unpaired electrons. Termination reactions can occur through radical-radical recombination or by reactions with other molecules present in the system (Ashenurst, 2022; Libretexts, 2022; Khan, 2012).

2.3 Fire Investigation

Fire investigation and analysis is a complex process that involves a variety of techniques and methods to determine the cause and origin of a fire. The general process of fire investigation and analysis includes scene examination, evidence collection, laboratory analysis, documentation, reconstruction, and report writing (Churchward *et al.*, 2004).

The scene examination is the first investigation step after the fire is extinguished. The investigator will look for any evidence that may help determine the origin and cause of the fire, such as burn patterns, heat damage, and the location of the most intense fire damage. The next step is to collect evidence from the scene, which can include physical samples of debris and materials, photographs, and documentation of any eyewitness accounts. Physical samples collected from the scene are sent to a laboratory for analysis. Depending on the suspected cause of the fire, various analytical techniques may be used, such as gas chromatography, mass spectrometry, and microscopy. These techniques can help identify the presence of accelerants or other substances that may have contributed to the fire. Throughout the investigation, the investigator must document all observations and findings. This includes photographs, diagrams, and written notes. The investigator may also need to interview witnesses and collect statements. Once all the evidence has been collected and analysed, the investigator will reconstruct the fire scene to determine the most likely cause and origin of the fire. This involves analysing the physical evidence and reconstructing the events leading up to the fire. Finally, the investigator will write a report summarizing the investigation and presenting the findings. The report will typically include a detailed description of the fire scene, evidence collected, laboratory analysis results, reconstruction, and conclusions regarding the cause and origin of the fire (Churchward *et al.*, 2004).

The process of conducting a fire investigation requires the application of scientific expertise and technology to form legally defensible conclusions. These conclusions must be based on objective and truthful compilation of factual data, ensuring the absence of prejudice, bias, or preconception.

2.4 Current Methods for Fire Debris Analysis

The following list consists of the standards related to fire debris analysis published by ASTM (American Society of Testing and Materials) International:

- ❑ ASTM E2451-21: Standard practice for preserving ignitable liquids and ignitable liquid residue extracts from fire debris samples.
- ❑ ASTM E3245-20e1: Standard guide for systematic approach to the extraction, analysis, and classification of ignitable liquids and ignitable liquid residues in fire debris samples.
- ❑ ASTM E3197-20: Standard terminology relating to examination of fire debris.
- ❑ ASTM E1412-19: Standard practice for separation of ignitable liquid residues from fire debris samples by passive headspace concentration with activated charcoal.
- ❑ ASTM E1413-19: Standard practice for separation of ignitable liquid residues from fire debris samples by dynamic headspace concentration onto an adsorbent tube.
- ❑ ASTM E1618-19: Standard test method for ignitable liquid residues in extracts from fire debris samples by gas chromatography-mass spectrometry.

2.5 Recent Advancement in Fire Debris Analysis

As was discussed previously fire debris analysis comprises of scene examination, evidence collection, and lab analysis. Various approaches in advancing the sampling and analytical methods have been developed to resolve the challenges in the chemical analysis of fire debris.

2.5.1 Fire Debris Sampling

Correct and adequate sampling of fire debris can increase the success rate of the subsequent chemical analysis, so knowing what to look for at the fire scene is essential. There are various forms of sampling techniques in arson investigation, including canines, the use of spectroscopic instruments, and electrochemical sensors.

Canines

The use of canines in detecting accelerants in fire debris is a common practice among investigators (Dalton, 2017). Canines possess an exceptional sense of smell, with a range of

300,000-500,000 times stronger than humans (K9s4COPs, 2023) enabling them to effectively sweep search for accelerant identification. Canines can detect trace amounts of accelerants (0.1ppm), thereby reducing the search time taken at the scene of fire to search for and locate accelerants that may be invisible to the human eye. In comparison, a canine can cover a much larger area of approximately 400-500m² in 10min, whereas a single investigator can only search up to 30m² in 4 hours (O'Hagan *et al.*, 2021).

Prior to commencing their operational duty, canines require an extensive training period of up to 14 weeks with a handler and an average continuous training time of 24.3 hours per month (An Garda Síochána, 2023; Lancashire Constabulary, 2023; Mesloh, 2006). Despite their strong sense of smell, there is a high incidence of incorrect alerts by canines due to the chemical similarity of ignitable liquids and petroleum derived background materials. Canines may also experience signal saturation and their sense of smell may be subject to refractory periods, leading to a temporary confusion and false alerts (O'Hagan *et al.*, 2021). To address this issue, Abel *et al.* conducted a study on confirmatory analysis of canine search results to improve the training and certification procedures (Abel *et al.*, 2022).

From an economic viewpoint, the cost of training a canine to operational standards is a high financial investment, making it a drawback of using canines. The cost of training a canine varies depending on the region of training. In Ireland, the approximate cost of training a canine is € 100,000 with an ongoing cost of € 40,000 per annum (Mulligan, 2020). In the UK, it is estimated to cost £18,500 for the first year, which includes the cost of the puppy, veterinary, training course, equipment, kennels, and food (South Yorkshire Police, 2017). In the US, the full operational canine training cost can range from \$30,000 to \$80,000 (Wright, 2019).

Spectroscopic Techniques

In arson investigation, the use of spectroscopic techniques has become a growing trend. Portable instruments are particularly useful in situations where a canine is unavailable or where the area is unsafe for the canine to access. While UV light was available in the 1970s for identifying pour patterns, it was not commonly used at that time due to inadequate technical equipment for production of satisfactory results (Griffin, 2020). However, the technique has since been successfully applied in fire investigation due to its simplicity, speed, and non-destructive nature, as well as minimising the chemical waste production in fire scene analysis (Griffin, 2020). White light is insufficient for identifying the presence, spread, or pour patterns of accelerants. Fluorescence techniques are effective in complementing sampling and liquid

pattern analysis by capturing scene images at different wavelengths (Ljungkvist *et al.*, 2019). This technique can be used in conjunction with canines, where canines can initially sweep the area to highlight a potential location of ignitable liquids, and then fluorescence cameras can be used to identify the exact location or collect debris for further lab testing. As no single method can provide positive results in arson investigation, cooperation between canines, investigators, and the lab is essential for enhancing the success rate.

Ljungkvist *et al.* highlighted that the detection of fluorophores relies entirely on the specific UV-light utilised and the product being examined (Ljungkvist *et al.*, 2019). This indicates that heavy petroleum distillate molecules generally absorb UV light at longer wavelengths due to their higher number of saturated bonds. Notably, Griffin observed that employing multiple light sources for illuminating accelerants leads to enhanced fluorescence detection compared to using a single light source, Table 1 (Griffin, 2020). Blue light (440-485nm) proved to be the most effective in inducing fluorescence in petrol and white spirit, red light (620-740nm) in BBQ lighter fluid and acetone, and UV light (100-400nm) in diesel. However, it was also noticed that diesel occasionally exhibited better fluorescence under blue light deviating from the optimal UV light source (Griffin, 2020). This suggests that utilising multiple light sources can prevent potential accelerants from being overlooked.

Table 1 Fluorescence of ignitable liquids under each light source

Ignitable liquids	Light source				
	UV 100-400nm	Blue 440-485nm	Blue/Green 485-500nm	Green 500-565nm	Red 620-740nm
Petrol	1	1	1	1	0
Diesel	4	4	2	2	0
BBQ lighter fluid	0	0	0	0	3
Acetone	0	0	0	0	4
White spirit	0	3	3	0	0

0 – no fluorescence observed; 1 – slight fluorescence observed; 2 – some fluorescence observed; 3 – fluorescence observed but difficult to distinguish between the ignitable liquid and background; 4 – bright fluorescence and liquid pattern can be observed easily (Griffin, 2020)

Fluorescence offers several advantages in the realm of detecting ignitable liquids. However, it also possesses inherent limitations. To effectively observe weak fluorescence, the screening environment must be entirely dark and the detector should be placed a short distance from the

sample. Additionally, the presence of background materials can overshadow the weak fluorescence emitted by accelerants can potentially lead to misinterpretation. Moreover, the presence of reflected light can further complicate the analysis (Ljungkvist *et al.*, 2019). Another factor to consider is the production of carbon monoxide during the combustion process, which can generate an increase in fluorescence. This phenomenon may cause confusion for investigators when attempting to identifying the potential presence of ignitable liquids (Griffin, 2020).

Electrochemical Techniques

A portable photoionization detector (PID) is a widely employed non-destructive instrument for the identification of volatile organic compounds (VOCs) (O'Hagan *et al.*, 2021). The compact and portable design of the PID makes it highly suitable for field investigations. It utilises UV light as the energy source to irradiate gas molecules while electrochemical sensors within the device measure the resulting electrical currents generated through reactions between the gas molecules and applied reagents (Baldwin, 2015). The PID offers a straightforward, quick, and precise means of detecting accelerants within concentration ranges of parts per million (ppm) and parts per billion (ppb). Additionally, the use of PID can mitigate false-positive results caused by pyrolysis (O'Hagan *et al.*, 2021). However, the application of PID is subject to certain limitations. One such limitation is its sensitivity to humidity, as high humidity levels (>70%) can reduce instrument sensitivity and necessitate frequent recalibration (O'Hagan *et al.*, 2021).

A new technology known as portable hydrocarbon noses has emerged for on-site detection of accelerants. These devices primarily rely on an integrated sensor capable of detecting combustible and hazardous vapours even at concentrations as low as 1ppm (Wu *et al.*, 2020; Baldwin, 2015). By employing a small vacuum pump and a narrow hose, the vapours are drawn into a chemical detector and subsequently detected by a sensor specifically designed for this purpose. The sensor measures electrical currents that arise from the reaction between the targeted gaseous molecules and the applied reagents within the sensor (Baldwin, 2015). While these electrochemical sensor devices can function similarly to canines, their ability to identify characteristic compounds of accelerants and degradation products resulting from pyrolysis is relatively limited in terms of specificity and sensitivity (Torres *et al.*, 2020). Nonetheless, the use of hydrocarbon noses can complement the capabilities of canines and fluorescence detectors in accelerant detection.

Ferreiro-González *et al.* conducted a study to explore the application of an electronic nose (E-Nose) as a non-separative technique for analysing ignitable liquids. They proposed that this method could serve as an environmentally friendly alternative to conventional analysis of ignitable liquid residues. The E-Nose system utilised in the study consisted of a headspace autosampler and a Kronos quadrupole mass spectrometer. The authors reported a total analysis time of 12 minutes for this system. Through the combined use of chemometric tools, such as hierarchical cluster analysis (HCA) and linear discrimination analysis (LDA), partial discrimination of ignitable liquids was achieved (Ferreiro-González *et al.*, 2016). Subsequently, the authors published another paper focusing on the validation of the headspace mass spectrometry electronic nose (HS-MS E-Nose) in conjunction with chemometric tools. The results showed that this developed method enabled the analysis of fire debris in 10 minutes without the need for solvents or sorbents, while achieving a 90% correct classification rate for the identification of ignitable liquids (Ferreiro-González *et al.*, 2017).

Although PID and hydrocarbon noses have been utilised in arson investigation, recent advancements and technological developments have significantly expanded their practical applications in the field of arson investigation and prevention (Baldwin, 2015). One notable development is the introduction of an E-nose equipped with a metal oxide sensor, specifically designed to monitor five commonly used commercial flammable liquids by bus arsonists, namely, ethanol, gasoline, lacquer thinner, tetrahydrofuran, and turpentine (Wu *et al.*, 2020). Additionally, the study demonstrated that certain E-Nose devices have the capability to filter out potential false alarms triggered by non-regulated liquids, such as mosquito repellent, perfume, and hair jelly, even though they contain flammable substances (Wu *et al.*, 2020). This advancement in arson investigation is particularly valuable as it enables the E-Nose to selectively detect ignitable liquids at concentrations as low as 1ppm (Wu *et al.*, 2020).

Chromatographic Sampling

Torres *et al.* conducted two studies evaluating the extraction and analysis of ignitable liquids using Capillary Microextraction of Volatiles (CMV) devices coupled with portable and benchtop Gas Chromatography Mass Spectrometry (GCMS) systems. In the first study, the CMV-portable setup did not exhibit sufficient chromatographic resolution due to limitations inherent to the portable GCMS device used. However, the CMV-benchtop setup successfully extracted and identified specific components of ignitable liquids. This study demonstrated the feasibility of using CMV extraction as a rapid (~5min) technique in conjunction with other

portable and benchtop GCMS systems (Torres *et al.*, 2020). In their second study, the CMV was further evaluated with a paper cup extraction method coupled with a portable GCMS for field sampling purposes. The CMV and paper cup approach demonstrated successful extraction of multiple target components of ignitable liquids. It outperformed the portable GCMS sampling and in terms of efficiency and exhibited greater sensitivity compared to traditional ignitable liquid headspace extraction techniques. These findings highlight the effectiveness of the CMV and paper cup method for field sampling and analysis of ignitable liquids (Torres *et al.*, 2022).

DeHaan (2021) conducted a comprehensive study on the application and limitations of portable GCMS systems in fire investigation. Various systems specifically designed for hazardous materials teams were tested. It was found that the portable GCMS system can generate comparable GC separation, consistent retention times, and sensitivity levels to a conventional benchtop GCMS system. However, the main limitation identified was the interpretation of data in the field as it often required extensive training that is not typically available to most fire investigators and personnel at the fire scene (DeHaan, 2021).

2.5.2 Sample Collection and Storage

The presence of ignitable liquid residues on partially burned items such as clothing, carpet, wood, soil, and paper should be collected, stored, and transported to a forensic lab without contamination or evaporation of volatile analytes. Taking preventive measures enhances the integrity of the analysis results by ensuring a legally sound chain of custody throughout the fire debris analysis process (Sandau, 2021). There is currently no universal method for sample collection given the variation in fire debris types and potential interferents resulting from the method of fire extinguishment (Carmona *et al.*, 2021). Generally, fire debris samples are collected using sterile tools and placed into inert, durable, and securely sealed containers with a preference for airtight containers over plastic bottles or bags. For example, a lined metal paint can is inert and can minimise the loss of volatile compounds due to its airtight properties. Conversely, plastic containers are more susceptible to puncturing and vapours may diffuse into or out of the plastic material. Some plastics may also be porous or react with volatile compounds, posing a risk of volatile organic compound loss from the debris samples or leading to false-negative analysis results (Nicholas, 2008). Proper sample collection and storage are crucial for ensuring successful lab analysis.

A new development in sample collection involves the use of hydrophobic pads. A hydrophobic pad is a sorbent designed to collect oil-based product over water surface. Totten *et al.* conducted a study to assess the effectiveness of hydrophobic pads in recovering oil-based products from water (Totten *et al.*, 2020). Their investigation revealed that hydrophobic pads were successful in capturing hydrocarbon compounds with carbon chains greater than C₈. This innovative approach to sample collection and extraction of hydrocarbon compounds has the potential to address the issue of dilution or removal of accelerants during fire control measures (Totten *et al.*, 2020).

While there have been limited advancements in the field of sample collection and storage for fire debris, ensuring proper and adequate storage of samples is crucial for maintaining the integrity of analysis results and aiding in the investigation of potential crimes.

2.5.3 Extraction

The sample preparation step plays a crucial role in the isolation of ignitable liquid residues from interferences prior to instrumental analysis. Various techniques have been developed for separating ignitable liquid residues from the fire debris matrix.

Samples collected at arson scenes often require pre-treatment. Overtime, the techniques for extracting and concentrating accelerants from different substrates have evolved. In the 1940s, a common practice involved the direct comparison of chemical and physical properties, such as light refraction coefficient, weight density, and boiling point, between the fire debris samples and reference samples (Yadav *et al.*, 2021; Borusiewicz, 2002). During the 1950s and 60s, conventional extraction methods such as steam distillation, vacuum distillation, and solvent extraction were employed to isolate accelerants from substrates (Yadav *et al.*, 2021; Borusiewicz, 2002). In the 1970s, headspace analyses emerged as modern extraction procedure. These include direct heated headspace analysis, dynamic (purge and trap) headspace analysis, and static (equilibrium) headspace analysis using the activated charcoal strip method, solid phase microextraction (SPME), or other adsorbents placed in temperature-controlled, airtight containers (Yadav *et al.*, 2021; Borusiewicz, 2002). Table 2 provides a summary of the extraction, instrumental, and chemometric applied to these new approaches based on the reviewed literatures.

Headspace analysis operates on the principle of examining the chemical composition of the gas phase above a sample, whether it is in liquid or solid form. These methods are considered to be

straightforward and rapid, requiring minimal sample preparation. However, it is important to note that the activated charcoal strip method carries the potential risk of exposure to toxic solvents such as carbon disulfide which is used for eluting the adsorbent is highly hazardous.

The reviewed advancements on headspace extraction conditions include the use of activated charcoal pellets as adsorbents (Carmona *et al.*, 2021), activated charcoal cloth as adsorbents (Sandercock, 2016), SPME employing polydimethylsiloxane (PDMS) (Martín-Alberca *et al.*, 2015), SPME using divinylbenzene/carboxen/polydimethylsiloxane (DVB/CAR/PDMS) (Fettig *et al.*, 2013), and the application of capillary microextraction of volatiles (CMV) in conjunction with a portable GCMS system (Torres *et al.*, 2020).

Activated Charcoal Strip

The extraction of ignitable liquids using Activated Charcoal Strips (ACS) is the designated standard method according to the American Society of Test and Material (ASTM) E1618, titled “Standard Test Method for Ignitable Liquids Residues in Extracts from Fire Debris Samples by Gas Chromatography-Mass Spectrometry.” While this method is recognised for isolating volatile compounds specific to ignitable liquids, it is also a time-consuming and expensive method of extraction. The extraction process typically requires 12 to 16 hours (Ferreiro-Gonzalez *et al.*, 2016) and commercial activated charcoal strips can cost over \$700 per 100 strips (ArrowheadForensics, 2023).

Baernkopf *et al.* evaluated the preservation of ignitable liquids on ACS over two-year period. They applied low and high volumes of gasoline and heavy petroleum distillate onto an inert substrate, which were then collected using passive headspace concentration. The collected samples were stored in three different vials at room temperature. The ACS were periodically analysed over the course of two years. It was observed that they effectively retained the ignitable liquid in all types of vials and with both low and high volumes (Baernkopf *et al.*, 2020).

Activated Charcoal Pellets (ACP)

Carmona *et al.* devised a technique using Activated Charcoal Pellets (ACP) for the sampling and extraction of gasoline and diesel fuel from fire debris. The ACP was prepared by pressing charcoal powder and D-glucose in a pellet form. The efficacy of this method was compared to the conventional ACS methods and the results demonstrated that the ACP method yields comparable outcomes to the established ACS method. An advantageous aspect of the ACP method is its ease of preparation requiring a short preparation time using inexpensive materials

readily available in lab. However, similar to the ACS method, the ACP method necessitates a 16 hour extraction duration for volatile compounds to be adsorbed onto the adsorbent. Additionally, the validation of this technique is crucial to determine its suitability and effectiveness in real-world fire scenarios (Carmona *et al.*, 2021).

Activated Carbon Cloth (ACC)

Sandercock assessed the extraction of ignitable liquids using Activated Carbon Cloth (ACC) and compared it to commercially available ACS. The findings revealed that ACC can extract a higher concentration of ignitable liquid compounds compared to ACS. The use of ACC offers several advantages over ACS, including cost-effectiveness, the possibility of regeneration through resistance heating using an electric current and reduced waste generation. Nevertheless, similar to the ACS and ACP methods, the ACC method requires a lengthy adsorption time prior to GCMS analysis (Sandercock, 2016).

Büchler *et al.* investigated the use ACC and ACS as collection methods for sampling ignitable liquids on hands. Similarly, the study found that ACC exhibited greater effectiveness in extracting gasoline compared to ACS. However, two crucial factors affecting the extraction efficiency were the distance between the adsorption material and the skin, as well as the available headspace during sample collection which were relevant for both ACC and ACS (Büchler *et al.*, 2021).

Solid Phase Microextraction (SPME)

The application of Solid Phase Microextraction (SPME) has been frequently reported as an alternative to the standard ACS method for extraction purposes. SPME involves the use of fibres coated with an adsorbent phase capable of extracting volatile compounds which can then be directly inserted into the injection port of a GC system for thermal desorption and subsequent analysis. SPME offers several advantages over ACS in the extraction of volatile compounds from fire debris. It is a non-destructive, rapid, highly sensitive, solventless, and selective method. Additionally, it is a straightforward and effective sampling technique that is portable and suitable for field deployment. However, SPME fibres are delicate and more susceptible to displacement, leading to higher operational costs compared to ACS (Harries *et al.*, 2021).

The application of SPME in arson investigation represents a significant advancement as the isolation process can selectively target aliphatic or aromatic compounds by employing different types of SPME fibres. Fettig assessed the use of DVB/CAR/PDMS fibre for the

extraction of ignitable liquids in fire debris. The study demonstrated that SPME with DVB/CAR/PDMS fibre effectively recovered ignitable liquids (gasoline and diesel fuel) from residues on burnt solid substrates (particleboard and carpet) within a total extraction time of only 35 minutes (Fettig *et al.*, 2013).

Dhabbah used SPME with PDMS fibre to detect gasoline residues in textiles made of cotton, wool, nylon, and polyester. This investigation showcased an effective approach to extracting characteristic volatile components of gasoline from both natural and synthetic textiles, eliminating the need for commercial ACS. The study concluded that the SPME PDMS fibre procedure was “simple, fast, efficient, solventless, cheap, and environmentally friendly” (Dhabbah, 2018).

Swierczynski *et al.* carried out an experiment where gasoline was introduced onto various household materials and allowed to dry for specific time intervals. The ignitable liquid was extracted using SPME combined with GCMS. The analysis revealed that gasoline residue could be detected in cotton fabric for up to seven days after drying while cardboard and carpet retained gasoline for over three weeks. The authors employed small vials for the headspace analysis, attributing the improved detection limit and the ability to identify residues even after an extended period of time (Swierczynski *et al.*, 2020).

Other Extraction Methods

Yadav *et al.* conducted a comparative analysis of hexane and diethyl ether as solvents for extracting diesel fuel from partially burned substrates. The study determined that diethyl ether exhibited better efficiency in extracting diesel fuel from the tested porous matrices, including wood, ceramic-based tile, and cotton. However, neither solvent was effective in extracting diesel fuel from the non-porous plastic material that was tested (Yadav *et al.*, 2021).

Summary

The established method for extracting ignitable liquid residues in fire debris analysis is the utilisation of activated carbon strips, as outlined in ASTM E1618. However, there is a growing shift in this analytical process towards replacing ACS with SPME. The patent for SPME coatings and separation methods has expired on 6th March 2023 (Pawliszyn, 2003). Subsequently, other manufacturers will be able to produce their own SPME fibres at a lower cost. This reduction in material expenses combined with the technique’s environmentally friendly nature encourages analysts to opt for SPME in the extraction of volatiles from fire debris as opposed to the lengthy activated carbon-based extraction methods.

2.5.4 Instrumental Analysis and Data Interpretation

GCMS is the primary method used in the chemical analysis of fire debris. It is widely adopted, following the reference guidance of ASTM E1618 (Büchler *et al.*, 2021; Carmona *et al.*, 2021; Totten *et al.*, 2020; Sandercock, 2016; Fettig *et al.*, 2013). Under this guidance, various protocols have been developed covering the extraction methods and advancements in analytical techniques. These advancements include multidimensional analysis and a shift from conventional destructive methods to non-destructive methods.

GCMS is a highly effective and sensitive analytical technique that offers several benefits to fire debris analysts. Extracted ion profiling, in particular, is valuable for distinguishing ignitable liquids from interference caused by pyrolysis products or contaminants (Nicholas, 2008). During analysis, each sample undergoes GCMS and the number of separated and detected compounds in ignitable liquids can range from a few to hundreds. However, one-dimensional GCMS has limitations in resolving compounds that serve as precursors from the manufacture, pyrolysis products, combustion products, or fire-suppression products (Nizio *et al.*, 2016). Consequently, alternative techniques have been introduced to assist in the analysis of ignitable liquid compounds.

Mártin-Alberca *et al.* conducted a comprehensive review of analytical tools for fire debris analysis. These include portable GCMS, supersonic-GCMS, GCMS with vacuum-UV ionisation, multidimensional GCMS (GC x GCMS), GC x GC with Flame Ionisation Detection (GC x GC-FID), GC-Fourier Transform Ion Cyclotron Resonance MS (GC-FT-ICR-MS), and Isotope Ratio Mass Spectrometry (IRMS) (Mártin-Alberca *et al.*, 2015). Furthermore, alternative techniques that use multidimensional GC in conjunction with chemometric and computational software are new developments in the realm of arson investigation.

2.5.5 Chromatographic Analysis

Multidimensional GC has emerged as a valuable approach to address the challenges associated with resolving target and matrix volatiles. Nizio *et al.* developed a two-dimensional GC coupled with Time-of-Flight MS (GC x GC-TOFMS) method for analysing petroleum-based ignitable liquids. The study demonstrated that GC x GC-TOFMS can achieve a peak capacity of approximately 9.3, which is close to the theoretical maximum of approximate 11.2 for a given resolution and maximum theoretical plates. This achievement was made possible by using computational software (ChromaTOF®) that corrects baselines and aligns peaks. The resulting chromatograms exhibited well-organised patterns of structurally related compounds,

enabling rapid classification of ignitable liquids according to the ASTM E1618 standard (Nizio *et al.*, 2016). Another method, as reported by Sampat *et al.* employing GC x GC-TOFMS achieved an 89% true positive identification rate for the presence of ignitable liquids in sample substrates with only a 7% false positive detection rate for ignitable liquid residues (Sampat *et al.*, 2018).

Barnett *et al.* introduced a novel and efficient method for analysing arson volatile compounds known as Direct Analysis in Real Time Mass Spectrometry (DART-MS) with QuickStrip and thermal desorption. Thermal desorption provided better detection capabilities for residues in the presence of substrates. They showed that DART-MS can analyse ignitable liquid residues without the need for complex extraction and chromatographic separation procedures. The application of DART-MS yielded mass spectra with a greater number of peaks in the higher mass range when compared to conventional GCMS. This improvement in peak generation facilitated the detection of less volatile compounds. By employing Partial Least Square Discriminant Analysis (PLS-DA) models in conjunction with DART-MS, they achieved rapid classification of ignitable liquids originating from various substrates, yielding an impressive correct classification rate of 98% (Barnett *et al.*, 2019). Sisco *et al.* conducted a literature review on the forensic application of DART-MS. It indicated that DART-MS offers a rapid screening method for detecting the presence of ignitable liquids. However, due to its limited separation capacity, chemometric techniques are generally required to differentiate between neat liquids and evaporated samples (Sisco *et al.*, 2021).

Aliaño-González *et al.* used Headspace Gas Chromatography Ion Mobility Spectrometry (HS-GC-IMS) in combination with chemometric tools, specifically Hierarchical Cluster Analysis (HCA) and Linear Discriminant Analysis (LDA) for arson investigation (Aliaño-González *et al.*, 2018). This approach presented an alternative to the conventional ACS-GC-MS method by offering advantages in preconcentration, analysis, and data interpretation. The researchers concluded that HS-GC-IMS along with HCA and LDA exhibited remarkable accuracy in classifying ignitable liquids with 95% correct discrimination rate. Moreover, this method significantly reduced the analysis time, completing the entire analysis in just 15 minutes. Notably, this approach is cost-effective, straightforward, solvent-free, and suitable for routine analysis, further enhancing its practicality (Aliaño-González *et al.*, 2018).

Roberson *et al.* developed a micro-bore capillary column (5m x 1.25 μ m x 50 μ m i.d.) as an alternative to commercially available GC columns commonly used in the chemical analysis of

fire debris, such as DB-5MS, HP-5MS (30m x 0.25mm x 0.25µm i.d.). The analysis was performed using the ASTM E1618 test mixture. The optimised GCMS separation conditions using the micro-bore capillary column resulted in rapid analysis, enabling the determination of compounds up to C₁₄ within 3 minutes as opposed to the traditional 30 minutes GCMS analysis (Roberson *et al.*, 2019).

Pandohee *et al.* employed two-dimensional GC with Flame Ionisation Detector (GC x GC-FID) to analyse a variety of ignitable liquids, including both neat and weathered samples. The study successfully differentiated the three categories of ignitable liquids by analysing the 2D patterns and applying principal component analysis (Pandohee *et al.*, 2020).

Boegelsack *et al.* conducted a study on optimising a flow-modulated GC x GCMS method for analysing ignitable liquids present in wildfire debris. Various GC columns and parameters, such as flow rate and oven programming were evaluated. The final method used a 5% diphenyl column coupled with a 50% diphenyl column. This GC x GCMS technique was successful in resolving the target compounds listed in ASTM E1618, enabling the classification of ignitable liquid residues within a complex matrix (Boegelsack *et al.*, 2021b). In a separate study, Boegelsack *et al.* developed a retention time index system for GC x GC analysis of ignitable liquids. A contour map for both neat ignitable liquids and samples obtained from fire scenes was created following the ASTM E1618 guidelines. The contour map in combination with the retention index system proved to be useful for standardising and comparing data (Boegelsack *et al.*, 2021a). The work of Boegelsack *et al.* was revolutionary in the field of arson investigation by attempting to standardise the method of chemical analysis.

Kates *et al.* applied comprehensive GC x GC-TOFMS to analyse fire debris samples collected from wildfires. The study revealed that the implementation of GC x GC-TOFMS resulted in improved separation of ignitable liquids from interfering compounds in the matrices, mainly due to lower detection limits. The number of tentative results was reduced to 6% and 76% successful identifications of ignitable liquids was achieved when debris was reanalysed by GC x GC-TOFMS after analysis with conventional GCMS (Kates *et al.*, 2020).

2.5.6 Statistical Analysis and Machine Learning

Akmeemana proposed the use of likelihood ratios calculated through the Naïve Bayes method to identify ignitable liquids in fire debris. The study employed data from the National Centre of Forensic Science Substrate and Ignitable Liquid Reference Collection to determine the occurrence frequency of compounds in substrates and ignitable liquids. The Naïve Bayes

method can effectively classify samples of pure substrates and ignitable liquids. However, it faced challenges in classifying mixtures of both due to the influence of burning on the presence of specific compounds (Akmeemana, 2019).

Bogdal *et al.* conducted a two-part study aimed at identifying gasoline in fire debris using machine learning techniques. The researchers developed a machine learning tool employing different algorithms in Part 1 of the study while Part 2 focused on creating a convolutional neural network specifically designed for analysing searchable bitmap images of GCMS data. Both approaches involved training the machine learning models using known samples and evaluating their performance on unknown samples. Although the datasets used in both studies were limited to gasoline, they demonstrated a high screening and classification accuracy rate of 98% (Bogdal *et al.*, 2022a; Bogdal *et al.*, 2022b).

Park *et al.* conducted a study where they developed three distinct machine learning models based on GCMS data derived from 728 real fire debris samples. The classification accuracy of the models varied between 63% and 84%. However, the accuracy for specific ignitable liquids was lower due to limitations in the data size for those liquids (Park *et al.*, 2021).

de Figueiredo *et al.* studied the connection between the residue and the source liquids with chemometrics by evaporating and burning gasoline samples on a substrate. Chemometrics played a crucial role in linking evaporated, burned, and unburned samples by identifying the most discriminative ratios for comparison. The nature of this study was exploratory and further research is required on a larger sample size to validate the findings (de Figueiredo *et al.*, 2019a).

de Figueiredo *et al.* employed an untargeted chemometric method using data obtained from 190 distinct gasoline samples with the aim of distinguishing between the liquids. The data was collected using headspace concentration with Tenax TA tubes followed by automated thermal desorption GCMS. The method was successful in differentiating all 190 samples from each other. However, the authors acknowledge the need for additional research on weathered samples and alternative extraction techniques to validate the applicability of method on a wider scale (de Figueiredo *et al.*, 2019b).

Falatová *et al.* explored the potential of an e-Nose in combination with chemometric tools for identifying ignitable liquids in simulated fire debris. The study focused on testing two substrates, cotton and cork, and two ignitable liquids, ethanol and diesel fuel. The results

suggested that the applied chemometric techniques were effective in distinguishing between the samples (Falatová *et al.*, 2019). However, it is important to note that the chosen ignitable liquids had distinct chemical compositions that would have been easily distinguishable even without the use of statistical treatments. The study highlighted the need for further investigation involving a broader range of ignitable liquids with overlapping chemical compositions to fully evaluate the performance of the e-Nose and chemometric tools in fire debris analysis.

Christy *et al.* investigated chromatographic features in 150 gasoline samples with the goal of establishing quantitative criteria to assist in identifying samples that were evaporated up to 90%. The study involved analysing peak height ratios from 64 groups of chromatographic peaks which were then subjected to statistical analysis to assess their relative significance. The resulting scores were used to construct a sufficiency graph providing a visual representation of the data that supports the identification of gasoline (Christy *et al.*, 2021). This work aimed to establish a framework for enhancing the process of data interpretation in fire debris analysis.

The use of machine learning to interpret analytical results is also a new development in the field of fire debris analysis. Traditional methods of data interpretation, such as visual comparison of mass spectra can be hindered by background contributions from substrate pyrolysis. Previous computer-based pattern recognition methods have faced challenges in explaining their methods in court due to operator error. Machine learning is a form of artificial intelligence which has the potential to prevent errors in decision-making (Sigman *et al.*, 2021), but reliability and explicability barriers must be overcome especially in light of proposed EU regulation of AI (Anon, 2021).

Despite these challenges, several approaches have shown potential for improving the classification of fire debris analysis results. Vergeer *et al.* explored the use of likelihood ratios to classify gasoline samples, but the analysis was limited to pure petroleum and did not include substrate contributions (Vergeer *et al.*, 2020). Thurn *et al.* proposed the use of Kohonen self-organising maps coupled with extracted ion spectra to group ignitable liquids and substrate pyrolysis samples (Thurn *et al.*, 2018). However, this method was only applied to pure materials, and the classification process was not applied to actual fire debris containing mixtures of substrates and ignitable liquids.

More recently, Thurn *et al.* investigated the classification performance of neural networks on fire debris samples with ignitable liquid added after the fire (Thurn *et al.*, 2021). Although the

classification ability remains relatively poor, the potential for machine learning to provide better decision making remains because rapid analysis of a large number of samples is possible. Future developments in this field have the potential to impact the analysis of fire debris by forensic practitioners.

2.5.7 Summary

Table 2 below shows the summary of literature review in fire debris analysis. The current GCMS techniques are adequate to meet the analytical requirements. GCMS is a well-established and cost-effective technology that demonstrates excellent sensitivity, reproducibility, and selectivity, making it highly suitable for routine detection of ignitable liquids. While recent developments have offered enhancements in terms of run time, sample preparation, portability, ease of use, and discrimination power, they are unlikely to replace GCMS analysis in the near future without further testing, cost improvements, and demonstration of reliability on a larger scale. Therefore, GCMS remains the gold standard of analysis for fire debris.

However, the analysis of data to determine the presence or absence of ignitable liquids in complex samples remains an area that requires significant development. No existing method has achieved 100% accuracy in identifying the presence or absence of ignitable liquids in all cases. With ongoing advancements in machine learning techniques, it is anticipated that these methods will eventually provide rapid and unbiased data analysis. Nevertheless, it is essential to conduct further investigations into the underlying chemistry to ascertain whether such identification is feasible in all scenarios.

2.5.8 Limitations

Despite numerous advancements had been added to the field of fire debris analysis, there are still some unresolved limitations that needs to be addressed. The limitations include weathering effect, sample contamination from matrix interference, and lack of standards.

Weathering Effect

Jin *et al.* conducted a study to investigate the impact of fire on the stability of target compounds by burning and reheating gasoline residues. The results showed that the thermal destruction impact was greater on polycyclic aromatic hydrocarbons (PAHs) more than alkylbenzenes. PAHs and indanes could not be effectively detected after heating. On the other hand, alkylbenzenes and naphthalenes exhibited relatively higher stability with ACS extraction. However, when the temperature reached 600 °C, nearly all target compounds were lost after a

reheating period of 2min (Jin *et al.*, 2020).

Background Interferent

1. Fabrics

Baernkopf conducted a study to examine the occurrence of ignitable liquids on new and worn shirts with prints, made with 100% cotton, cotton blend with polyester, rayon, or both and 100% polyester. The research involved analysing 141 shirts using passive headspace ACS with GCMS. The results showed that 34% of the tested shirts exhibited signs of potential heavy normal alkane compounds, while 41% showed the presence of aromatic products. Although not all the identified aromatic patterns were sufficiently strong to be definitively identified, the high frequency of occurrence indicated the need for caution when identifying aromatic products in printed clothing (Baernkopf, 2020)

Dhabbah investigated the duration for which gasoline could be detected on burned and unburned fabrics using SPME with GCMS. The findings of the research indicated that gasoline remained detectable for a longer period (up to 4 hours) on unburned synthetic fabrics, such as polyester and nylon compared to cotton or wool. However, residues on burned fabrics were no longer detectable after 2 hours. Retained ignitable liquids were less volatile compounds as their retention time was greater than 5min (>50 °C) (Dhabbah, 2018). No detectable compounds from unburned or burned substrate materials without addition of gasoline. This suggested that the substrates did not produce interfering background components.

Guerrera *et al.* conducted a study to investigate whether the compounds found in clothing and body products could potentially affect the analysis of ignitable liquids. The research involved analysing samples of both worn and unworn clothing, as well as various body products with passive headspace ACS and GCMS. It was observed that some body products exhibited patterns like those of heavy petroleum distillates. The examined clothing contained compounds commonly found in ignitable liquids. However, although these compounds could potentially interfere with the identification of an ignitable liquid, a trained examiner would be capable of distinguishing between contributions from the substrate (clothing) and the ignitable liquid itself (Guerrera *et al.*, 2019).

2. Rubber

Jin *et al.* conducted a study aiming to differentiate between gasoline and different types of polystyrene-based rubbers using specific target compounds. The pyrolysis products generated from these materials exhibited numerous similar compounds, with alkylbenzenes being the

most common interferences. The findings of the study further support the proposal that the chemical compositions of the materials are correlated with the extent of interference (Jin *et al.*, 2021).

Lack of Standards

Although there is continuous publication of research on developing new techniques on different aspects of arson investigation, including sampling, extraction, instrumental, and data analysis, the standardised protocols remain absent. To address this gap, it requires the collaboration between the disciplines of fire investigation, analytical chemistry, and forensic science. By integrating the knowledge and expertise from these fields, the development of more comprehensive approaches to fire debris analysis can be achieved leading to the establishment of standardised methods and protocols.

Table 2 Summary of literature review on chemical analysis of fire debris

References	Ignitable Liquids	Substrates	Fire Debris Simulation Method	Storage Method	Extraction	Analysis Instrument	Chemometric	Result
Abel <i>et al.</i> , 2022	Gasoline, diesel	Kimwipe™ (cellulose)	IL spiked onto substrate without burning	Airtight lined cans	SPME (Carbon-wide range PDMS)	GC x GC-TOFMS	N/A	Method of extraction effective in generating comparative result to references
Aliaño-González <i>et al.</i> , 2018	Gasoline, diesel, ethanol, paraffin	Pinewood, cork, paper, cotton sheet	IL spiked onto substrates before burning for 2min	10mL GC vial	GC autosampler oven	GC-IMS	HCA, LDA	95% correct discrimination
Aqel <i>et al.</i> , 2016	Gasoline, diesel	Cotton, polyester, silk, nylon	IL spiked onto substrates before burning for 2min	Airtight nylon bags	SPME (100µm PDMS)	GCMS	N/A	Cotton and silk retained IL longer
Baerncopf <i>et al.</i> , 2020	Gasoline, diesel	Kimwipe™ (cellulose)	IL spiked onto substrate without	Airtight gallon can	ACC	GCMS	N/A	No obvious loss or changes on replicates

			burning					
Barnett <i>et al.</i> , 2019	Kerosene, diesel, Japan drier, charcoal starter fluid, naphtha, prestain, lighter fluid gasoline	Carpet, wood, cloth, sand, paper	IL spiked onto substrate without burning	N/A	Solvent extraction for GCMS; no extraction for DART-MS	GCMS and DART-MS	PLS-DA	98% correct discrimination
Büchler <i>et al.</i> , 2021	Gasoline	Suspect's hands	IL spiked onto volunteer's hands	Nylon-11 bags	ACC	GCMS	N/A	Method of extractive effective in isolating IL
Carmona <i>et al.</i> , 2021	Gasoline, diesel	Cotton fabric, paper	IL added onto substrates after direct flame burning	N/A	ACP	GCMS	N/A	Method of extraction effective in isolating ILs
Dhabbah, 2018	Gasoline	Cotton, wool, polyester, nylon	IL spiked onto substrate before direct flame burning	Nylon arson bag	SPME (100µm PDMS)	GCMS	N/A	Residual hydrocarbons can be accurately characterised
Falatová <i>et al.</i> , 2019	Ethanol, diesel	Cotton, cork	IL spiked onto substrates before burning the bottom of metal can for	Airtight metal can	E-Nose	MS	HCA, PCA, LDA	Method effective in classifying IL categories

			2min					
Ferreiro-Gonzalez <i>et al.</i> , 2016	Gasoline, diesel fuel, citronella, kerosene, paraffin	Wood, cotton, cork, paper, paperboard	N/A	N/A	E-Nose	Kronas-quadrupole MS	HCA, LDA	90% correct classification
Fettig <i>et al.</i> , 2013	Gasoline, diesel	Particleboard, nylon-66 (carpet)	IL spiked onto substrates without burning	N/A	SPME (50/30µm DVB/CAR/PDMS)	GCMS	N/A	Method of extraction effective in isolating ILs
Guerrera <i>et al.</i> , 2019	Vaseline® Petroleum Jelly, Secret® Shower Fresh women's deodorant, Aspercreme®, Johnson® Baby Oil, Coconut Pineapple Fragrance Mist perfume, Nivea® Essentially Enriched lotion	Sports bras (10% spandex, 90% nylon), mesh shorts (100% polyester), short sleeve t-shirts (100% cotton), ladies socks (44% cotton, 52% polyester, 1% nylon, 2% rubber, 1% spandex)	N/A	N/A	ACS	GCMS	N/A	Interferents from body products detected
Jin <i>et al.</i> , 2021	Gasoline	SBR, PS, PB, SBS	IL spiked onto substrates before direct flame	N/A	Solvent extraction	GCMS	N/A	Proposed substrates chemical composition correlated with

			burning					interference
Nizio <i>et al.</i> , 2016	Gasoline, kerosene, mineral spirits, diesel	N/A	N/A	N/A	N/A	GC x GC-TOFMS	ChromaTOF®	Method of analysis capable of achieve overall peak capacity gain that is ~17% below the system's theoretical maximum
Pandohee <i>et al.</i> , 2020	Gasoline, kerosene, unleaded petrol, methylated spirits, mineral spirit, oil of turpentine, pure turpentine	N/A	N/A	Airtight vials	N/A	2D GC-FID	PCA	ILs categories successfully differentiated
Roberson <i>et al.</i> , 2019	Gasoline, E85 fuel, lighter fluid	Carpet	IL spiked onto substrates before burning	Airtight cans	ACS	GCMS	N/A	Analysis time shorten significantly from 30 min to 3min
Sampat <i>et al.</i> , 2018	White spirit, lamp oil, gasoline	Flooring materials, fabrics, papers	IL spiked onto substrates before	Airtight cans	Anasorb CSC coconut shell charcoal	GC x GC-TOFMS	Binary decision model	89% true positive identification

			burning					
Sandercock, 2016	Gasoline, diesel fuel	Lens cleaning paper	IL spiked onto substrate without burning	Airtight can	ACC	GCMS	N/A	Cheaper alternative extraction adsorbent in comparison to ACS
Swierczynski <i>et al.</i> , 2020	Gasoline	Cotton fabric (cellulose), cardboard (cellulose), carpet (polyethylene-based)	IL spiked onto substrate without burning	Airtight nylon bags	SPME (100µm PDMS)	GCMS	N/A	IL detectable after a week for all substrates
Torres <i>et al.</i> , 2020	Gasoline, diesel	N/A	N/A	N/A	CMV (TRIDION-9)	GCMS (portable and benchtop)	N/A	Method effective in rapid field analysis (~ 5min)
Totten <i>et al.</i> , 2020	Gasoline, charcoal lighter fluid, kerosene, fuel oil, torch fuel, naphtha	Water	N/A	N/A	Hydrophobic pads followed by ACC or ACS	GCMS	N/A	Method of extraction effective in isolating ignitable liquids as low as 10µL
Thurn <i>et al.</i> , 2021	Diesel	ABS, polystyrene	N/A	N/A	N/A	GCMS	Neural network	0.59 true positive rate
Yadav <i>et al.</i> , 2021	Diesel	Cotton cloth, wood, glaze tile, PVC	IL spiked onto	N/A	Solvent extraction	GCMS	N/A	Diethyl ether method of



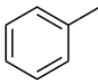
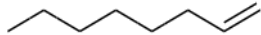
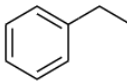

			substrates before direct flame burning for 30s				extraction effective in porous materials
--	--	--	---	--	--	--	--

Chapter 3: Materials & Methods

3.1 Standards

Ignitable liquid standard mixtures were prepared for the optimisation of GCMS procedure. The standard mixture included 1-hexene, toluene, m-xylene, p-xylene, o-xylene, decane, tert-butylbenzene (Sigma-Aldrich), ethylbenzene (Acros Organics), and 1-octene (Alfa Aesar). 50 μ L of each standard was added to a 100mL volumetric flask and filled to mark with pentane (Fishers Scientific). Chemical information of each standard is given in Table 3. Additional aromatic standard was obtained from the EPA 610 polynuclear aromatic hydrocarbons (PAH) mix (Supelco CRM48743). PAH standard chemical information is provided in Table 4.

Table 3 Chemical information of standard mixture

Compound	Structure	Molecular Formula	Molecular Mass (g/mol)	Density (g/cm ³)	Boiling Point (°C)	Elution Order	Purity (%)	Supplier	Cas No.
Pentane		C ₅ H ₁₂	72.15	0.626	35-37	N/A	95.0	Fishers scientific	109-66-0
1-hexene		C ₆ H ₁₂	84.16	0.678	60-66	1	97.0	Sigma-Aldrich	592-41-6
Toluene		C ₇ H ₈	92.14	0.865	110-111	2	99.7	Sigma-Aldrich	108-88-3
1-octene		C ₈ H ₁₆	112.22	0.715	102	3	97.0	Alfa Aesar	111-66-0
Ethylbenzene		C ₈ H ₁₀	106.17	0.860	136	4	99.8	Acros Organics (Janssen Pharmaceutical)	100-41-4
p-xylene		C ₈ H ₁₀	106.17	0.861	138	5	99.0	Sigma-Aldrich	106-42-3
m-xylene		C ₈ H ₁₀	106.17	0.863	138-139	5	99.0	Sigma-Aldrich	108-38-3

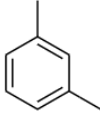
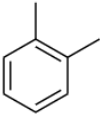
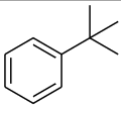

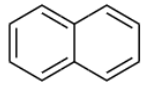
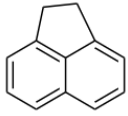
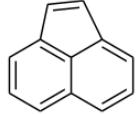
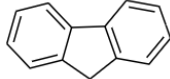
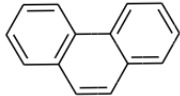
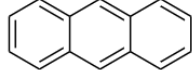
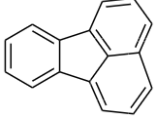
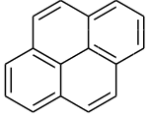
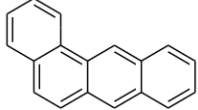
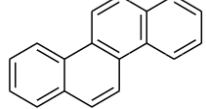
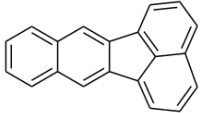
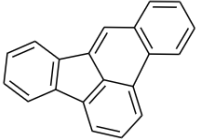
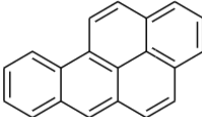
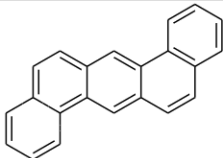
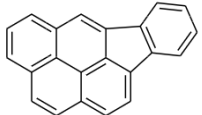
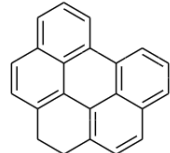
									
o-xylene		C_8H_{10}	106.17	0.879	143-145	6	99.0	Sigma-Aldrich	95-47-6
Tert-butylbenzene		$C_6H_5C(CH_3)_3$	134.22	0.867	169	7	99.0	Sigma-Aldrich	98-06-6
Decane		$C_{10}H_{22}$	142.28	0.730	174	8	99.0	Sigma-Aldrich	124-18-5

Table 4 Polynuclear aromatic hydrocarbons chemical information

Compound	Structure	Concentration ($\mu\text{g/mL}$)	Molecular Formula	Molecular Mass (g/mol)	Boiling Point ($^{\circ}\text{C}$)	Elution Order
Naphthalene		1000	$C_{10}H_8$	128.17	218	1
Acenaphthene		1000	$C_{12}H_{10}$	154.21	279	2
Acenaphthylene		2000	$C_{12}H_8$	152.19	280	3

						
Fluorene		200	$C_{13}H_{10}$	166.22	295	4
Phenanthrene		100	$C_{14}H_{10}$	178.23	340	5
Anthracene		100	$C_{14}H_{10}$	178.23	340	6
Fluoranthene		200	$C_{16}H_{10}$	202.26	375	7
Pyrene		100	$C_{16}H_{10}$	202.25	404	8
Benz[<i>a</i>]anthracene		100	$C_{18}H_{12}$	228.29	438	9
Chrysene		100	$C_{18}H_{12}$	228.28	448	10

Benzo[<i>b</i>]fluoranthene		100	C ₂₀ H ₁₂	252.31	481	11
Benzo[<i>k</i>]fluoranthene		200	C ₂₀ H ₁₂	252.31	480	12
Benzo[<i>a</i>]pyrene		100	C ₂₀ H ₁₂	252.31	495	13
Dibenz[<i>a,h</i>]anthracene		100	C ₂₂ H ₁₄	278.35	524	14
Indeno[1,2,3- <i>cd</i>]]pyrene		100	C ₂₂ H ₁₂	276.3	536	15
Benzo[<i>ghi</i>]perylene		200	C ₂₂ H ₁₂	276.33	550	16

3.2 Optimisation

This section contains the optimisation procedures employed in the study, which involve the construction of the pyrolysis compartment and tilting platform, calibration of the furnace, sample preparation, as well as the optimisation of extraction and instrumental conditions. The experimental approach used is adapted from Sandercock's 2012 recreation of pyrolysis products however in this work all glass reaction vessels were used to permit higher temperatures and deliberately investigate the secondary reaction products created during sustained pyrolysis (Sandercock, 2012).

3.2.1 Pyrolysis Compartment & Tilting Platform

For the initial pyrolysis of samples, an aluminium block measuring 50mm x 62mm x 70mm was utilised. This block had been pre-drilled with seven 8mm x 50mm holes and had a maximum pyrolysis capacity of 600 °C, considering that the melting point of aluminium is 659°C (Ryan, 2018). As an alternative to the aluminium block, a steel block measuring 50mm x 50mm x 115mm was employed. The steel block also had four 8mm x 70mm pre-drilled holes and a higher maximum pyrolysis capacity of up to 1200 °C, considering the melting point of steel is 1371°C (Ryan, 2018). The steel block was deemed preferable between the two options as it allowed for the determination of slow pyrolysis at higher temperatures.

To facilitate the safe removal of pyrolyzed ampoules from the pyrolysis compartment, a tilting platform was constructed, Figure 8. The tilting platform primarily consisted of aluminium profiles measuring 40mm x 40mm (code: 761-3319, RSPRO). A non-ceramic millboard thermal insulating sheet (code: 203-5133, RSPRO) with a withstanding temperature of 1000 °C was used as the insulating layer. Steel and aluminium plates were employed to adjust the height, ensuring that the samples from the steel block could fall into the insulating block

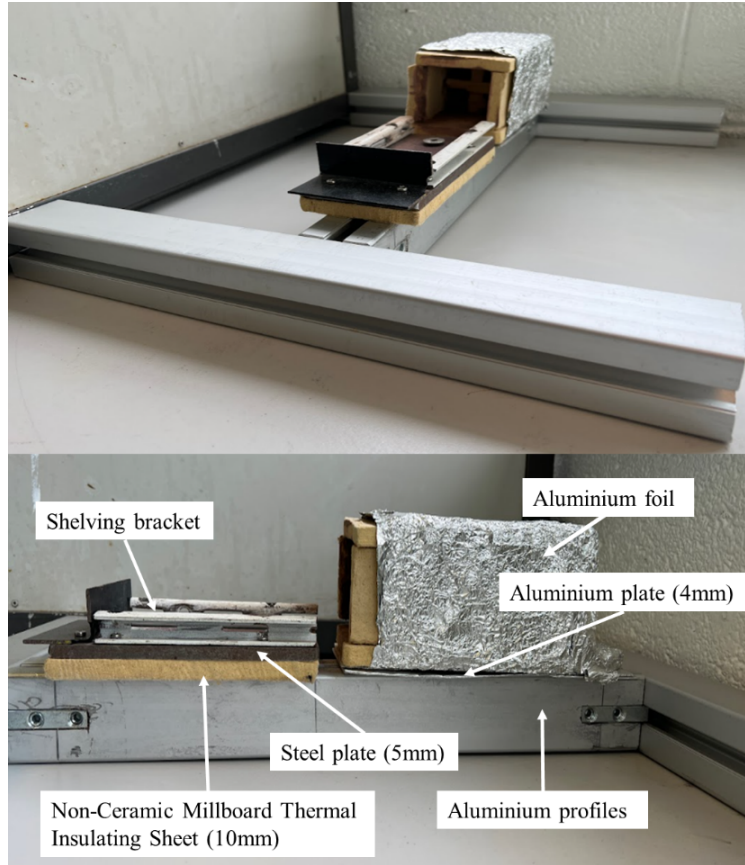


Figure 8 Image of tilting platform

3.2.2 Furnace Calibration

A Phoenix electric muffle furnace (serial no. 97-J-78) was used to pyrolyze all samples in the research. No technical information about the furnace can be found online. As a result, a manual calibration procedure was carried out with a Lascar EL-GFX-DTC temperature data logger (code: 775-1073, RSPRO) equipped with two K-type thermocouples (code: 219-4365, RSPRO). One thermocouple was positioned in the middle of furnace under the heating coil, while the other thermocouple was placed inside the steel block, Figure 9.

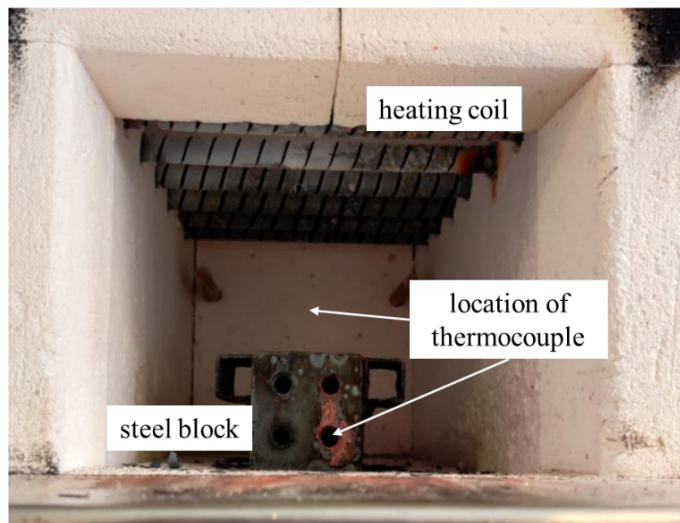


Figure 9 Furnace calibration

3.2.3 Sample Preparation

Sample ampoules were created by sealing the ends of glass tubes after adding the substrate. For the purpose of optimisation, two types of glass tubes were used to prepare the sample ampoules, FisherBrand™ glass pipette (code: 1154-6963) and Schott AG glass tubing (code: SCOR1028407). The glass pipette had an internal diameter of 6mm and a wall thickness of 0.5mm with an average ampoule length of 52mm prepared with the glass pipette, the ampoule average volume was calculated to be 1.47cm³. However, during the initial sample pyrolysis conducted in the aluminium block using the glass pipette ampoules, the process was unsuccessful. The ampoules were unable to withstand the pressure build-up when the temperature increased, resulting in explosion of the ampoule.

As an alternative, sample ampoules prepared with the glass tubing and pyrolyzed in the steel block were used. The glass tubing had an internal diameter of 3.2mm and a wall thickness of 0.9mm. The length of the ampoules prepared with the glass tubing was approximately 60mm to ensure a proper fit into the steel block, with an estimated ampoule volume of around 0.54cm³. To prevent ampoule explosions, the sample size was reduced to 2mg, ensuring an adequate pressure volume.

Polypropylene was chosen as the substrate for the optimisation and initial analysis of the pyrolysis procedure. The polymer possesses a relatively simple chemical structure and is abundantly used in the manufacture of various household items. The chemical structure of polypropylene is illustrated in Figure 10. It has a molecular formula of (C₃H₈)_n, a molecular mass of 44, a density of 0.905 gcm⁻³, a melting point of 160 °C, and a boiling point of 173 °C.

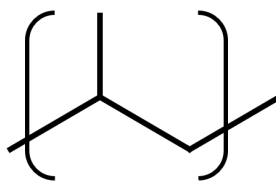


Figure 10 Polypropylene chemical structure

3.2.4 Extraction

As mentioned in the literature review section, the standard extraction method for fire debris analysis involved the use of an Activated Charcoal Strip (ASTM, 2019). However, recent advancements in the field, as reported in multiple studies (Büchler *et al.*, 2021; Carmona *et al.*, 2021; Sandercock, 2016), have introduced a new approach using an activated charcoal as their base of extraction either in pellet or cloth form. Nevertheless, the application of the solid phase microextraction (SPME) procedure has gained significant popularity in fire debris analysis due to its remarkable reduction in analysis time. In addition to the patent expiration, this will lead to the availability of more affordable fibre options for future research in the field. Compared to the conventional ACS extraction method, which typically takes 16 hours, the SPME method can be completed in just 30 minutes. Considering this breakthrough change, the extraction method chosen for this research was SPME.

Fibre Selection

Polydimethylsiloxane (PDMS) fibre is the commonly used SPME adsorbent for fire debris analysis, primarily for extracting non-polar volatile compounds typically found in petroleum-based ignitable liquids. However, they have limitations in extracting polar volatile compounds, such as methanol, ethanol, and acetone (Swierczynski *et al.*, 2020; Aqel *et al.*, 2016). Since petrol and diesel fuel are the major accelerants used in arson cases, PDMS fibres are sufficient for the analysis. However, when experimenting with ignitable liquids from the oxygenated classification, a Carboxen® fibre, based on polyethylene glycol (PEG), may be more effective in extracting the polar volatile compounds from fire debris.

For this analysis, a 100µm PDMS non-bonded assembly SPME fibre was chosen (SUPELCO®). It was used in conjunction with a manual SPME holder (SUPELCO®). Prior to use, the fibre was conditioned according to the instructions provided by SUPELCO®, which involved placing it in a GC injection port set at 250 °C for 30 min.

Heating Apparatus

The literature suggests that the optimal extraction temperature is 70 °C (Torres *et al.*, 2020). In this study, a sand bath was initially used as a temperature control system. However, it was hypothesised that the sand bath might not distribute heat evenly throughout the system, with the area near the heating source being hotter than the area further away. To address this concern, three types of sand bath extraction systems were evaluated to determine the optimal temperature control system for SPME, (1) a sand bath without water on a temperature controlled hot plate (Stuart® SCT1), (2) a sand bath with water on a temperature controlled hot plate, (3) a sand bath with water in an oven. The concept for method 3 was adapted from a previous study by Fettig *et al.*, in which the authors incubated the sample in an oven prior to extraction (Fettig *et al.*, 2013). The experimental setup for assessing the temperature control system is illustrated in Figure 11. Throughout the experiments, the position of the temperature probe remained undisturbed. The thermocouple was placed at three different locations to measure temperature variations within the system (i) near the heating source in a glass pipette, (ii) at the centre of the system in a glass pipette, and (iii) at the centre of the system in a headspace vial.

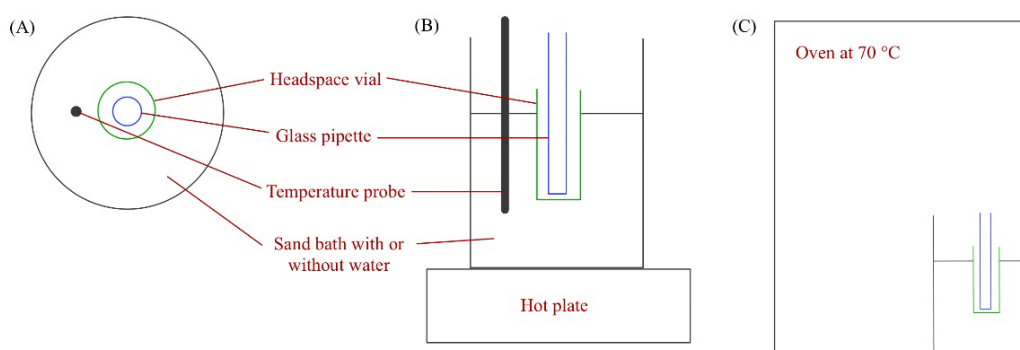


Figure 11 Experimental setup for SPME temperature optimisation (A) aerial view of sand bath, (B) hot plate as heating source with a temperature controller, (C) oven as heating source

Extraction Time

The study used the selected SPME temperature control system, i.e., sand bath with water on temperature controlled hot plate. Three different extraction times were employed for the optimization process, 10, 20, 30 minutes with a PDMS fiber. Samples were pyrolyzed at 400 °C and extracted with SPME fiber according to the test duration. For the GCMS analysis, a DB-1MS (dimethylpolysiloxane) column with a length of 30m, a film thickness of 0.25mm, and an internal diameter of 0.25µm was used as the stationary phase, with helium as the mobile phase. The inlet temperature was set at 250 °C and the flow rate was maintained at 1.2mL/min. It was

temperature programmed as follows: initial temperature of 35°C with a hold time of 2min followed by a ramp at 10 °C/min to 250 °C, and finally hold for 6.5min. The scan mode was set to 50–550m/z. Blank runs were performed between the analyses at 250 °C for 10min.

3.2.5 GCMS

The optimisation conditions used for the analysis are presented in Table 5. To determine the resolution between each standard peak, the retention times and baseline width of each individual peaks were recorded from the Agilent Mass Hunter Qualitative Analysis Software and calculated using the following equation:

$$R_{AB} = \frac{2 \Delta t_r}{w_B + w_A}$$

Equation (2)

R_{AB} is the resolution between two neighbouring peaks, Δt_r is the difference between retention times of components, w_A is the base width of peak A, w_B is the base width of peak B. The ideal resolution value between neighbouring peaks is 2 but may not be possible for all cases, a R_s value of 1.5 will be adequate for separation.

Table 5 GC optimisation conditions

Condition #	Split mode	GC temperature program	MS scan range (m/z)
1	Splitless	1min solvent delay; 35°C for 2min, ramp to 250 °C at 10 °C/min, and hold for 6.5min°C	50-550
2	Splitless	1.5min solvent delay; 35°C for 2min, ramp to 100 °C at 5°C/min, ramp to 150 °C at 10 °C/min, ramp to 250 °C at 20 °C/min	50-550
3	Splitless	2min solvent delay; 35°C for 2min, ramp to 250 °C at 10 °C/min, and hold for 5min°C	50-300
4	Split (100:1)	2min solvent delay; 35°C for 2min, ramp to 250 °C at 10 °C/min, and hold for 5min°C	50-300
5	Split (75:1)	2min solvent delay; 35°C for 2min, ramp to 250 °C at 10 °C/min, and hold for 5min°C	50-300
6	Split (50:1)	2min solvent delay; 35°C for 2min, ramp to 250 °C at 10 °C/min, and hold for 5min°C	50-300

7	Split (20:1)	2min solvent delay; 35°C for 2min, ramp to 250 °C at 10 °C/min, and hold for 5min°C	50-300
---	--------------	---	--------

Various literature sources have reported different mass-to-charge (m/z) ranges for their studies, such as 35-400m/z (Nizio *et al.*, 2018), 40-650m/z (Dutra *et al.*, 2011), 45-200m/z (Falatová *et al.*, 2019), 29-450m/z (Martin-Fabritius *et al.*, 2018), 42-300m/z (Torres *et al.*, 2020), and 30-550m/z (Harries *et al.*, 2021). However, for this specific experimental analysis, the selected m/z range was 50-300m/z. This selection was based on Table 6, which displays the indicative fragments for the relevant ignitable liquids according to the ASTM E1618 (OSAC, 2021) and it was observed that the fragments of interest were predominantly below 200m/z.

Table 6 Indicative fragments for ignitable of interest (Rankin *et al.*, 2014)

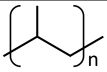
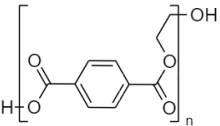
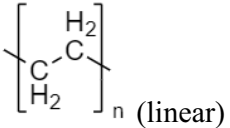
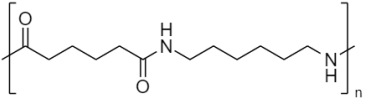
Compound Type	m/z
Alkane	57, 71, 85, 99
Cycloalkane/Alkene	55, 69, 83, 97
Alkylbenzene	91, 92, 105, 106, 119, 120
Indane	117, 118, 131, 132
Naphthalene	128, 142, 156, 170

3.3 Validation of Pyrolysis

The polymers used in this research were from household packaging sources, including polypropylene (PP), high density polyethylene (HDPE), polyethylene terephthalate (PET), sourced from a food container, shampoo container, and water bottle, respectively. Nylon was also investigated, sourced from clothing. Ignitable liquids used in this research were propan-2-one, butan-2-one, pentan-3-one, hexane, and ethyl acetate (Sigma-Aldrich). The chemical information of selected substrates and ignitable liquids are given in Table 7 and Table 8. Substrates were analysed with FTIR to confirm sample identity prior analysis. FTIR spectrum provided in *Appendix 1: FTIR of Selected Substrates*. Sample ampoules, pyrolysis compartment, and GCMS analysis conditions were optimised in *3.2 Optimisation*. Data analysis was conducted using Agilent Mass Hunter Qualitative Analysis Software programs with installed NIST (National Institute of Standards and Technology) search library and AMDIS (Automated Mass Spectral Deconvolution and Identification System). The summed

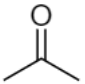
extracted ion profiles consisted of the following categories: alkanes (57m/z), cycloalkanes (55m/z), alkylbenzenes (91+104+105m/z), naphthalenes (128+142+156+170m/z), and indanes (117+118m/z) were analysed. Some examples of target compounds were listed in Table 9 with their indicative m/z as well as PAHs compounds are shown in Table 10.

Table 7 Chemical information of selected substrates

Polymer	Monomer Structure	Molecular Formula	Composition (%)				mm (g/mol)	Density (g/cm ³)	M.P (°C)	B.P (°C)	Pyrolysis Mechanism
			C	H	O	N					
PP		(C ₃ H ₈) _n	81.7	18.3	-	-	44.10	0.905	160	173	RS
PET		(C ₁₂ H ₁₄ O ₄) _n	64.9	6.3	28.8	-	222.24	1.38	260	350	RS
HDPE		(C ₂ H ₄) _n	85.6	14.4	-	-	28.05	0.941	110-130	112	RS
Ny		(C ₁₂ H ₂₂ N ₂ O ₂) _n	63.7	9.8	14.1	12.4	226.32	1.47	250-260	452	RS

RS – random scission; SGC – side group scission

Table 8 Chemical information of selected ignitable liquids

Compound	Structure	Molecular Formula	Composition (%)				mm (g/mol)	Density (g/cm ³)	BP (°C)	Purity (%)
			C	H	O	N				
Propan-2-one		C ₃ H ₆ O	62.0	10.4	27.5	-	58.08	0.791	56.0	99.5

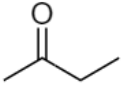
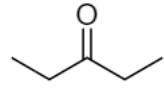
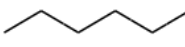
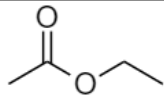
Butan-2-one		C_4H_8O	66.6	11.2	22.2	-	72.11	0.805	80.0	99.0
Pentan-3-one		$C_5H_{10}O$	69.7	11.7	18.6	-	86.13	0.813	101.5	99.0
Hexane		C_6H_{14}	83.6	16.4	-	-	86.18	0.659	69.0	95.0
Ethyl Acetate		$C_4H_8O_2$	54.5	9.2	36.3	-	88.11	0.902	76.5-77.5	99.5

Table 9 Target compounds for the identification of gasoline in fire debris samples provided by ASTM standards E1618 (Contreras et al., 2012)

Target Compounds	Main m/z	Compound Group
Toluene	91,92	C1 alkylbenzene
Ethylbenzene	91,106	C2 alkylbenzene
meta-xylene, para-xylene	91,106	
ortho-xylene	91,106	
Propylbenzene	91,120	C3 alkylbenzene
1-ethyl-3-methylbenzene	105,120	
1-ethyl-4-methylbenzene	105,120	
1,3,5-trimethylbenzene	105,120	
1-ethyl-2-methylbenzene	105,120	
1,2,4-trimethylbenzene	105,120	
1,2,3-trimethylbenzene	105,120	
1,3-diethylbenzene	105,119,134	
1-methyl-3-propylbenzene	105,134	
1,4-diethylbenzene	91,105,119,132	
4-ethyl-1,3-dimethylbenzene	119,134	
4-ethyl-1,2-dimethylbenzene	119,134	
2-ethyl-1,3-dimethylbenzene	119,134	
1,2,3,4-tetromethylbenzene	119,134	
1,2,3,5-tetramethylbenzene	119,134	
Indane	115,117,118	indane
Naphthalene	128	C0 naphthalene
2-methylnaphthalene	115,141,142	C1 naphthalene
1-methylnaphthalene	115,141,142	

Table 10 PAHs compounds major m/z and compound group

PAHs	Main m/z	Compound Group
Acenaphthylene	152	
Biphenylene	152	
Acenaphthene	152,153,154	

Fluorene	165,166	2-aromatic rings
Chamazulene	169,184	
Phenanthrene	178	3-aromatic rings
Anthracene	178	
Fluoranthene	202	4-aromatic rings
Pyrene	202	
Benz[a]anthracene	228	
Triphenylene	228	

3.3.1 Experimental Simulation

Experimental pyrolysis was conducted in an oxygen free environment. The steel block was preheated to the desired temperature in the muffle furnace with a thermocouple measuring the internal temperature of the steel block. Sample ampoules were pyrolyzed inside the heated steel block and dwell time was measured using a timer. The steel block was removed from the muffle furnace and transferred onto a tilting platform. The pyrolyzed sample ampoules were removed from the steel block and allowed to cool in a non-ceramic millboard thermal insulating container.

Cooled pyrolyzed sample ampoules were scored using a glass cutter approximately halfway along the ampoule and opened by cracking in half with a layer of tissue wrapping the scored ampoule. The ampoule was placed into a headspace vial immediately and sealed with a crimped cap. The vial was heated to 70°C in a water-sand bath on a Stuart temperature controller. A separated headspace vial with a thermometer inserted was used to monitor the extraction temperature. The SPME PDMS fibre was inserted and extracted the volatile compounds for 30 min. The SPME fibre was withdrawn and inserted into the GC-MS for analysis.

3.3.2 Real World Simulation

Real world simulation was conducted under two pyrolysis methods. The first method involved pyrolyzing a sample that was placed on a sand surface and covered with a 2mm thick steel plate. The sample was heated with a propane torch until a temperature of >600°C was reached. A layer of aluminium foil was used to cover the sand bath to retain the heat until the sample

cooled to $<50^{\circ}\text{C}$. The remaining debris was collected into a headspace vial and sealed. The headspace sample was collected using a PDMS fibre as described previously and analysed by GCMS.

The second method was through direct flame burning of a sample that was placed on a sand bath for 1min, subsequently a layer of sand was added onto the burned sample followed by 1min pyrolysis with a torch gun. The pyrolyzed sample was covered with a clock glass until the surface temperature reached $<50^{\circ}\text{C}$. The debris was collected into a headspace vial and sealed for SPME-GCMS analysis.

3.4 Slow Pyrolysis Profiles

3.4.1 Preparation of Samples

The selected substrates for pyrolysis were polypropylene (PP), polyethylene terephthalate (PET), polyethylene (PE), polystyrene (PS), polyester (PER), and nylon (Ny). The chemical information of substrates is given in Table 11. The selected flammable liquids include hexane, acetone, butan-2-one, 3-pentanone, ethyl acetate, and isopropanol. The chemical information of selected flammable liquids is given in Table 12. Three temperatures were selected to initially generate the library, 20°C (room temperature), 300°C , and 550°C . The 300°C and 550°C pyrolysis were carried out in the same manner described in 3.3.1 *Experimental Simulation*. The internal standard (IS) solution prepared for the quantitative analysis was 0.03M 2-nitrobenzaldehyde in dichloromethane. $1\mu\text{L}$ of IS solution was injected into the headspace vial with sample and immediately sealed with a crimped cap. Each sample type was subjected to three replicates of measurements, except for NyA550, PERA550, and PPMEK550 due to malfunction of the furnace. A total of 126 samples were generated.

3.4.2 Instrumental & Data Analysis

The pyrolyzed samples were subjected to GCMS analysis under conditions described in 4.1.5 *Optimised Analysis Method*. The GCMS peaks in each chromatogram were identified using the NIST library with the AMDIS software. The data analysis consisted of normalisation of chromatograms and classification of peaks using principal component analysis (PCA). Normalisation of chromatograms was conducted prior to performing calculations. The normalisation process comprised of two stages, internal standard normalisation, and total area normalisation. The aim of the internal standard normalisation was to ensure that there was the same order of magnitude for the highest peak in all chromatograms of the data set. The total area normalisation aimed to reduce variability among replicates arising from differences in

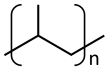
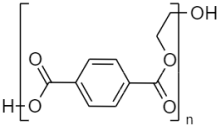
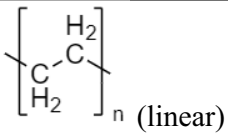
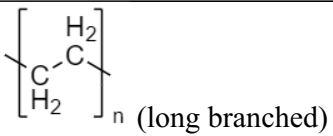
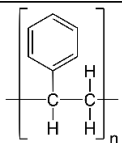
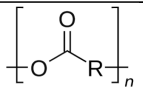
injection volume. The similarities and differences among samples were graphically represented in the form of scores plot using PCA.

To achieve internal standard normalisation, the peak area at each retention time (PA_i) was initially divided by the peak area of the internal standard (PA_{IS}) present in the corresponding chromatogram. For total area normalisation, the peak area of each chromatogram in the data set was summed and the average area of all chromatograms was calculated. Lastly, the peak area at each retention time was divided by the area of the respective chromatogram and multiplied by the average area of all chromatograms, general equation given in Equation (3). All normalisation calculations were carried out using Microsoft Excel.

Equation (3)

The normalised data were subjected to PCA analysis in both Microsoft Excel and RStudio. The code for PCA analysis in RStudio attached in Appendix 2: RStudios Code for PCA.

Table 11 Chemical information of selected substrates

Polymer	Monomer Structure	Molecular Formula	Composition (%)				MM (g/mol)	Density (g/cm ³)	M.P (°C)	B.P (°C)	Pyrolysis Mechanism
			C	H	O	N					
PP		(C ₃ H ₈) _n	81.7	18.3	-	-	44.10	0.905	160	173	RS
PET		(C ₁₂ H ₁₄ O ₄) _n	64.9	6.3	28.8	-	222.24	1.38	260	350	RS
HDPE		(C ₂ H ₄) _n	85.6	14.4	-	-	28.05	0.941	110-130	112	RS
LDPE		(C ₂ H ₄) _n	85.6	14.4	-	-	28.05	0.925	106-112	170-200	RS
PS		(C ₈ H ₈) _n	92.3	7.7	-	-	104.15	0.96	210-249	430	SGC
PER		(C ₂ H ₂ O ₂) _n	41.4	3.5	55.1	-	58.04	1.20	295	350	RS

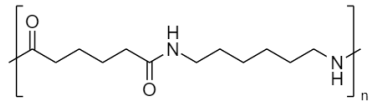
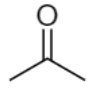
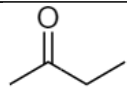
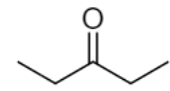
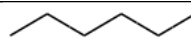
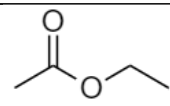
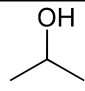
Ny		(C ₁₂ H ₂₂ N ₂ O ₂) n	63.7	9.8	14.1	12.4	226.32	1.47	250- 260	452	RS
----	---	---	------	-----	------	------	--------	------	-------------	-----	----

Table 12 Chemical information of selected flammable liquids

Compound	Structure	Molecular Formula	Composition (%)				MM (g/mol)	Density (g/cm ³)	BP (°C)	Purity (%)
			C	H	O	N				
Propan-2-one		C ₃ H ₆ O	62.0	10.4	27.5	-	58.08	0.791	56.0	99.5
Butan-2-one		C ₄ H ₈ O	66.6	11.2	22.2	-	72.11	0.805	80.0	99.0
Pentan-3-one		C ₅ H ₁₀ O	69.7	11.7	18.6	-	86.13	0.813	101.5	99.0
Hexane		C ₆ H ₁₄	83.6	16.4	-	-	86.18	0.659	69.0	95.0
Ethyl Acetate		C ₄ H ₈ O ₂	54.5	9.2	36.3	-	88.11	0.902	76.5-77.5	99.5
Isopropanol		C ₃ H ₈ O	60.0	13.4	26.6	-	60.10	0.786	82.5	99.5

Chapter 4: Results & Discussion

4.1 Optimisation

4.1.1 Furnace Calibration

The furnace temperature was systematically set to 300, 450, 500, and 850 °C for the calibration process. The obtained results were recorded in Table 7 and depicted in Figure 12. The calibration equation derived from this analysis was $y = 0.9527x + 5.8446$, with a R^2 value of 0.9986. The y represents the furnace temperature setting required for sample pyrolysis and x represents the furnace temperature setting. The specific values for different sample pyrolysis conditions can be found in Table 8.

Table 7 Furnace calibration

Furnace temperature (°C)	Measured furnace temperature (°C)	Measured temperature inside steel block (°C)
300	321.7 ± 22.4	301.0 ± 7.0
450	385.0 ± 12.9	425.7 ± 1.0
500	561.2 ± 37.7	477.6 ± 8.1
850	813.3 ± 15.6	819.7 ± 1.0

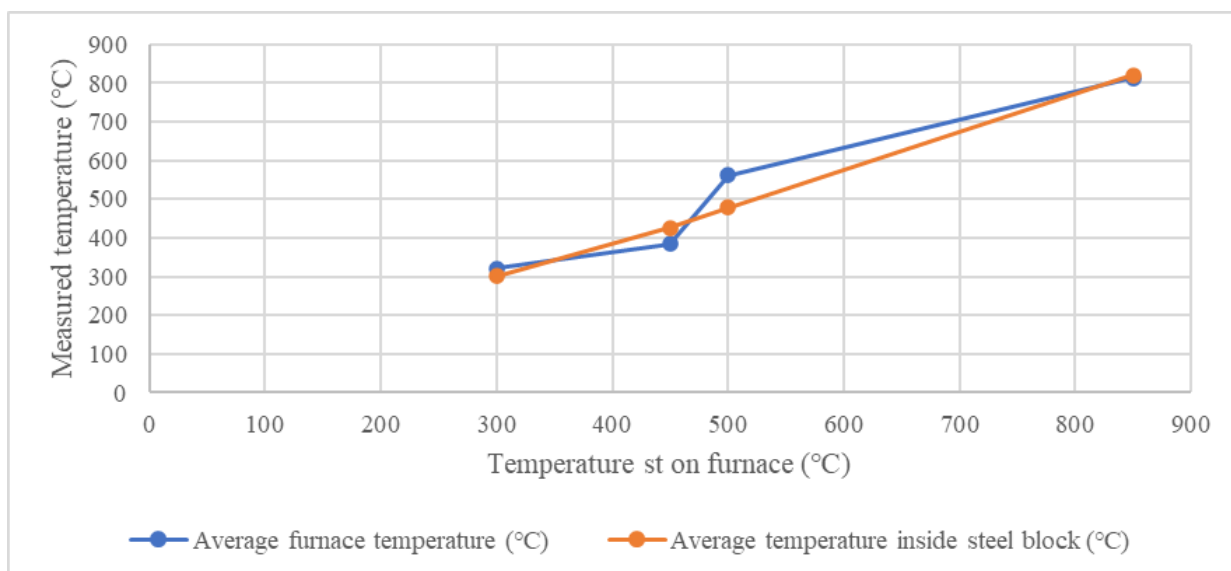


Figure 12 Graph of furnace calibration

Table 8 Temperature setting for sample pyrolysis

Experimental temperature required (°C)	300	400	500	550	600	700	800
Furnace temperature setting calculated from equation of line (°C)	308.8	413.7	518.7	571.2	623.7	728.6	833.6
Actual furnace temperature setting for sample pyrolysis (°C)	309	414	519	571	623	729	834

4.1.2 Heating Apparatus

The temperature measurement data were given in Table 8 sand bath only, Table 9 sand bath with water, Table 10 in an oven. The temperature measurements near the hot plate, as shown in Figure 13(1.1), exhibited the highest temperature variation over a 10-min period, ranging from 61.3°C to 84.2°C, with a standard deviation of 10.86°C. Similarly, the temperature measurements near the heating source with water in the sand bath, depicted in Figure 13(2.1), also displayed significant temperature variations. The temperature difference during the 10-minute interval ranged from 25.2°C to 26.7°C, with a standard deviation of 3.34°C. To test the hypothesis, temperature measurements were taken at the centre of the heating system Figure 13(1.2 and 2.2). Without water, the temperature difference ranged from -7.1°C to 5.7°C, with a standard deviation of 5.71°C. With water in the sand bath, the temperature difference ranged from 6.6°C to 8.3°C and the standard deviation was 0.73. The smaller standard deviation indicated that adding water to the sand bath improved temperature stability during the extraction process.

To simulate the extraction conditions and determine the actual temperature experienced by the samples, the temperature was measured at the centre of the sand bath using a headspace vial Figure 13(1.3 and 2.3). In the sand bath alone (1.3), the temperature difference ranged from -12°C to 3.7°C, with a standard deviation of 7.31°C, while in the sand bath with water (2.3), the temperature difference ranged from -2.4°C to 3.1°C, with a smaller standard deviation of 2.25°C. These results further support the hypothesis that the sand bath does not provide consistent temperature distribution, but the addition of water improves heat transfer consistency.

Extraction temperature in sand bath with water incubated in an oven was evaluated Figure 13 (3). This method exhibited the smallest temperature differences, ranging from 0.7°C to 1.0 °C,

with a standard deviation of 0.13°C. However, the practicality of this method could not be achieved due to the separated location of the oven and the GCMS.

Table 8 Temperatures measured with temperature probe and thermocouple in sand bath at different positions

Time (min)	1	2	5	10
Position of thermocouple	Near heating source			
Temperature on probe (°C)	78	80	83	81
Temperature on thermocouple (°C)	139.8	145.2	167.2	142.3
Differences in temperature (°C)	61.8	65.2	84.2	61.3
Standard deviation (°C)	10.86			
Position of thermocouple	Centre of system			
Temperature on probe (°C)	78	77	74	70
Temperature on thermocouple (°C)	70.9	72.9	75.5	75.7
Differences in temperature (°C)	-7.1	-4.1	1.5	5.7
Standard deviation (°C)	5.71			
Position of thermocouple	Centre of system inside a headspace vial			
Temperature on probe (°C)	69	69	70	74
Temperature on thermocouple (°C)	57	65.6	73.1	77.7
Differences in temperature (°C)	-12	-3.4	3.1	3.7
Standard deviation (°C)	7.31			

Table 9 Temperatures measured with temperature probe and thermocouple in sand bath with water at different positions

Time (min)	1	2	5	10
Position of thermocouple	Near heating source			
Temperature on probe (°C)	73	72	71	71
Temperature on thermocouple (°C)	99.7	97.7	96.2	90.3
Differences in temperature (°C)	26.7	25.7	25.2	19.3
Standard deviation (°C)	3.34			
Position of thermocouple	Centre of system			
Temperature on probe (°C)	70	70	70	69
Temperature on thermocouple (°C)	76.6	77.1	77.6	77.3
Differences in temperature (°C)	6.6	7.1	7.6	8.3
Standard deviation (°C)	0.73			
Position of thermocouple	Centre of system inside a headspace vial			
Temperature on probe (°C)	70	70	72	70

Temperature on thermocouple (°C)	67.6	70.7	72.7	73.1
Differences in temperature (°C)	-2.4	0.7	0.7	3.1
Standard deviation (°C)	2.25			

Table 10 Temperature measured in an oven

Time (min)	1	2	5	10
Position of thermocouple	Centre of system			
Oven temperature (°C)	70	70	70	70
Temperature on thermocouple (°C)	69	69.1	69.2	69.3
Differences in temperature (°C)	1	0.9	0.8	0.7
Standard deviation (°C)	0.13			

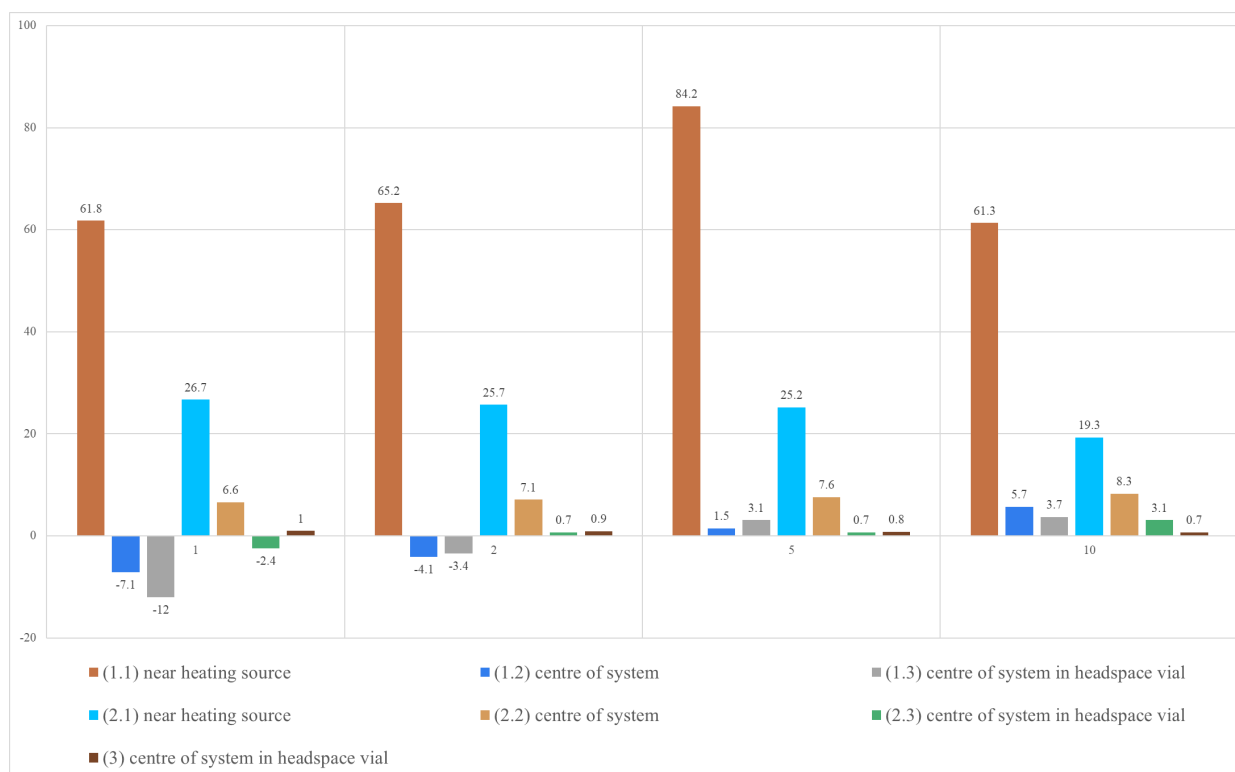


Figure 13 Temperature differences between temperature probe and thermocouple in (1) sand bath, (2) sand bath with water at different position, and (3) in oven

4.1.3 Extraction Time

Based on the results depicted in Figure 14, all tested extraction times were effective in extraction of target compounds above the limit of detection for GCMS analysis. The optimal extraction time was determined to be 30 min. This extraction duration yielded the highest peak

area for all major compounds in the chromatograms. Therefore, a 30 min extraction time was selected for the further analyses.

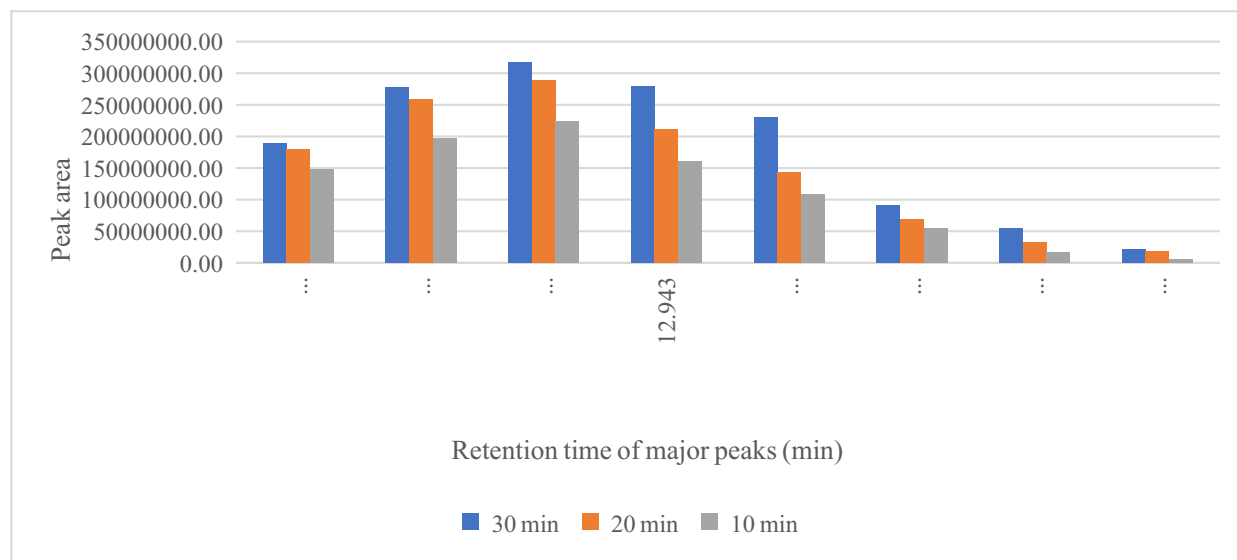


Figure 14 The effect of time on the extraction of volatile compounds

4.1.4 GCMS

The chromatograms and results obtained were recorded in Table 11 and Table 12. Resolution values highlighted in blue were found to be less than 1.5, indicating that the neighbouring peaks were not fully separated. By comparing the resolution values and visually examining the chromatograms, condition 7 was identified as the optimal GC condition for analysing the pyrolyzed samples. Although the resolution between peaks 4 and 5 had a R_s value of 0.923, indicating some overlap, it was considered acceptable for further analysis since two distinct peaks could be distinguished from the chromatogram. EPA 610 PAH mixture was separated under condition 7. Table 13 shows the mixtures had some overlap between neighbouring peaks but two distinct peaks could be distinguished from the chromatogram, Figure 15.

Table 11 GC optimisation conditions

Condition #	Chromatogram
1	
2	

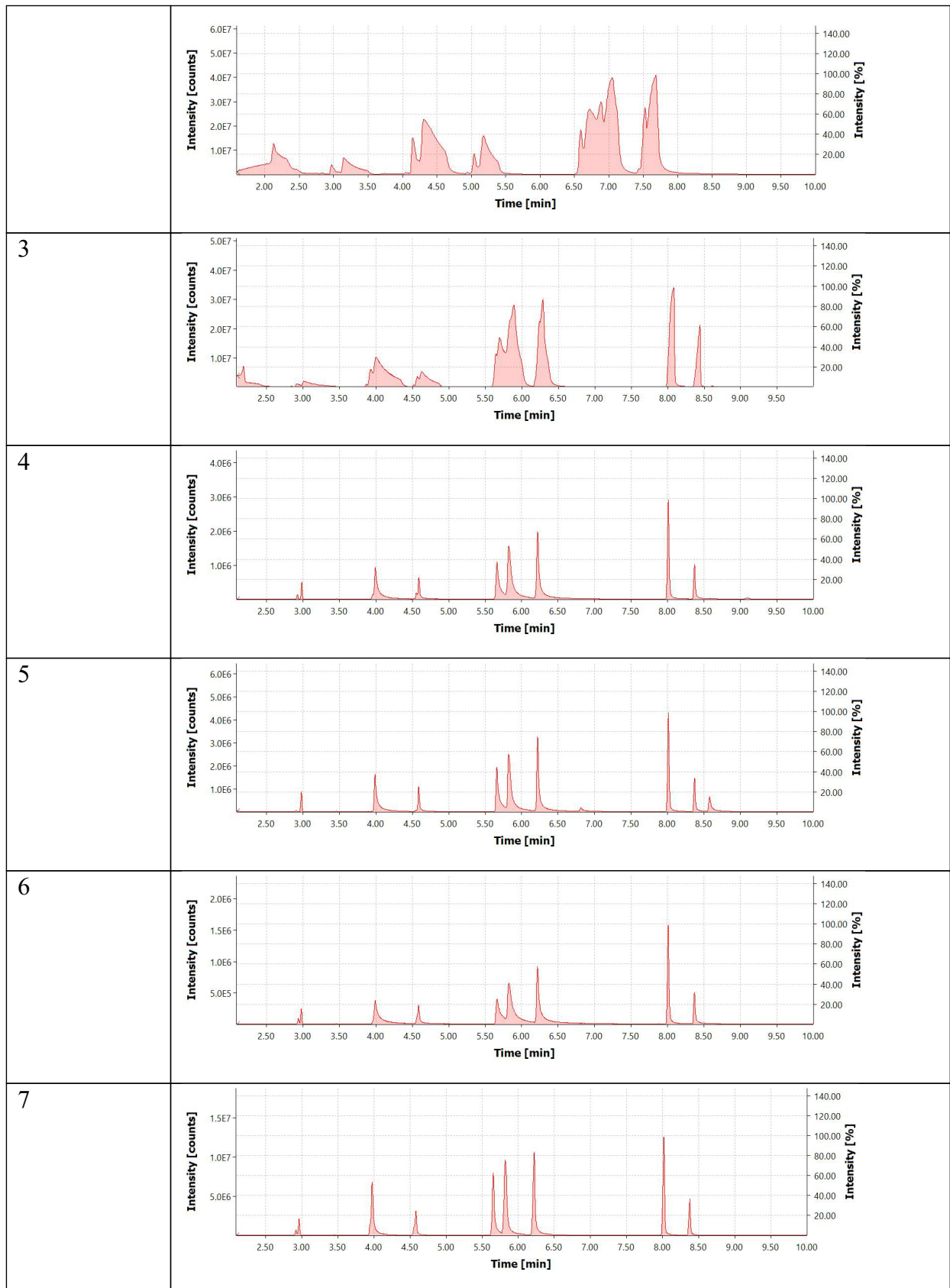


Table 12 Peak resolution using standard mixture solution

Peak numbers	1,2	2,3	3,4	4,5	5,6	6,7	7,8
Condition 1	3.49	1.21	3.48	1.28	0.95	5.03	1.82

Condition 2	2.12	1.35	4.01	0.99	1.58	8.09	2.12
Condition 3	3.58	1.40	4.28	0.81	1.35	9.33	2.13
Condition 4	6.05	3.57	8.45	0.74	1.88	12.37	2.92
Condition 5	7.25	4.22	8.25	0.81	2.13	14.01	3.03
Condition 6	5.60	2.76	7.80	0.90	2.05	12.56	2.93
Condition 7	7.60	3.92	7.00	0.92	2.32	12.65	2.75

Table 13 Peak resolution using PAHs standard

Peak numbers	1,2	2,3	3,4	4,5	5,6	6,7	7,8	8,9	9,10
Resolution	3.25	0.61	1.54	4.84	0.30	4.64	1.11	9.16	0.25

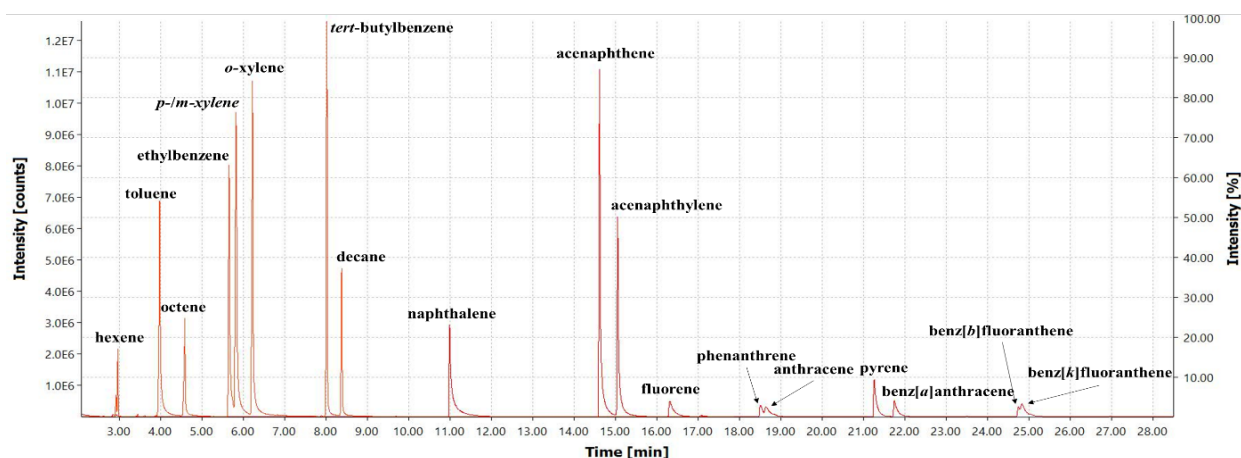


Figure 15 Reference standard separation under condition 7

4.1.5 Optimised Analysis Method

Sample pyrolyse in a steel block under preset temperature and time. Score the ampoule at halfway point with a glass cutter. Break the ampoule in half and transfer into a headspace vial, immediately crimp the lid to minimise escape of gaseous compounds. Extract with PDMS fibre for 30 min at 70 °C in a water-sand bath. Analyse with GCMS equipped with DB-1MS column in 30 m length, 0.25 mm film thickness, 0.25 µm internal diameter, helium mobile phase at 1.2 mL/min. The injection temperature set at 250 °C and oven temperature programmed as follows: initial temperature of 35 °C with a hold time of 2 min followed by a ramp at 10 °C/min to 250 °C and finally hold for 5 min. The scan mode set to 50-300 m/z. Split ratio of 20:1 for experimental simulation samples and split-less setting for real world simulation samples. SPME fibre was cleaned between analysis by exposing the PDMS fibre in the injector at 250 °C

for 10 min.

4.2 Validation of Pyrolysis

This section consists of the qualitative analysis with the aims to determine the effect of time, temperature, and presence of ignitable liquids on the pyrolysis of substrates.

4.2.1 Time Variation Analysis

To explore the effect of time on the pyrolysis of polymer, an initial experiment was conducted using polypropylene (PP). The PP samples were subjected to pyrolysis at a temperature of 500 °C for various durations: 1, 5, 10, 15, and 30 min. The pyrolysis process took place in a heated steel block to simulate oxygen-free thermal degradation. The temperature of 500 °C was chosen as it falls within the typical range for pyrolysis, allowing the determination of optimal duration for conducting experimental pyrolysis. The objective was to observe the appearance of aromatic compounds in the chromatograms derived from the polymer substrate at temperatures commonly associated with pyrolysis. Additionally, the pyrolysis of acetone and its introduction to the PP substrate were investigated to evaluate the influence of an external source of flammable liquid on the pyrolysis profile.

Figure 16 presents the results of the time variation analysis of pyrolysis in the form of a heatmap. Alkane and cycloalkane/alkene products were predominant in the 1-15min pyrolysis samples, while alkylbenzenes and naphthalene dominated the 30 min pyrolysis samples. The addition of acetone to the PP substrate accelerated the formation of alkylbenzene, as seen in the 15min pyrolysis sample.

Figure 17 presents the total ion chromatograms (TICs) of PP subjected to pyrolysis at 500 °C for different durations. Figure 17 (a) to (d) show pyrolyzed fragments consisting solely of alkanes, cycloalkanes/alkenes, with no presence of aromatics. Aromatic fragments are only observed in Figure 17 (e), corresponding to a 30 min pyrolysis duration, where C1-C5 alkylbenzenes, C2-C3 styrenes, C0-C3 naphthalene, and C1 indanes are detected.

Figure 18 displays the TICs of PP pyrolyzed at 500 °C for various durations in the presence of acetone. Pyrolysis durations of 1-10min primarily produced C7-C19 alkanes, cycloalkanes/alkenes, with no aromatic products. A 15min pyrolysis yielded C1-C3 alkylbenzenes, carboxylic acids, and alcohols products. The longest pyrolysis duration of 30 min, with the addition of acetone to the PP substrate, resulted in the highest production of aromatic products, including C0-C5 alkylbenzenes, C0-C3 naphthalene, as well as aldehydes,

ketones, and alcohols.

Figure 19 illustrates the TICs of acetone subjected to pyrolysis at 500 °C for different durations. The pyrolysis of acetone produced isophorone as the major product in 1, 5, 10, and 15min durations, while 2,4-dimethyl-2-pentene was the sole aldol product observed in the 30 min pyrolysis. Pyrolysis products in the alkyne group were observed in durations of 1-15min, with substituted alkanes and alcohols present only in the 1 min pyrolysis samples, and aldehyde only detected in the 15min pyrolysis samples. A 30 min pyrolysis yielded target compounds listed in the ASTM E1618, including C0-C4 alkylbenzene and naphthalene, along with other products from carboxylic acids, alcohols, and ketones. The presence of aldehyde, ketone, and alcohol in the products can be attributed to the presence of acetone.

The results from the time variation study demonstrated the 30 min pyrolysis duration significantly influenced the product distribution of PP, resulting in a product matrix resembling profiles found in gasoline or diesel. Thus, the 30 min pyrolysis duration was selected for further analysis. The introduction of acetone as an external source of flammable liquid further impacted the pyrolysis profile, promoting the formation of products from other functional groups. These findings provide valuable insights into the pyrolysis behaviour of polymer materials and can contribute to the development of a reference library that aids in the identification of matrix backgrounds that may have been misinterpreted as ignitable liquids.

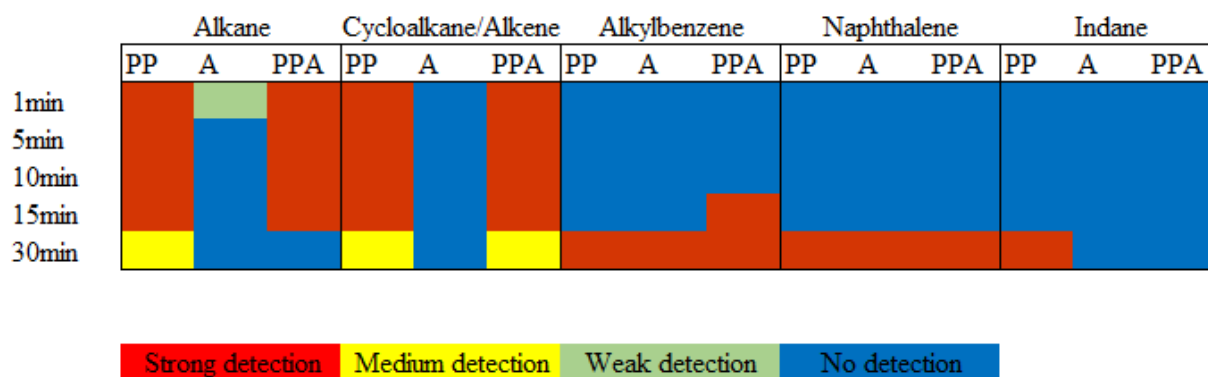


Figure 16 Heatmap comparison of pyrolysis results for time variation

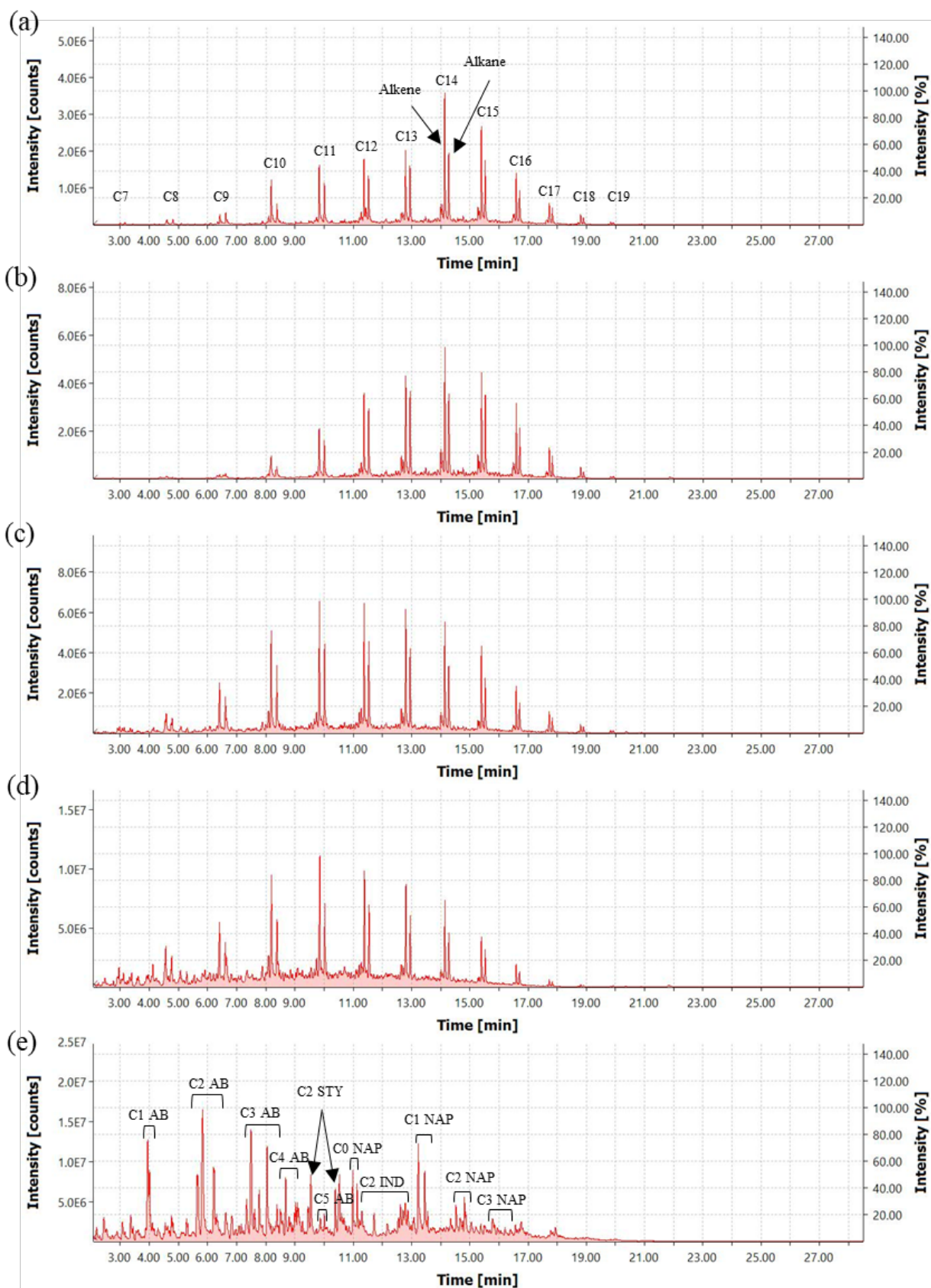


Figure 17 Chromatograms from time variation analysis on PP only - (a) 1min, (b) 5min, (c) 10min, (d) 15min, and (e) 30 min [AB - alkylbenzene; STY - styrene; NAP - naphthalene; IND - indane]

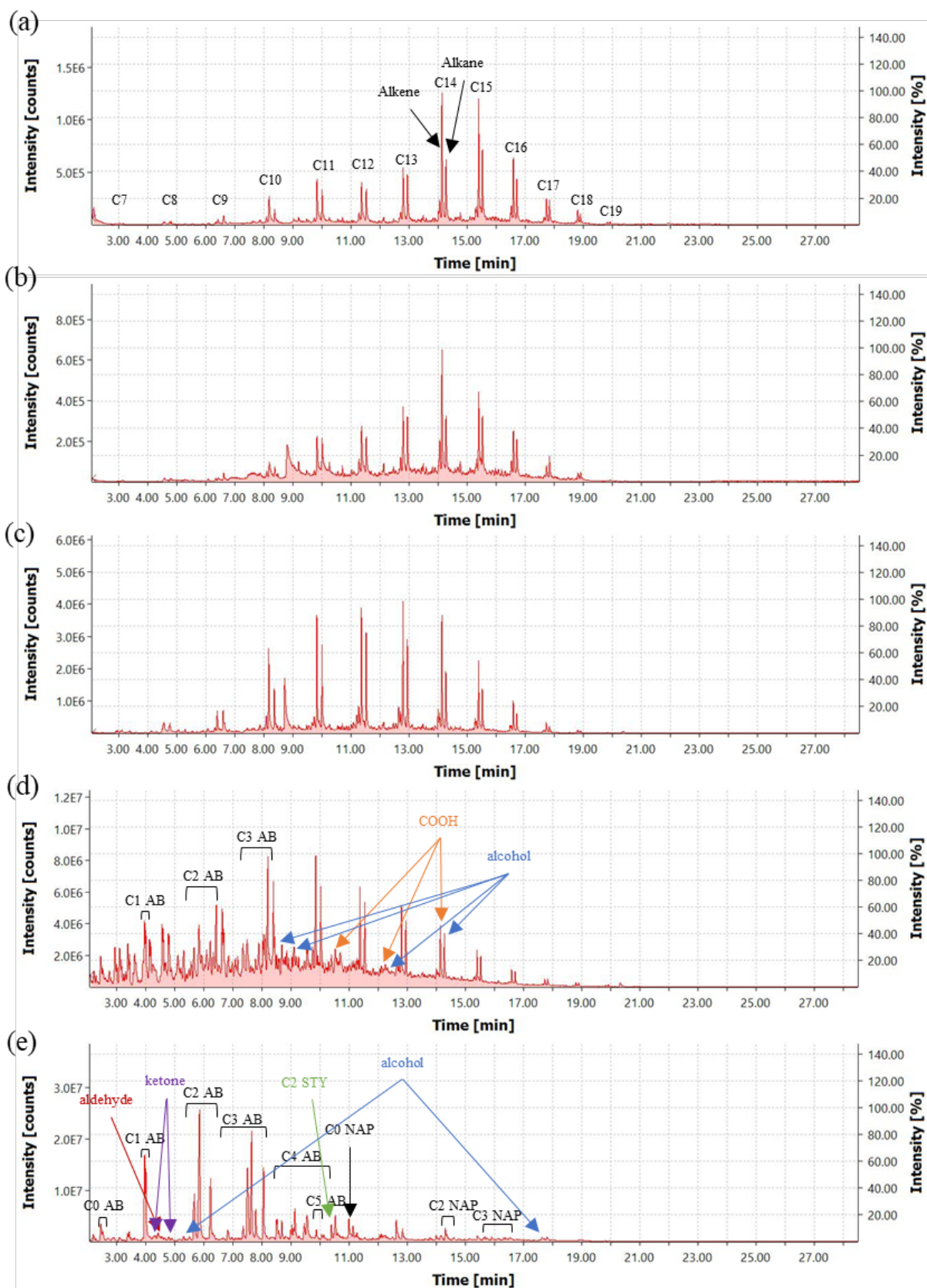


Figure 18 Chromatograms from time variation analysis on PP with the presence of acetone - (a) 1min, (b) 5min, (c) 10min, (d) 15min, and (e) 30 min [AB - alkylbenzene; STY - styrene; NAP - naphthalene; IND - indane; COOH - carboxylic acid]

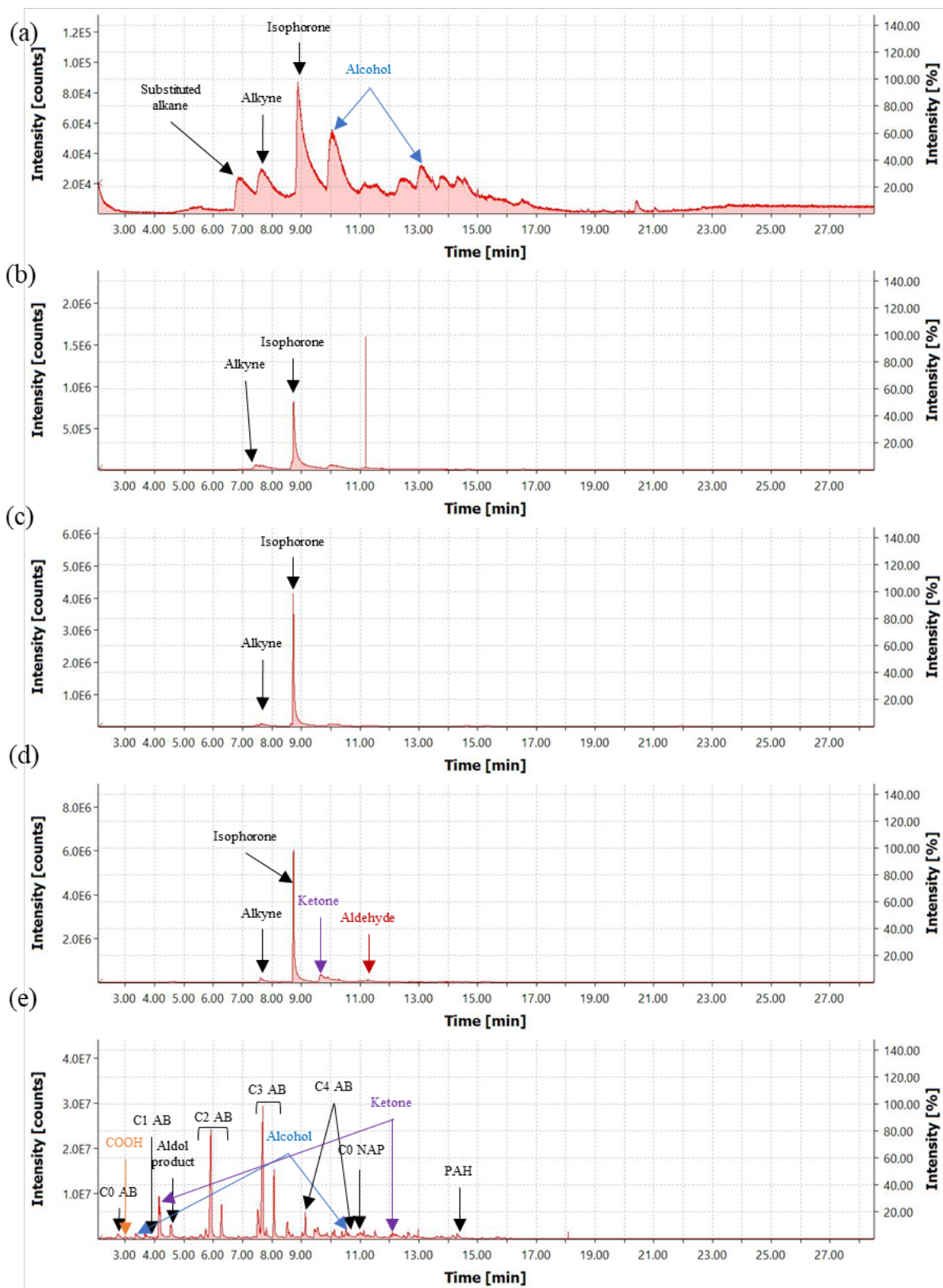


Figure 19 Chromatograms from time variation analysis on acetone - (a) 1min, (b) 5min, (c) 10min, (d) 15min, and (e) 30 min [AB - alkybenzene; NAP - naphthalene; COOH - carboxylic acid; PAH – polyaromatic hydrocarbon]

4.2.2 Pyrolysis Temperature Analysis

Many literature studies have examined the effect of pyrolysis temperature on the degradation products of common polymers and concluded that the temperature of pyrolysis has a significant influence (Nisar *et al.*, 2022; Zafar, 2021; Esmizadeh *et al.*, 2020; Das *et al.*, 2018; Huang *et al.*, 2017; Ahmad *et al.*, 2014; Lee *et al.*, 2007). It had been observed that temperatures below 450 °C result in solid products, while temperatures exceeding 800 °C lead to gas products (Nisar *et al.*, 2022; Zafar, 2021). During the flashover phase of a compartment fire, when the room is filled with hot smoke, pyrolysis of materials present in the room occur as the temperature reaches approximately 600 °C. In the fully developed phase, the temperature inside the compartment can rise to 800-1000 °C (Janssens, 2012).

To investigate the influence of pyrolysis temperature on the formation of various cracking products of PP, a temperature range of 300-600 °C was chosen. This range was selected due to constraints associated with the preparation of sample ampoules of pyrolysis. As the temperature increases, the pressure inside the glass ampoule also increases, leading to the risk of ampoule rupture during pyrolysis and preventing the generation of oxygen-free thermal degradation products.

Figure 20 illustrates the outcomes of the temperature variation study on pyrolysis. The detection of alkane and cycloalkane/alkene products decreased as the pyrolysis temperature increased. Conversely, the detection of alkylbenzene and naphthalene products showed an upward trend with increased temperature. Notably, when acetone was present within the temperature range of 300-500 °C, the detection of alkane and cycloalkane/alkene products was reduced. This observation suggests that the production of aldol products masked the typical alkane and cycloalkane/alkene products originating from the substrate itself. It implies that the presence of an external flammable liquid can influence the detection of the substrate type but not the presence of the flammable liquid itself.

Figure 21 presents the TICs of PP subjected to pyrolysis at 300, 400, 500, 550, and 600 °C for 30 min. Aromatic products were observed at pyrolysis temperatures >500 °C. In Figure 21(c), the detected aromatics included C1-C5 alkylbenzene, C2-C3 styrene, C0-C3 naphthalene, and C1 indanes. At 550 °C, the detected aromatics encompassed C0-C4 alkylbenzenes, C0-C1 indene, C0-C2 naphthalene, as well as polyaromatic hydrocarbons such as acenaphthene, acenaphthylene, fluorene, 2-methyl-9H-fluorene, and phenanthrene. Likewise, at 600 °C, the detected aromatics consisted of C0-C3 alkylbenzene, C0-C1 indene, C0-C2 naphthalene, along with the same polyaromatic hydrocarbons observed at 550 °C.

Figure 22 depicts the TICs of PP subjected to pyrolysis at 300-600 °C in the presence of acetone. A prominent aldol product, 4-methyl-3-penten-2-one, was detected in the 300-400 °C pyrolysis samples. This aldol product masked the extraction and detection of other compounds derived from the pyrolysis of substrate matrix at 300 °C. At 400 °C, a C3 alkylbenzene product was detected, suggesting that the presence of an external flammable liquid or an oxygenated component can enhance the degradation and production of aromatic compounds. At a pyrolysis temperature of 500 °C, various products from functional groups such as aldehydes, ketones, and alcohols were observed, which were attributed to the presence of acetone. Similarly, the pyrolysis products from the alcohol group were observed at 550 °C, but their occurrence significantly decreased as the temperature was raised to 600 °C, where only hydrocarbon products were observed.

Figure 23 illustrates the TICs of acetone subjected to pyrolysis at temperatures ranging from 300 to 600 °C for 30 min. In the 300-400 °C pyrolysis range, the presence of strong signals corresponding to aldol products was observed. A C3 alkylbenzene was detected in the 400 °C pyrolysis sample. Increasing the pyrolysis temperature to 500 °C revealed the presence of functional groups such as carboxylic acids, alcohols, and ketones. On the other hand, the alcohol functional group was the only one observed in addition to hydrocarbons at 550 °C. No detection of alkylbenzenes or other functional groups, except for polyaromatic hydrocarbons comprising C0-C2 naphthalene, substituted biphenyl, and phenanthrene was observed at 600 °C.

These findings offered valuable understanding of polymer pyrolysis behaviour and highlights the significance of accounting for temperature variations when examining the generation of degradation products. Understanding the thermal degradation pathways can potentially facilitate the establishment of comprehensive databases for identifying and distinguishing substrate characteristics and external flammable liquids. Such resources would aid forensic investigations in fire incidents. The pyrolysis temperature of 550 °C was selected for further analysis in this study.

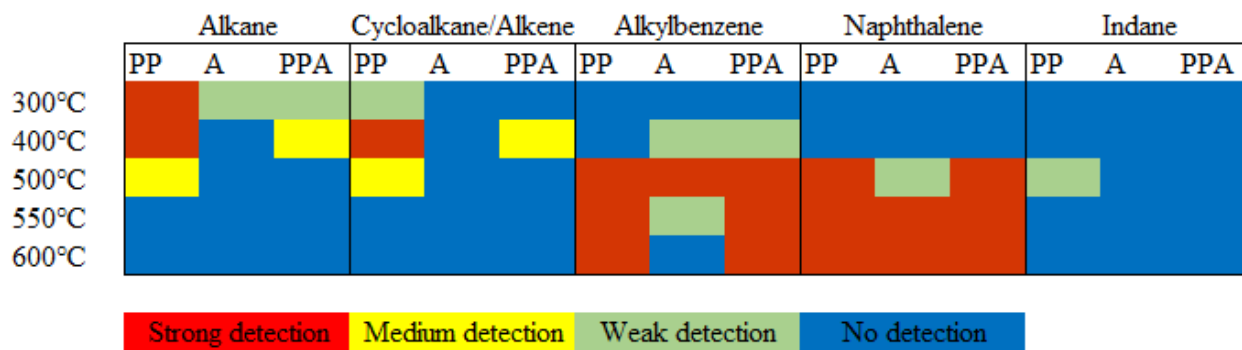


Figure 20 Heatmap comparison of pyrolysis results for temperature variation

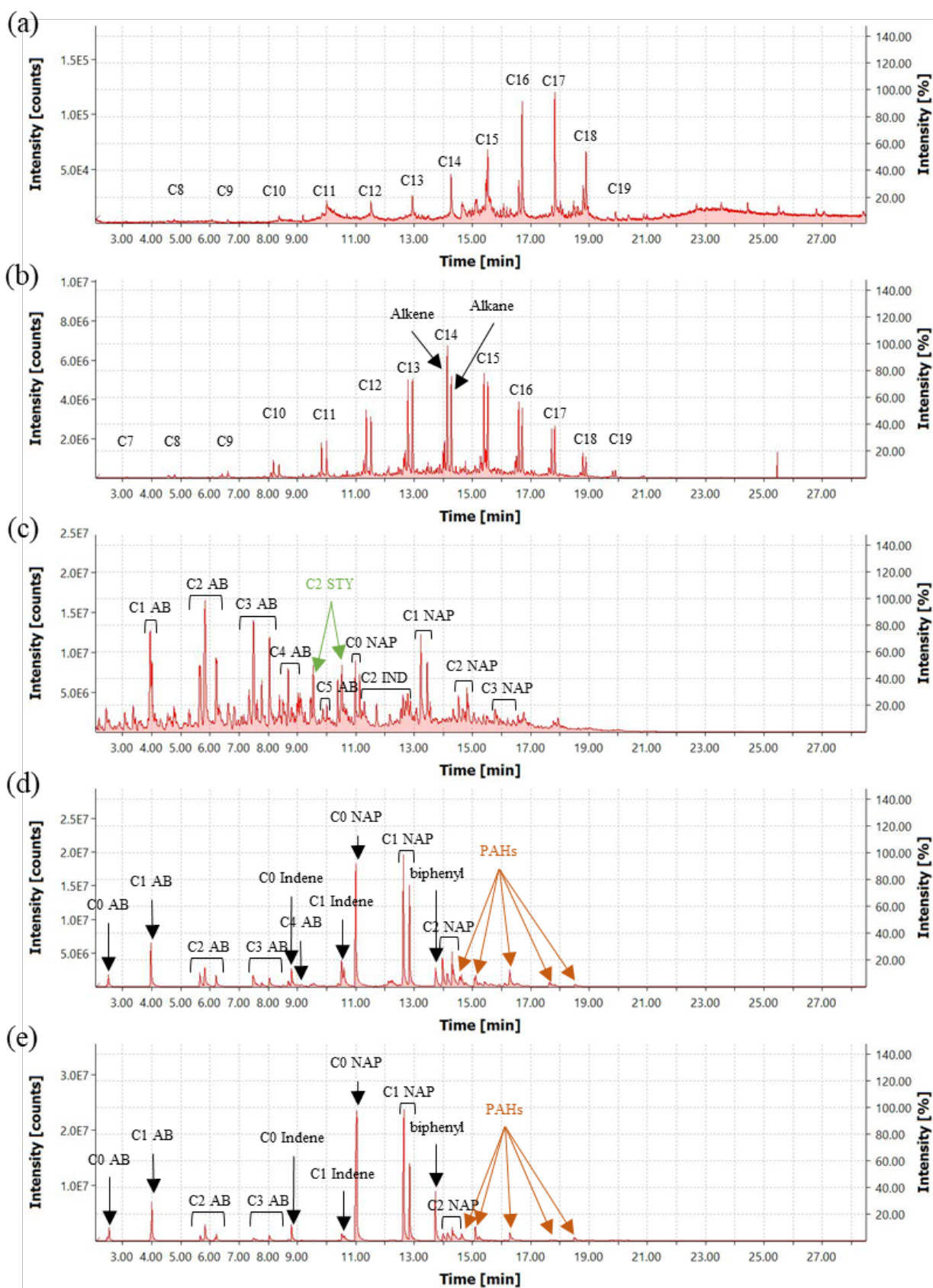


Figure 21 Chromatograms from temperature variation analysis on PP - (a) 300 °C, (b) 400 °C, (c) 500 °C, (d) 550 °C, and (e) 600 °C [AB - alkylbenzene; NAP - naphthalene; IND - indane; STY - styrene; PAH - polyaromatic hydrocarbon]

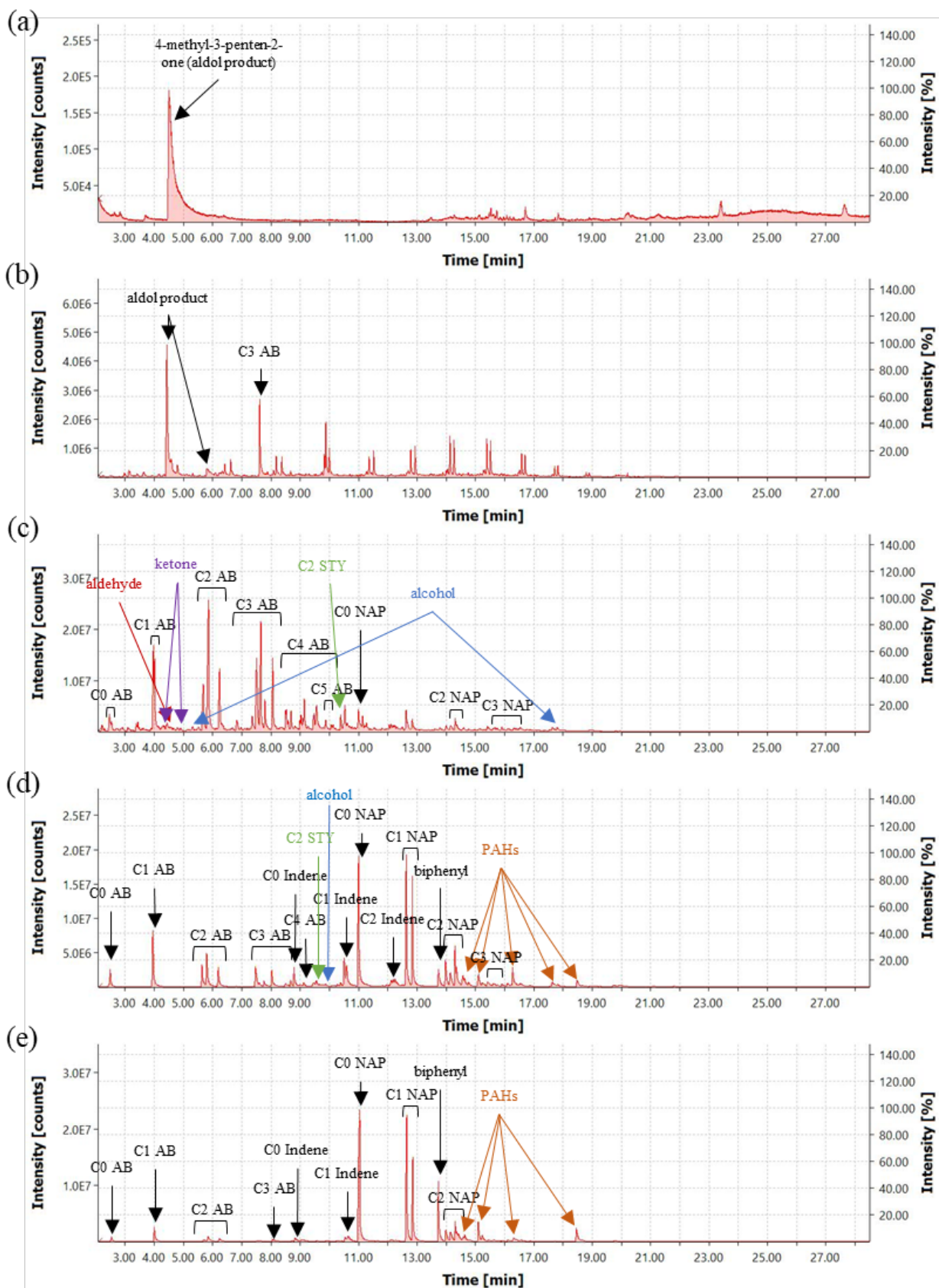


Figure 22 Chromatograms from temperature variation analysis on PP with the presence of acetone - (a) 300 °C, (b) 400 °C, (c) 500 °C, (d) 550 °C, and (e) 600 °C [AB - alkylbenzene; NAP - naphthalene; STY - styrene; PAH – polyaromatic hydrocarbon]

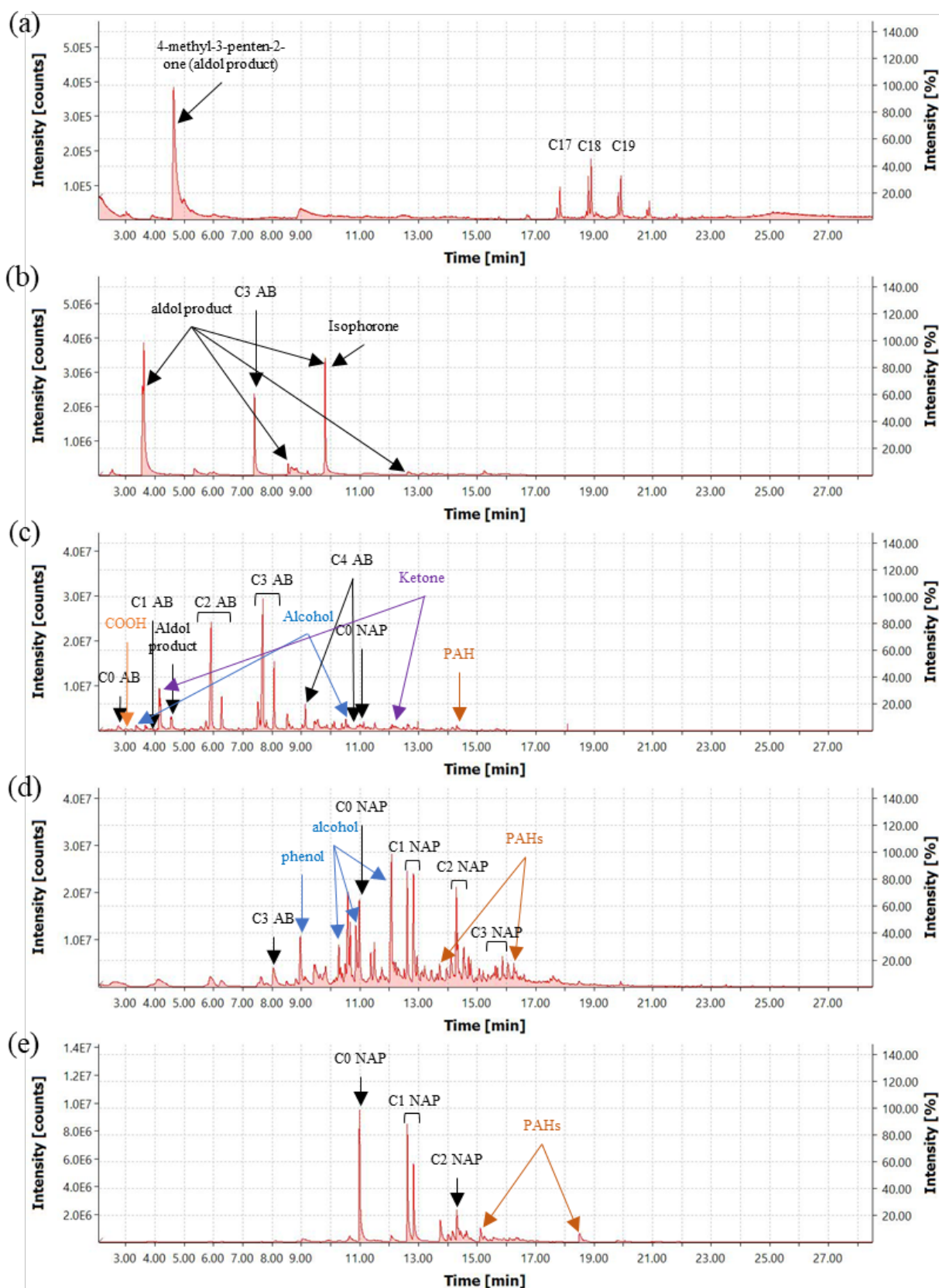


Figure 23 Chromatograms from temperature variation analysis on acetone - (a) 300 °C, (b) 400 °C, (c) 500 °C, (d) 550 °C, and (e) 600 °C [AB - alkylbenzene; NAP - naphthalene; COOH – carboxylic acid; PAH – polyaromatic hydrocarbon]

4.2.3 Ignitable Liquid Ratio Analysis

This qualitative study aimed to identify fuel-like pyrolysis products while also examining the influence of varying ratios of ignitable liquid on polymer samples. As discussed earlier, the presence of acetone was found to impact the pyrolysis profiles of PP. In order to investigate the ratio effect of ignitable liquid on the polymer, PP was combined with acetone at ratios of 1:1, 1:5, 1:10, 5:1, and 10:1. As shown in Figure 25, the mixtures were subjected to pyrolysis at a temperature of 550 °C for a duration of 30 min.

Similar to previous analyses, the absence of alkane and cycloalkane/alkene products was observed when the pyrolysis temperature exceeded 550 °C, Figure 24. In contrast, strong detection of alkylbenzene and naphthalene products were observed across all investigated ratios. Weak detection of indane and ketone products was only observed in the 5:1 ratio sample. Alcohol products were detected in samples with an equal or greater presence of acetone, specifically in the ratios of 1:1, 1:5, and 1:10. The number of detected polyaromatic hydrocarbon peaks decreased as the acetone ratio increased, suggesting that the presence of acetone or oxygenated compounds in the pyrolysis of PP did not promote the generation of polyaromatic hydrocarbons during the pyrolysis process. These findings contribute to the understanding of the pyrolysis behaviour of polymer-ignitable liquid mixtures and have implications for forensic investigations involving fire incidents.

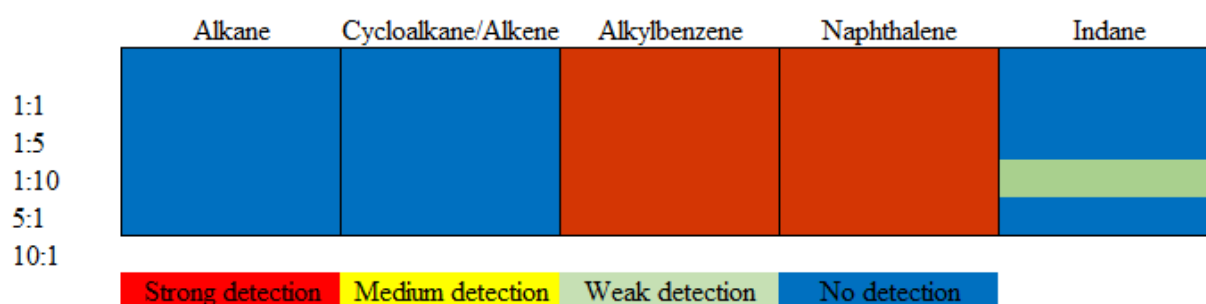


Figure 24 Heatmap comparison of ratio effect on pyrolysis of PP and acetone

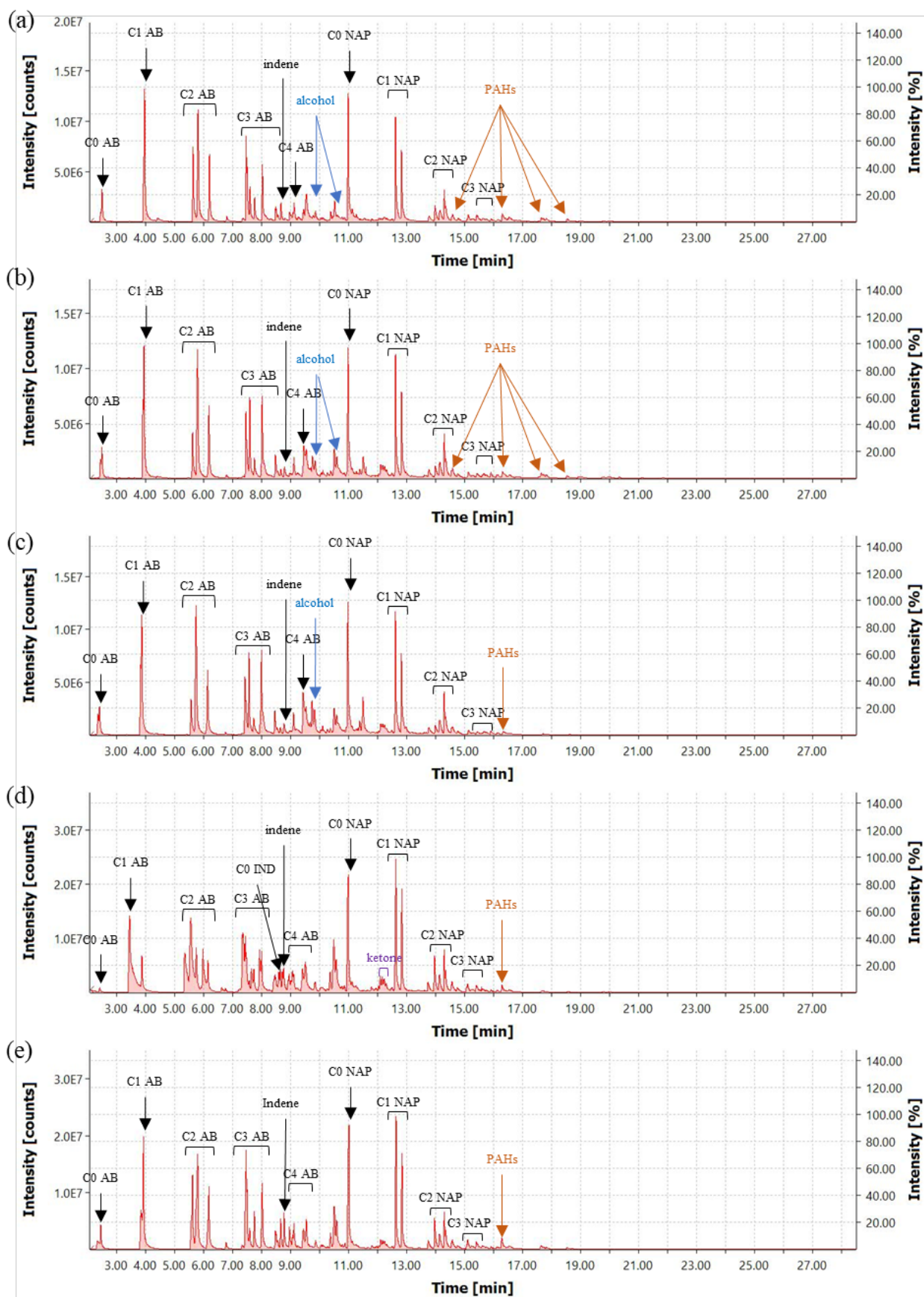


Figure 25 Chromatograms from ratio variation analysis on PP:acetone - (a) 1:1, (b) 1:5, (c) 1:10, (d) 5:1, and (e) 10:1 [AB - alkylbenzene; NAP - naphthalene; IND - indane; PAH - polyaromatic hydrocarbon]

4.2.4 Pyrolysis of Common Polymers

To investigate the differences in pyrolysis products generated from the substrate, additional polymers including high density polyethylene (HDPE), polyethylene terephthalate (PET), and nylon were subjected to pyrolysis at 550 °C for 30 min. The resulting chromatograms are given in Figure 26.

Across all substrates, no detection of alkane or cycloalkane/alkene products was observed. The pyrolysis products of PP consisted of C0-C4 alkylbenzene, C0-C2 naphthalene, C0-C1 indene, and five types of PAHs including acenaphthene, acenaphthylene, fluorene, C1 fluorene, and phenanthrene. Similar pyrolysis products were observed for HDPE, which included C0-C4 alkylbenzenes, C0-C3 naphthalene, C0-C1 indene, and the same five types of PAHs as PP. This similarity can be attributed to the linear aliphatic chemical structure of both PP and HDPE, which undergo random chain scission during the pyrolysis (Huang *et al.*, 2018; Huang *et al.*, 2017; Stauffer, 2003).

PET produced C0-C2 alkylbenzenes, C0-C1 naphthalene, as well as two types of PAHs, namely fluorene and phenanthrene. Additionally, compounds from other functional groups such as alcohol, ketone, and aldehyde were also detected in the pyrolysis products of PET. Biphenyl was the most abundant pyrolysis product of PET. This can be explained by the presence of phenyl group in the PET structure, where the bond dissociation energy between the phenyl group and its neighbouring carbon was approximately 452.6kJ/mol, while the C-C bond dissociation energy within the ester was around 358.2kJ/mol (Huang *et al.*, 2018). Consequently, the formation of phenyl group products was preferred as opposed to aromatic products during the pyrolysis process.

The pyrolysis of nylon resulted in the production of C0-C3 alkylbenzene, C0-C1 naphthalene, as well as various nitrogen-containing compounds including pyridine, C2 benzenemethanamine, benzonitrile, benzenamine, and C0-C1 quinoline. The production of non-hydrocarbon compounds derived from the substrate itself can aid the identification of substrate types, allowing for the subtraction of matrix effect accordingly to determine the presence of ignitable liquid.

The general pyrolysis mechanism of polymers is presented in Figure 27. The thermal energy from the pyrolysis process initiates the formation of free radical products based on the bond dissociation energy of each bond. These free radicals propagate to form aliphatic structures.

Aromatic products will form at higher pyrolysis temperature where greater thermal energy are present into the process.

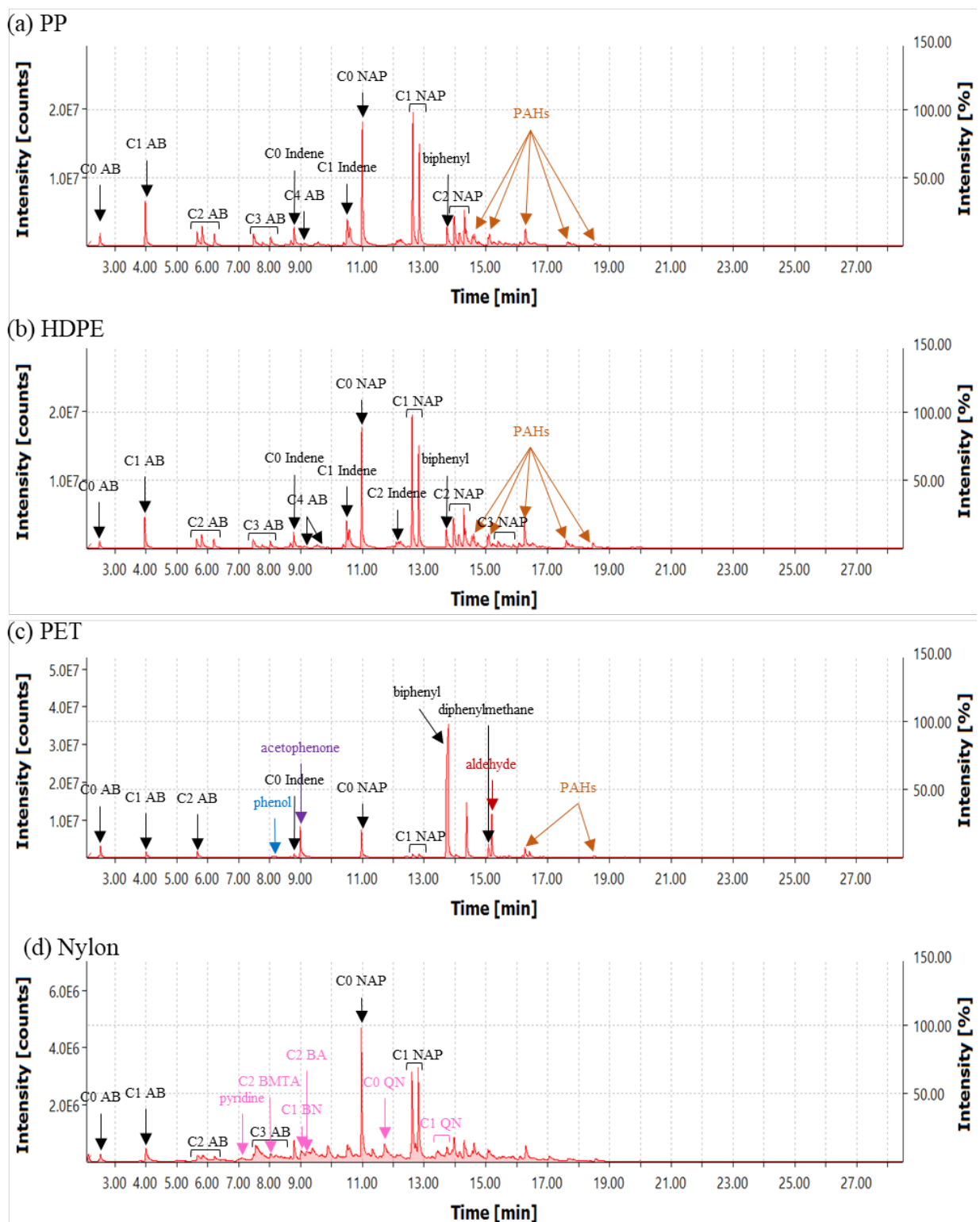


Figure 26 Chromatograms from pyrolysis of substrates at 550 °C for 30 min [AB - alkylbenzene; NAP - naphthalene; PAH – polyaromatic hydrocarbon; BMTA – benzenemethanamine; BN – benzonitrile; BA – benzenamine; QN - quinoline]

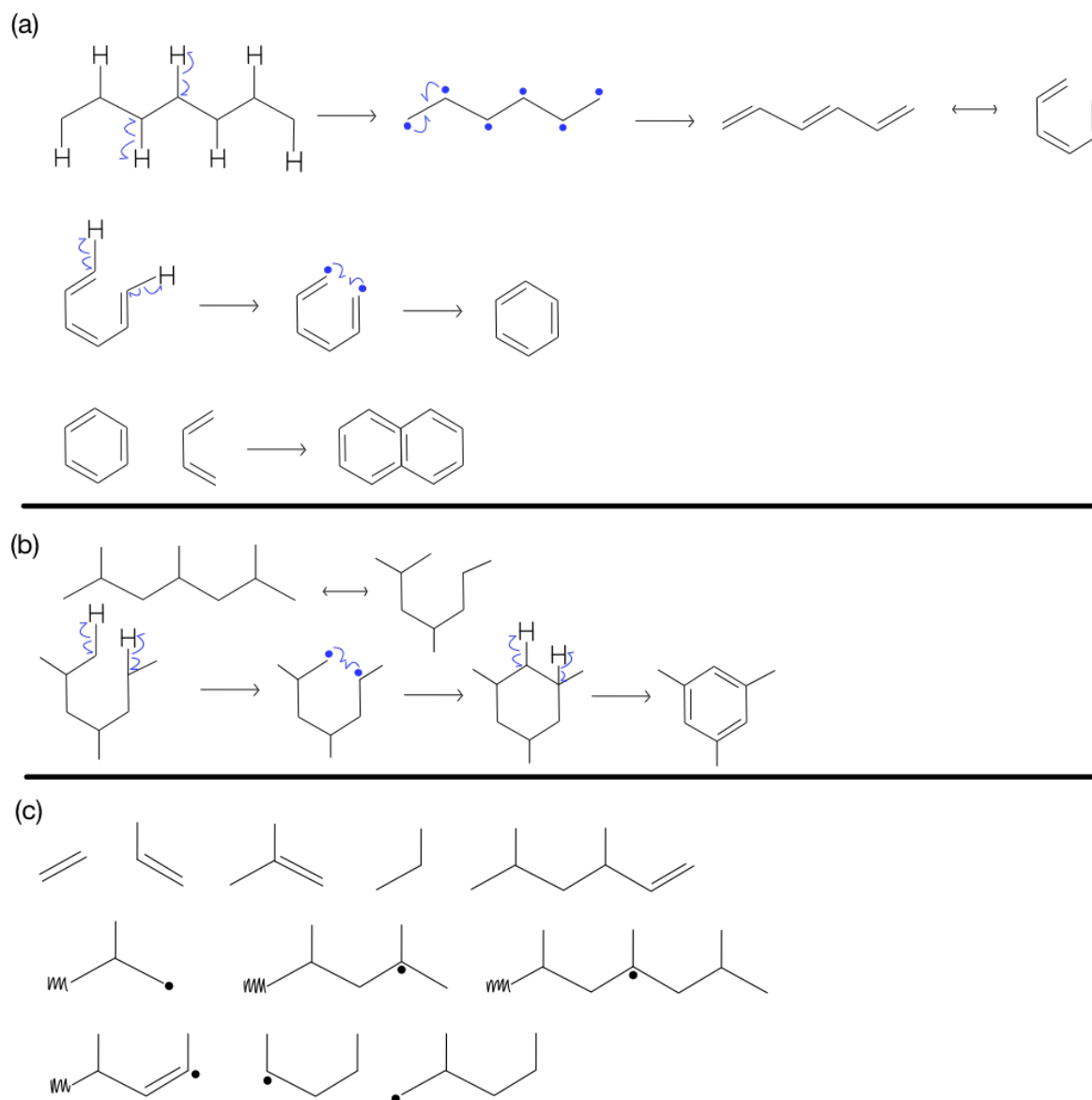


Figure 27 General pyrolysis mechanisms for the formation of aromatic products (a) polyethylene, (b) polypropylene, (c) degradation and free radical products from propagation

4.2.5 Pyrolysis of Common Polymer with Acetone

To investigate the influence of a foreign ignitable liquid on the pyrolysis profiles, the substrates were subjected to pyrolysis at 550 °C for 30 min in the presence of acetone. The resulting chromatograms are depicted in Figure 28. No detection of alkane or cycloalkane/alkene products was observed in any of the samples.

PP with acetone (PPA) exhibited pyrolysis products consisting of C0-C4 alkylbenzene, C0-C3 naphthalene, C0-C1 indene, and five types of PAHs, namely acenaphthene, acenaphthylene, fluorene, C1 fluorene, and phenanthrene. Additionally, an alcohol product was detected. Similarly, HDPE with acetone (HDPEA) yielded similar pyrolysis products, including C0-C4

alkylbenzene, C0-C3 naphthalene, C0-C1 indene, the same five PAHs as PPA, and an alcohol product. The only variation in the pyrolysis profile was the presence of indane in HDPEA.

PET with acetone (PETA) produced C0-C4 alkylbenzene, C0-C1 naphthalene, C0 indene, along with two types of PAHs, fluorene and phenanthrene. Furthermore, compounds from other functional groups, such as alcohol, ketone, and aldehyde were also detected in the pyrolysis of PETA.

The pyrolysis of nylon with acetone (NyA) resulted in the generation of C0-C3 alkylbenzene, C0-C2 naphthalene, C0 indane, C0 indene, as well as products from other functional groups, including ketone, nitrogen-containing compounds, alcohol, and carboxylic acid.

The comparison of substrate pyrolysis with or without acetone is presented in Figure 28. In the presence of acetone, notable differences were observed in the pyrolysis products. When acetone was added to PP, the production of naphthalene with a higher carbon number was observed compared to the pyrolysis of PP without acetone. The detection of indane was only observed in the pyrolysis of HDPEA and NyA while it was not detected in the pyrolysis of the respective substrates alone.

The addition of acetone to PET led to the formation of alkylbenzene products with higher carbon numbers compared to the pyrolysis of PET without acetone. In the case of NyA, functional groups including ketone, alcohol, and carboxylic acid were detected, which can be attributed to the presence of acetone in the pyrolysis process. Additionally, the presence of acetone in NyA also resulted in the production of naphthalene with a greater carbon number.

These findings emphasised the influence of ignitable liquids on the pyrolysis behaviour and product profiles of polymers. The identification and characterisation of these pyrolysis products can help in determining the presence of specific substrate types and foreign ignitable liquids.

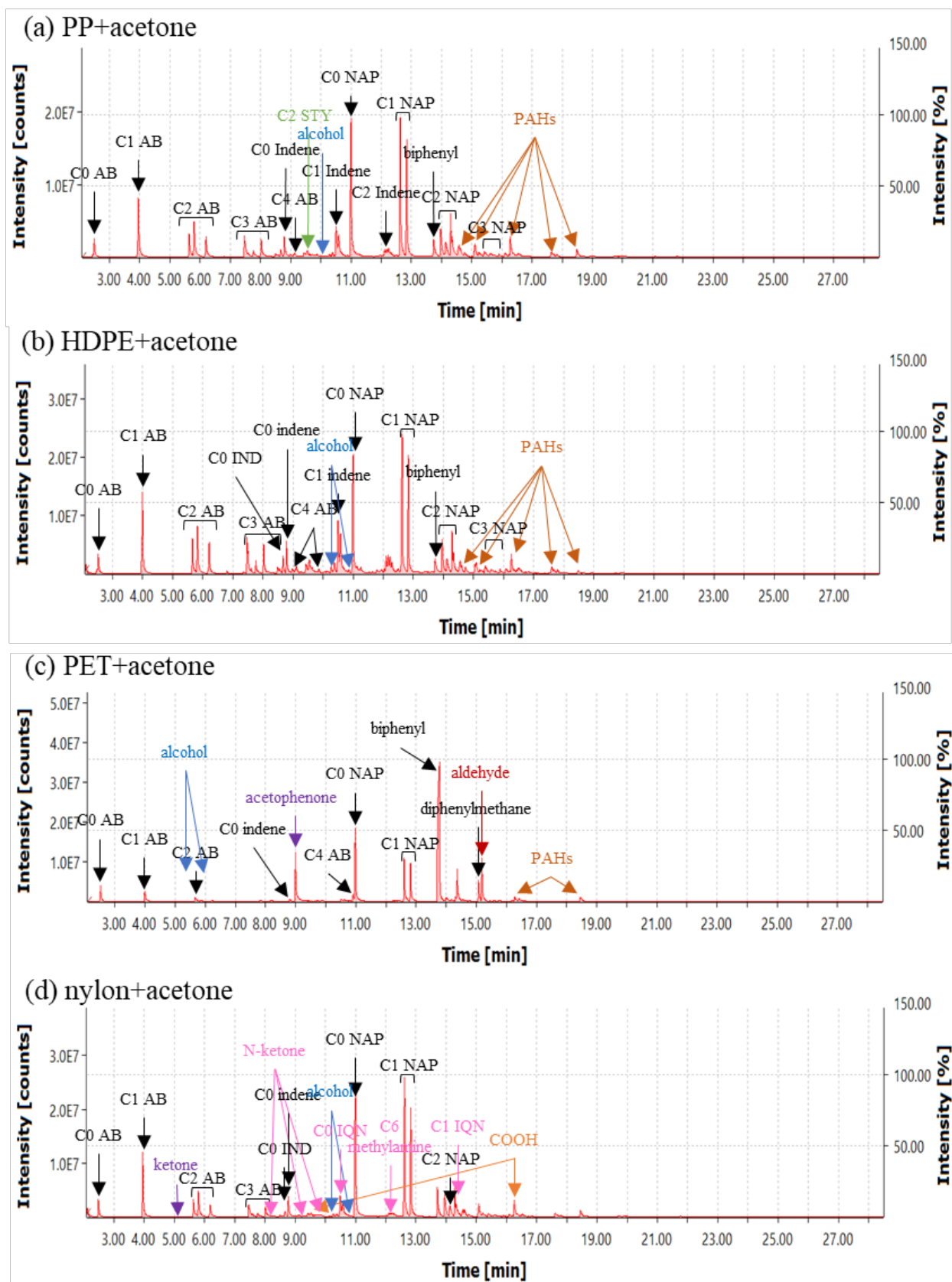


Figure 28 Chromatograms from pyrolysis of substrates in the presence of acetone at 550 °C for 30 min [AB - alkylbenzene; NAP - naphthalene; STY - styrene; PAH – polyaromatic hydrocarbon; IND – indane; N-ketone – nitrogen-containing ketone; IQN – isoquinoline; COOH – carboxylic acid]

4.2.6 Pyrolysis of Polypropylene with Common Ignitable Liquids

To investigate the changes in pyrolysis profile of the substrate in the presence of different ignitable liquids, PP was subjected to pyrolysis at 550 °C for 30 min with acetone, hexane, ethyl acetate, butan-2-one (methylethylketone/MEK), and 3-pentanone. None of the samples exhibited detection of alkane or cycloalkane/alkene compounds. The results obtained from this investigation are presented in Figure 29.

Hexane and PP shared a similar chemical composition, consisting solely of carbon and hydrogen in their structures. Therefore, it was hypothesised that the pyrolysis profiles of PP with or without the presence of hexane as ignitable liquid would exhibit similarities due to their comparable chemical structures. However, notable differences were observed between the two profiles, PP and PPH, including additional peaks corresponding to indane, C2 indene, C3 naphthalene, and reduced peaks of PAHs. These findings suggest that the presence of hexane facilitates the conversion of compounds with higher carbon numbers while simultaneously reducing the formation of PAHs.

Ethyl acetate, acetone, butan-2-one, and pentan-3-one were ignitable liquids containing oxygen atoms. It was postulated that the presence of oxygen during the pyrolysis process would alter the pyrolysis profiles of the substrates, potentially leading to a partial combustion reaction and generating a reduced number of peaks. Comparative results are given in Figure 30.

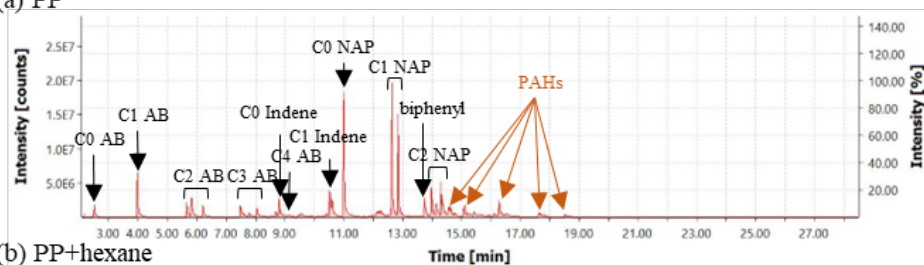
The resulting pyrolysis products of PPEA included C0-C3 alkylbenzene and naphthalene, C0 indane and indene, as well as two PAHs, namely fluorene and phenanthrene. On the other hand, PPA yielded C0-C4 alkylbenzene, C0-C3 naphthalene, C0-C1 indene, and the same five PAHs as the original PP profile. Pyrolysis of PPMEK produced C0-C4 alkylbenzene, C0-C3 naphthalene, C0 indane and indene, as well as three PAH peaks including acenaphthene, fluorene, and phenanthrene. The resulting pyrolysis products of PP3P included C0-C4 alkylbenzene, C0-C1 naphthalene, C0 indane and indene, and three PAH peaks, namely acenaphthylene, fluorene, and phenanthrene.

The carbon number in alkylbenzene remained unchanged for all ignitable liquid except for ethyl acetate. This implies that ketone-based ignitable liquids had no effect on the carbon numbers of the identified alkylbenzene compounds, while the presence of a carboxylate ester resulted in a reduction in the carbon number of detected alkylbenzene. In contrast, the addition of an ignitable liquid during the pyrolysis of PP led to an increase in the carbon number of

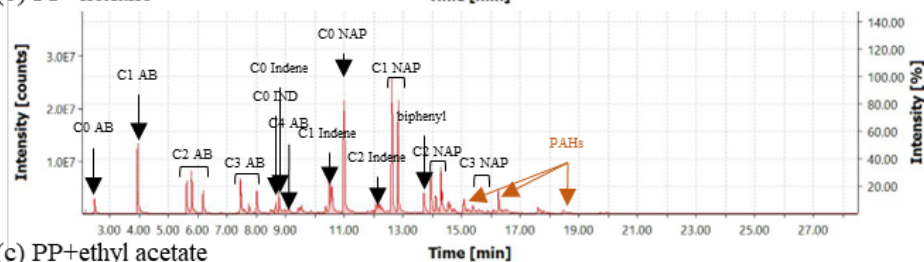
detected naphthalene, except in the case of pentan-3-one where the carbon number of naphthalene decreased. Peaks corresponding to indane were detected when an ignitable liquid was added during pyrolysis, while they were absent in the pyrolysis of PP and PPA. The detected peaks of indene products varied depending on the specific ignitable liquid used. Furthermore, the overall number of detected PAHs decreased when an ignitable liquid was present during the pyrolysis of PP.

These findings provided useful insights into the effects of different ignitable liquids on the pyrolysis profiles of PP and highlight the importance of considering the chemical composition of ignitable liquids in understanding the resulting pyrolysis products. Further research required is to explore the underlying mechanisms driving these observations and to investigate the implications of these findings with in the field of arson investigation.

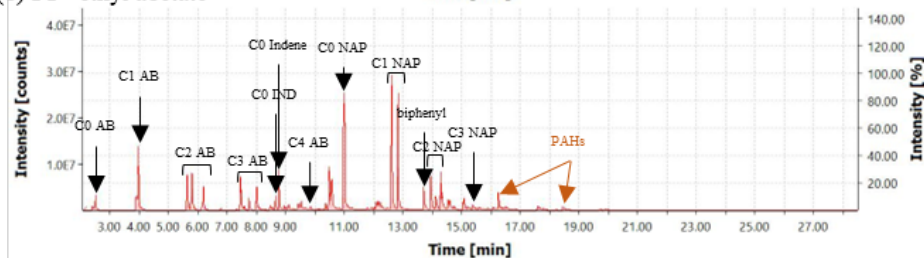
(a) PP



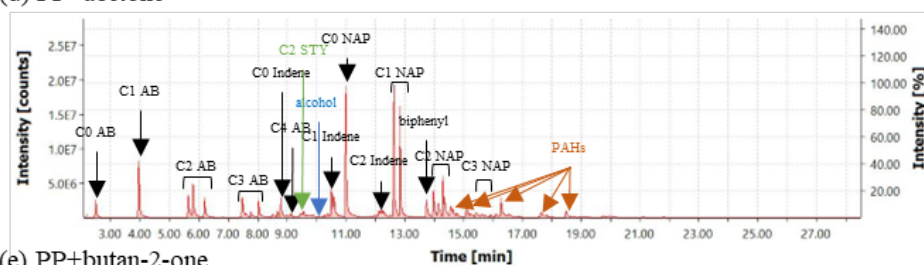
(b) PP+hexane



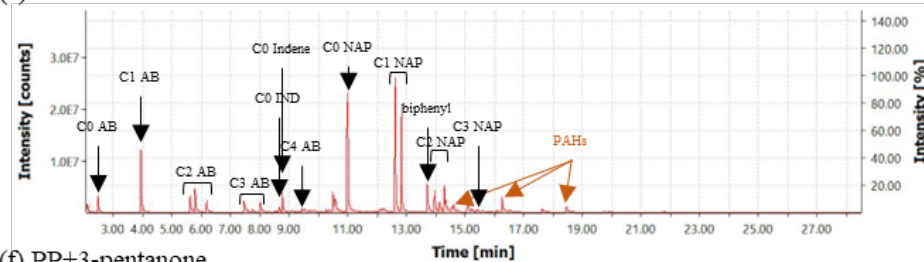
(c) PP+ethyl acetate



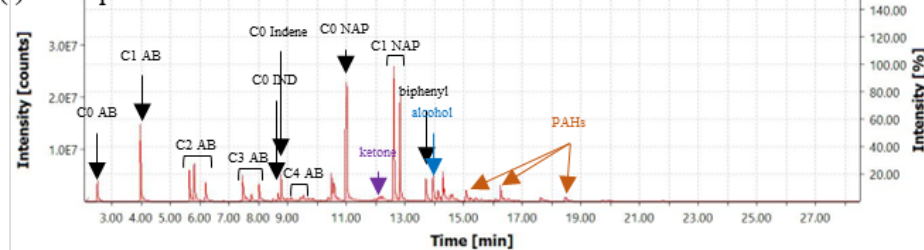
(d) PP+acetone



(e) PP+butan-2-one



(f) PP+3-pentanone



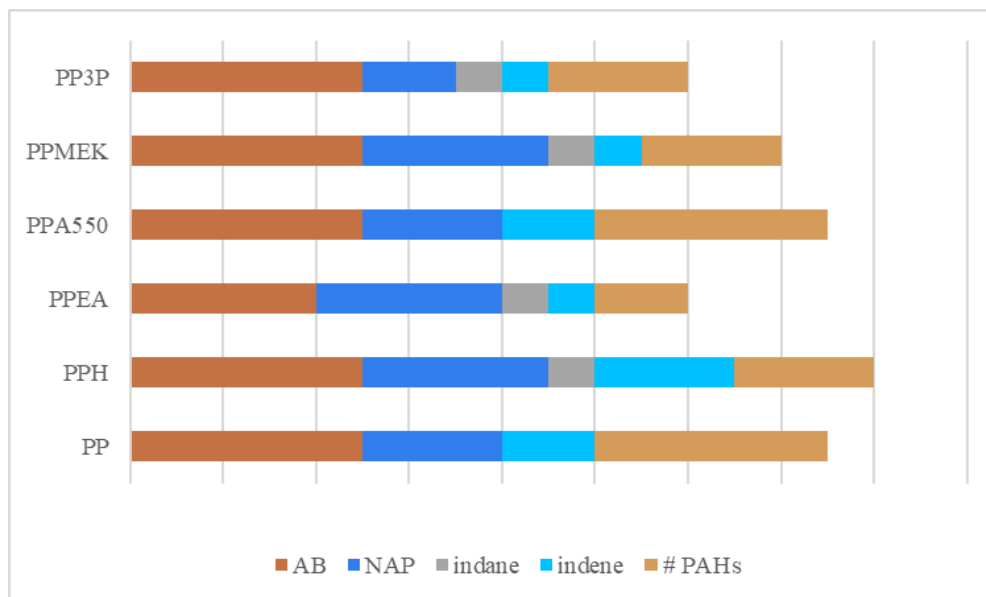


Figure 30 Comparison of carbon number at each category and number of PAHs from pyrolysis of PP with ignitable liquids at 550 °C for 30 min

4.2.7 Re-evaluation of Importance of Temperature in Pyrolysis of Substrates with Ignitable Liquid

Previous discussion emphasised that temperature played a crucial role in the formation of aromatic pyrolysis products. When the temperature exceeded 500 °C, substrates formed aromatic products irrespective of the substrate type. Upon subjecting substrates and ignitable liquids to pyrolysis at 550 °C for 30 min, the predominant pyrolysis products were aromatic compounds. Some of these aromatic compounds matched the indicative compounds listed in the E1618 ASTM standard. To further investigate the influence of temperature, pyrolysis at 300 °C (mild pyrolysis temperature) was conducted to compare the differences in pyrolysis profiles.

The differences in pyrolysis product detection between 550 °C and 300 °C are depicted in Figure 31 to Figure 33, and tabulated in Table 19. It was confirmed that a pyrolysis temperature of 550 °C led to higher levels of aromatic products, highlighting the significance of temperature in the conversion of petroleum fuel-like aromatic products.

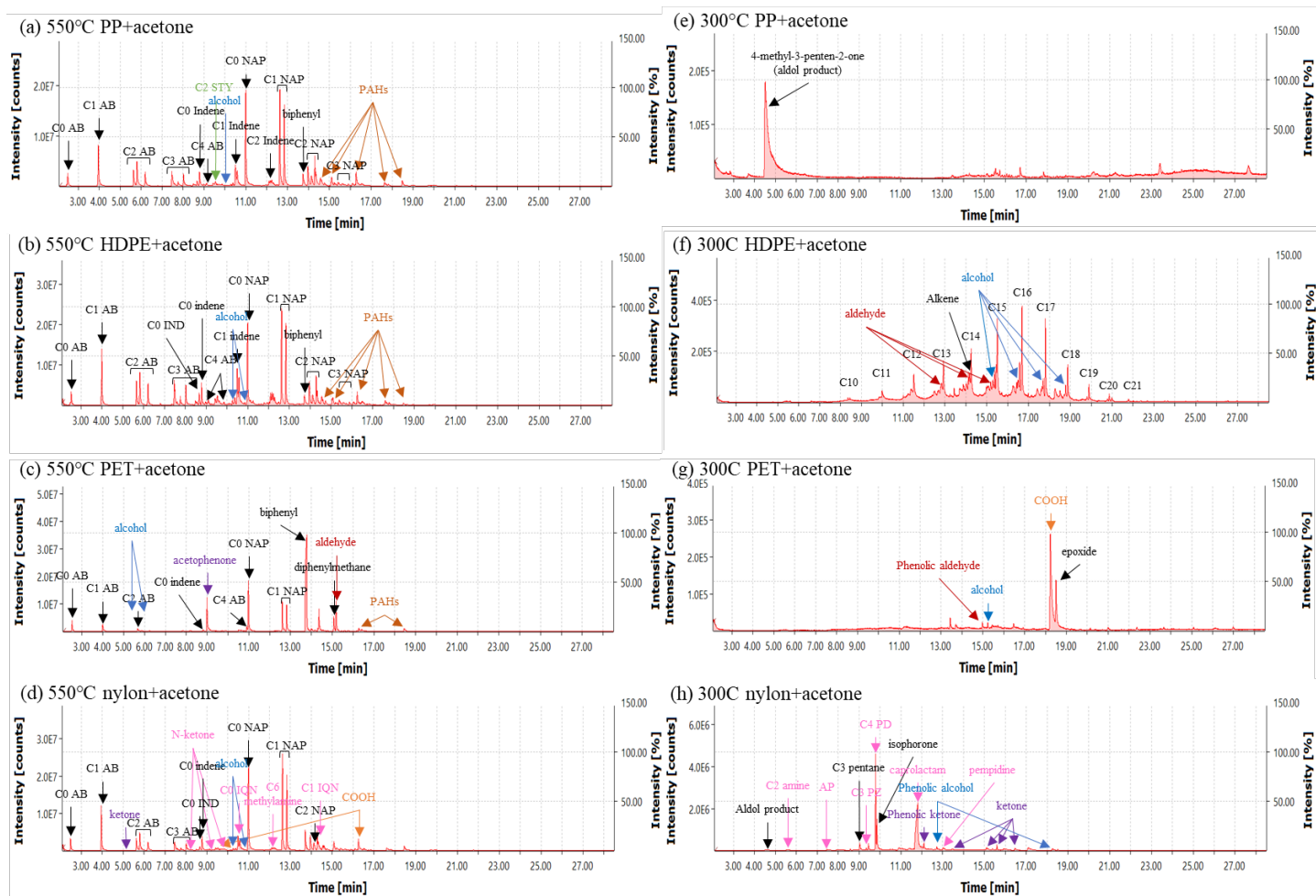
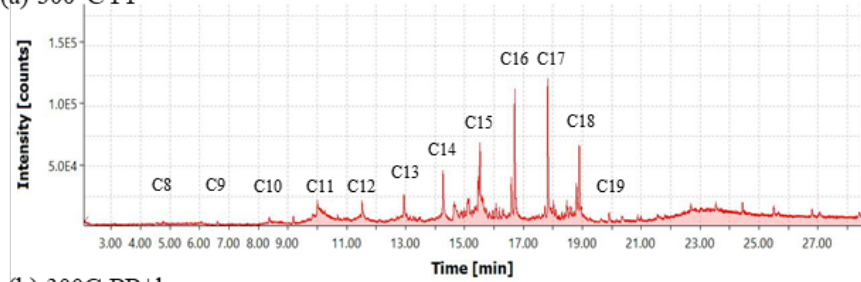
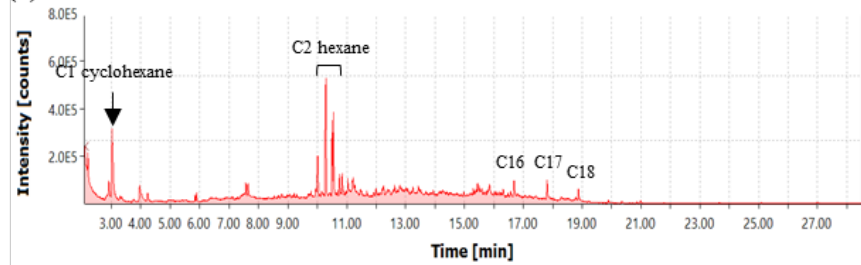


Figure 31 Chromatograms from pyrolysis of substrate in the presence of acetone at 300 °C and 550 °C for 30 min to determine the importance of temperature effect [AB - alkylbenzene; NAP - naphthalene; STY- styrene; PAH – polyaromatic hydrocarbon; IND – indane; COOH- carboxylic acid; N-ketone – nitrogen-containing ketone; IQN – isoquinoline; AP – aminopyridine; PZ –

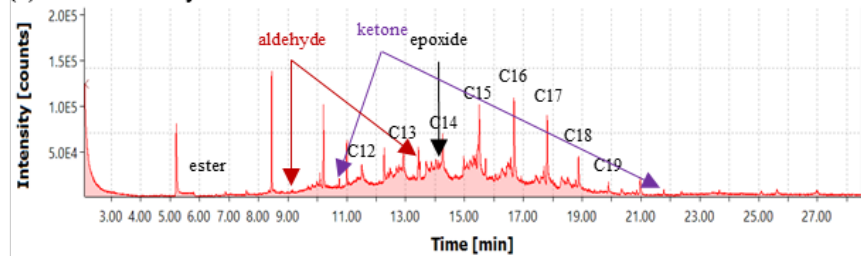
(a) 300°C PP



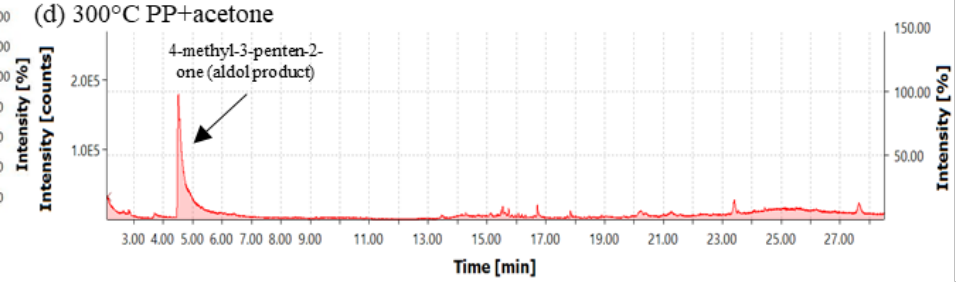
(b) 300C PP+hexane



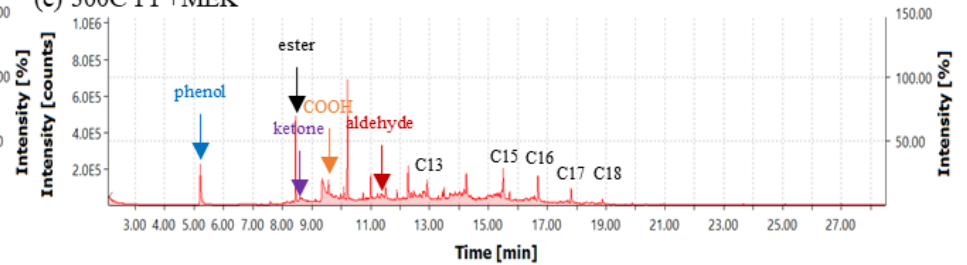
(c) 300C PP+ethyl acetate



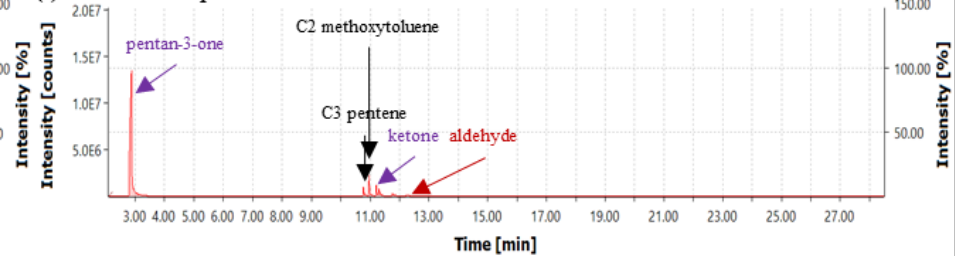
(d) 300°C PP+acetone



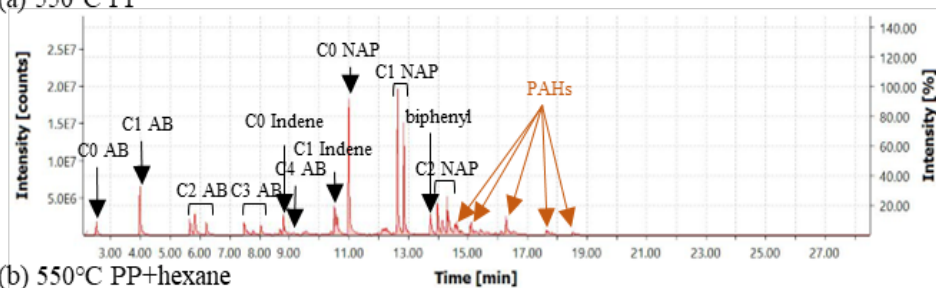
(e) 300C PP+MEK



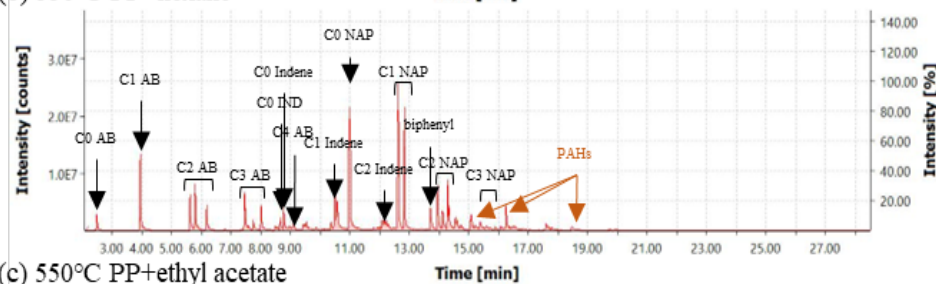
(f) 300C PP+3-pentanone



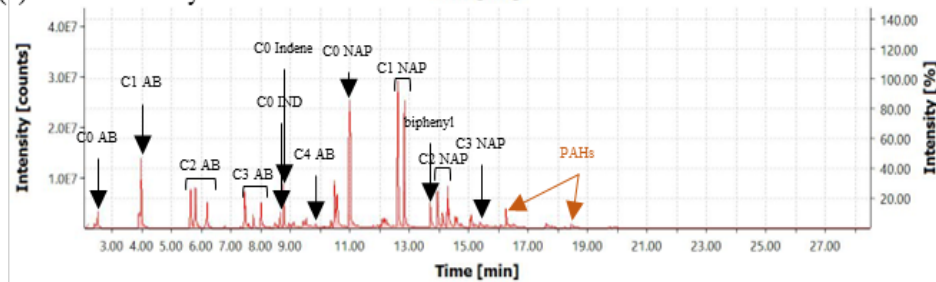
(a) 550°C PP



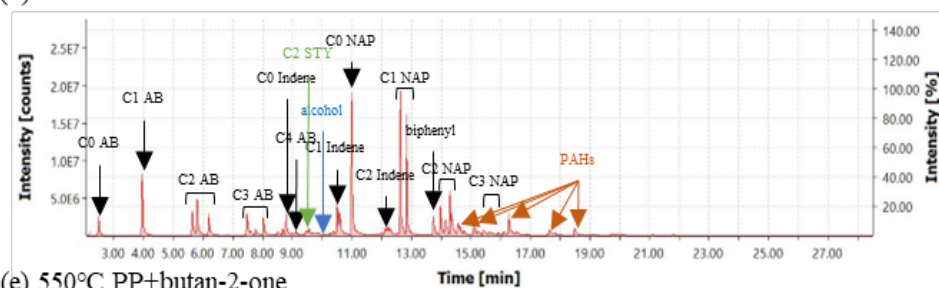
(b) 550°C PP+hexane



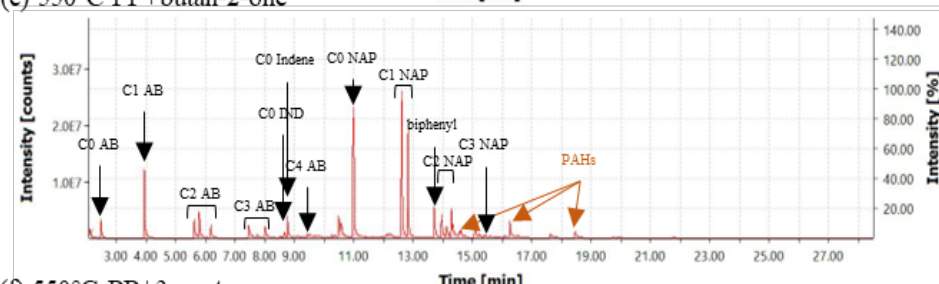
(c) 550°C PP+ethyl acetate



(d) 550°C PP+acetone



(e) 550°C PP+butan-2-one



(f) 550°C PP+3-pentanone

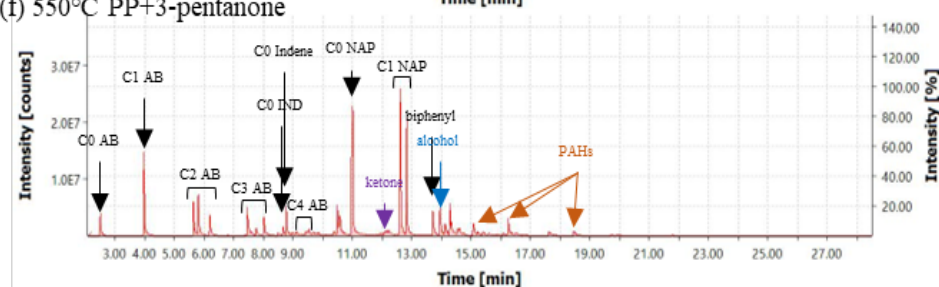


Table 19 Presence of aromatic product types in samples for 550 °C and 300 °C

	AB					NAP				IND	Indene			Other PAHs
	C0	C1	C2	C3	C4	C0	C1	C2	C3	C0	C0	C1	C2	#
PPA550														5
PPA300														0
HDPEA550														5
HDPEA300														0
PETA550														2
PETA300														0
NyA550														0
NyA 300														0

4.2.8 Real World Simulation

Two methods were employed to simulate real world pyrolysis samples of substrates, pyrolysis under a thin metal sheet and direct flame burning. The preliminary findings of this simulation study demonstrated the feasibility of collecting and analysing the debris from pyrolyzed polymers with ignitable liquids under a metal cover in an open container. The experimental data revealed that the phenomena observed in closed ampoules could be replicated in this setup.

The pyrolysis products obtained from the thin metal sheet pyrolysis method indicated the presence of indicative compounds found in gasoline even though there was only weak detection of C3 alkylbenzene and C0-C1 naphthalene in the pyrolyzed PP samples. In contrast, no aromatic compounds were detected when PP was subjected to direct flame burning.

However, there were certain limitations associated with the real world analysis using the thin metal sheet method, which hindered the qualitative analysis of the samples. These limitations included variations in pyrolysis duration, inconsistent heating of the surface, sampling location, sampling technique, and weathering effects. The duration of pyrolysis could be influenced by the distance between the heating source and the metal cover. Moreover, room temperature could impact the cooling rate of the sample, thereby affecting the overall pyrolysis duration. The heating temperature variation depended on the location of the heating source on the metal surface, with the centre receiving more heat compared to the edges. The sampling location and technique also affected the results due to the liquefaction of PP, which seeped through the sand and increased the distance from the heat source. The experimental pyrolyzed samples with secondary cracking exhibited charred compounds instead of solidified burnt polymers. This observation suggested that the sampling of pyrolyzed samples was influenced by the degree of substrate pyrolysis and the appearance after cooling.

Additionally, weathering effects posed a common limitation in fire debris analysis. The real world simulation results did not detect low molecular aromatic compounds commonly found in most experimental simulation samples. Although weak detections of certain indicative gasoline compounds were observed, the absence of major characteristic products indicated that the evidence collected was insufficient to conclude the presence of accelerants in a fire incident.

4.3 Slow Pyrolysis Profiles

Each peak observed in the chromatograms was identified and classified into 24 component groups based on their chemical composition. These components were composed of isomers with varying chain lengths but belonging to the same functional group. A detailed list of these component groups can be found in Table 22.

Table 22 List of component groups

Compound types	Symbol	Function groups
alkyne aromatic	AAr	Alkyne
alkylbenzene	AB	C0 - C4 isomers
alkane	alkane	C10 - C20
alkene	alkene	C12 - C17
alkyne	alkyne	Alkyne
cycloalkane	cycloalkane	C4 – C6
indane	indane	Indane
indene	indene	C0 – C2 isomers
naphthalene	NAP	C0 – C3 isomers
nitrogen-containing aliphatic	NCAI	Hydrocarbons with nitrogen
nitrogen-containing aromatic	NCAr	
nitrogen-containing cyclic	NCC	
nitrogen-containing heterocyclic	NCH	
nitrogen-containing heterocyclic aromatic	NCHAR	
oxygenated aliphatic	OAI	Alcohol, aldehyde, ester, ether, ketone
oxygenated aromatic	OAr	Alcohol, ester, ether, ketone, carboxylic acid
oxygenated cyclic	OC	
oxygenated cyclic aliphatic	OCAI	
oxygenated nitrogen-containing	ONCA	
oxygenated nitrogen-containing aliphatic	ONCAI	
oxygenated nitrogen-containing aromatic	ONCAr	
oxygenated nitrogen-containing cyclic	ONCC	
oxygenated nitrogen-containing heterocyclic aromatic	ONCHAR	
polyaromatic hydrocarbon	PAH	Fluorene, acenaphthene,

		acenaphthylene
--	--	----------------

Figure 34 illustrates the contribution of the variables to the principal components through a scree plot. It was determined that the first three principal components accounted for a significant proportion of the variation, accounting for 74.8% of the total variation. Specifically, alkylbenzene, oxygenated aromatic, and naphthalene were the primary contributors to these three components. The first variable, alkylbenzene, accounted for the highest proportion of variance at 43.8%, indicating its abundance in the samples. Although the second (oxygenated aromatic) and third (naphthalene) variables explained a relatively smaller proportion of variance, 15.8% and 15.2% respectively, their contributions were significant compared to the variances moving further down plot. These three main principal components were characterised by aromatic structures, indicating the significance of aromatic compounds in the dataset and their influence on the observed variation. These findings emphasized the importance of aromatic compounds in explaining the variation observed in the dataset. These aromatic compounds formed during the secondary cracking of pyrolysis process where cyclisation reaction takes place. Secondly, the oxygenated aromatic formed from cyclisation of pyrolyzed substrates and the presence of foreign oxygenated ignitable liquids. Lastly, naphthalene was formed where degraded substrates undergo cyclisation without oxygenated compound.

Figure 35 displays the correlation matrix from the data. Negative correlations were observed between unburned substrates and all pyrolysis samples conducted at 550 °C, except for unburned PS. The unburned PS showed positive correlations with PS550 and PSA550 due to its identical substrate type and chemical structure. Among the 550 °C pyrolysis samples, strong positive correlations were observed between PPMEK550, PPIP550, PPH550, PP550, PP3P550, LDPEA550, LDPE550, HDPEA550, and HDPE550, with R^2 values close to 1. This finding provides additional evidence in favour of the theory that polymers undergo aromatisation when exposed to elevated temperatures during a fire. It also underscores the inadequacy of the current Py-GCMS database in accurately forecasting the outcomes of prolonged, high temperature combustion events typical of fire scenarios. Similar observations are shown in Figure 36, this indicated a high degree a similarity in their pyrolysis products resulting from random scission. Samples such as PSA550, PS550, PPEA550, PETA550, PET550, PERA550, and PER550 exhibited R^2 values around 0.5, suggesting moderate

correlation. These samples consisted of substrates with a phenyl ring in their chemical structure. The presence of ignitable liquids did not significantly impact the correlations among the 550 °C pyrolysis samples, as seen on the strong correlation between substrates pyrolyzed with ignitable liquids on the right. However, the substrates do affect the correlation intensities between samples. PP, HDPE, and LDPE of which with similar chemical structure had higher correlation level while PER and PET of which structured with phenyl ring were correlated closer together. Strong positive correlation between samples observed in the top right corner. Samples were from 300 °C pyrolysis temperature. Unburned samples on the left (HDPE, LDPE, PP) had similar correlation due to their chemical structures. Furthermore, the weak positive correlation between samples from 300 °C and 550 °C pyrolysis, as well as weak negative correlations between samples from 300 °C and unburned samples were also observed. This correlation matrix highlighted that the presence of flammable liquids has a minimal effect on the pyrolysis products when the temperature exceeded 550 °C. In Figure 37, all unburned samples and those subjected to pyrolysis at 300 °C exhibited a negative correlation with PC1 (alkylbenzene). In contrast, all samples from the pyrolysis conducted at 550 °C showed a positive correlation with PC1. Among the 550 °C samples, those containing a phenyl ring in their chemical structure demonstrated a weak negative correlation with PC2 (oxygenated aromatic), except for PS550 and PSA550, which exhibited a weak positive correlation with PC2. This graph further supports that presence of foreign ignitable liquid in pyrolysis of substrates over 550 °C will not affect the product similarity when the starting substrates have similar chemical structure. Lower correlation level from samples pyrolyzed ≤ 300 °C observed. This was due to the absence of secondary cracking process for which the degradation product did not undergo cyclisation to form highly similar products like those pyrolyzed at 550 °C.

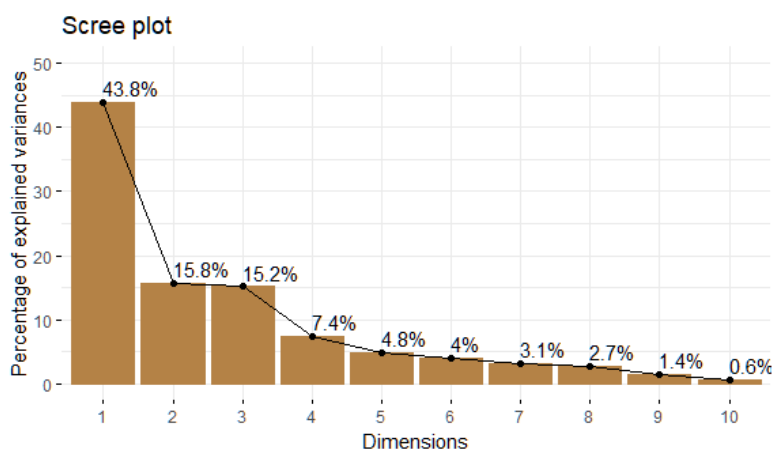


Figure 34 Scree plot of the components

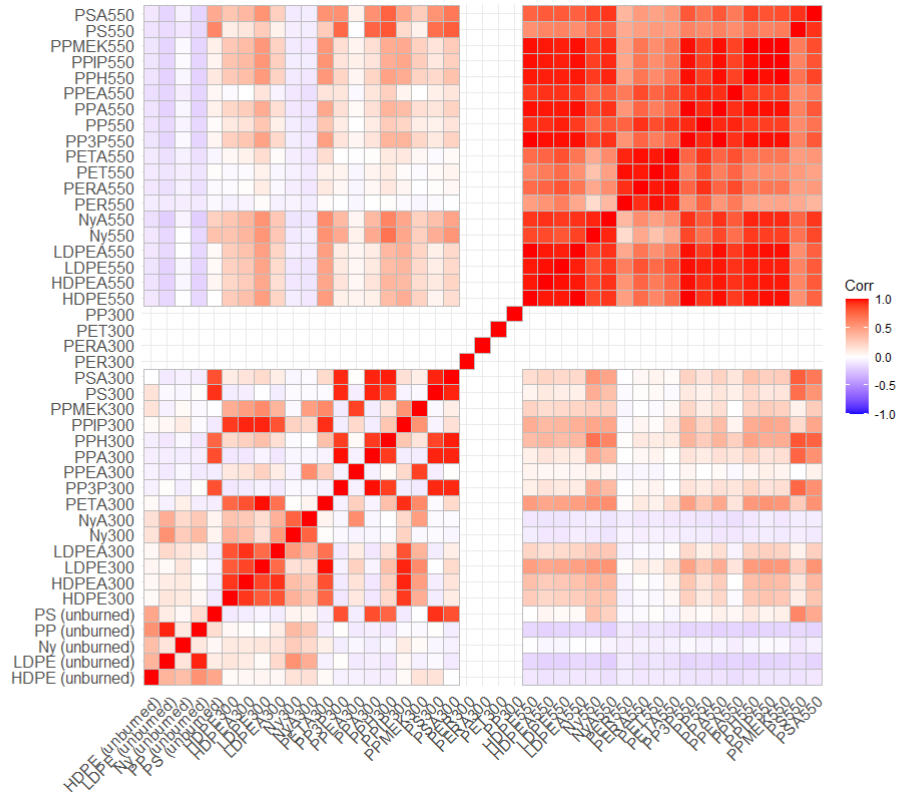


Figure 35 Correlation matrix from the data

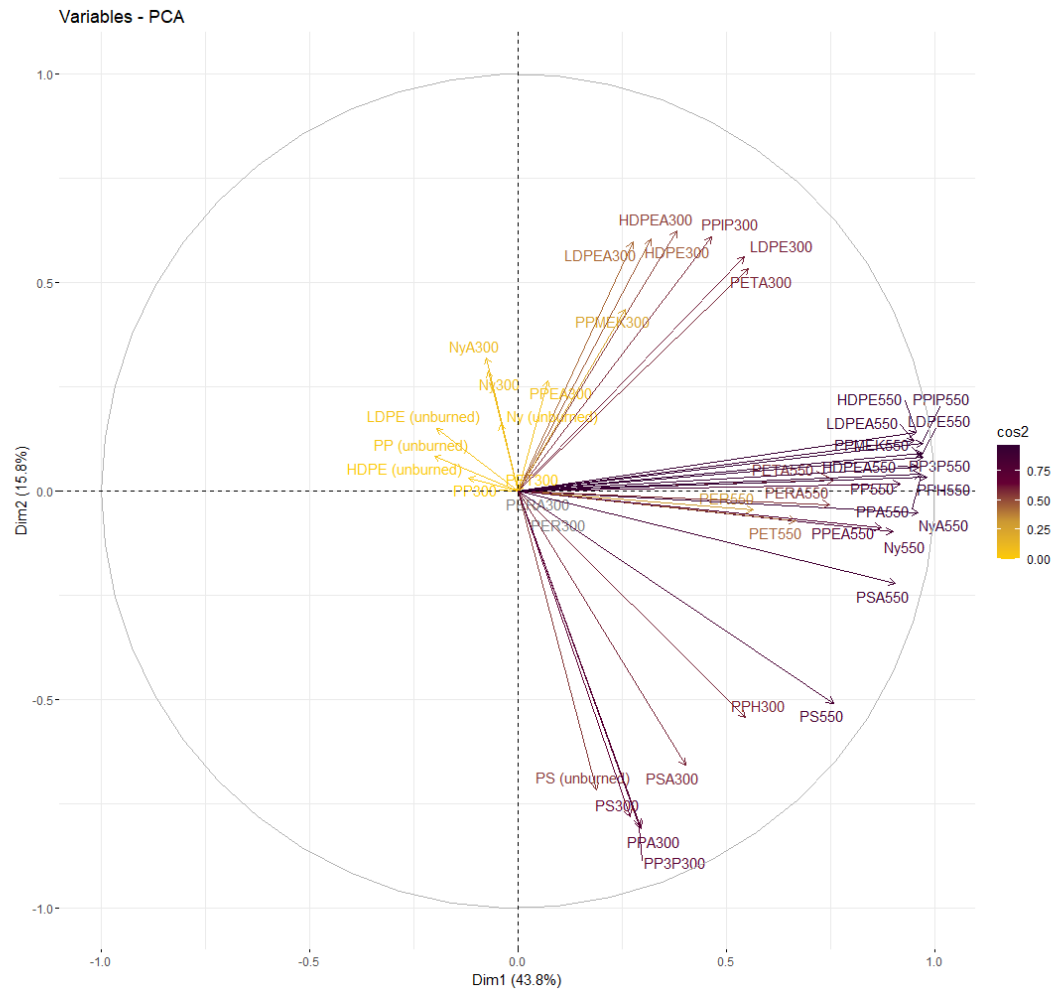


Figure 36 Cos2 plot of the samples

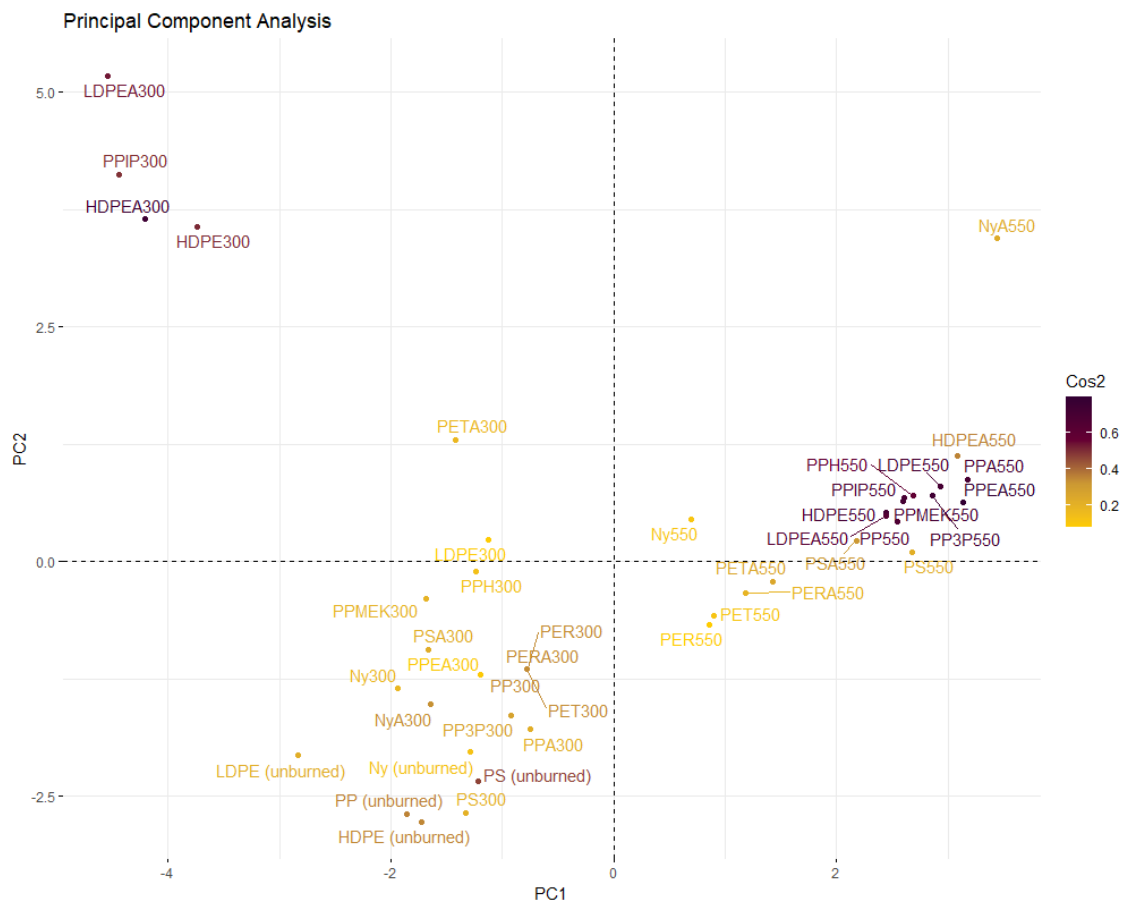


Figure 37 PCA plot of samples

Chapter 5: Conclusion

In conclusion, the experimental simulation and real world simulation conducted in this study provided insights into the pyrolysis behaviour of substrates and the influence of various factors on the formation of degradation products. The time variation analysis revealed that the duration of pyrolysis significantly influenced the product distribution of the polymer substrate. A 30 min pyrolysis duration resulted in a product matrix resembling profiles found in gasoline or diesel, while the addition of acetone as a foreign ignitable liquid further impacted the pyrolysis profile, promoting the formation of products from other functional groups.

The temperature variation analysis demonstrated the crucial role of pyrolysis temperature in the generation of degradation products. As the temperature increased, the detection of alkane and cycloalkane/alkene products decreased, while the detection of aromatic products, such as alkylbenzenes and naphthalene showed an upward trend. The presence of acetone within the temperature range influenced the product distribution, with aldol products masking the typical alkane and cycloalkane/alkene products.

Evaluation of ignitable liquid ratio indicated the ratio of the polymer substrate to acetone affected the formation of aromatic compounds, with higher ratios resulting in increased production of alkylbenzenes, naphthalene, and other functional groups.

Overall, these findings emphasize the importance of considering time, temperature, and the presence of ignitable liquid when analysing pyrolysis products for forensic investigations in fire incidents. Understanding the thermal degradation pathways and product distribution can aid in the identification and differentiation of substrate characteristics and the presence of potential ignitable liquids. This knowledge can contribute to the development of comprehensive databases and reference libraries, facilitating more accurate interpretations in fire investigations.

The findings from slow pyrolysis profile study provide insights into the pyrolysis characteristics of various substrates and their correlation patterns through the examination of chromatograms and the application of PCA. The use of PCA further improved the investigation of the relationship between samples through graphical demonstration. The results highlighted the complex relationships between pyrolysis conditions, chemical compositions, and the resulting pyrolysis products. It emphasized the importance of considering variables such as temperature, substrate composition, and functional groups in understanding the pyrolysis

process. A limitation in this study was the use of PDMS fibre, which inhibited the extraction of oxygenated compounds. Development of a new SPME fibre capable of extracting various compound types would enhance the generation of a library data base.

Chapter 6: Future Work

Py-GCMS was insufficient in reproducing pyrolysis samples and profiles similar to those collected from fire scenes. The investigation in the field of arson did not primarily focus on pyrolysis conditions such as time, temperature, and substrate type. Limited information regarding the pyrolysis duration and temperature of substrates was available in the field. To address these knowledge gaps and questions, it is important to conduct investigations and generate a library of data on substrates commonly subjected to pyrolysis in arson cases. This would enable the determination of the matrix identity by comparing it to the library data and the possibility of identifying the presence of accelerants by subtracting the substrate pyrolysis profile from the debris profile.

Future studies could investigate the influence of additional factors, such as heating rate, reaction time on the pyrolysis process to develop a data base that better represents real world fire conditions. Moreover, expanding the sample size and including wider range of substrates would provide a more comprehensive understanding of the correlation patterns and pyrolysis behaviour. These investigations will contribute to the advancement of fire investigation techniques and the development of more accurate forensic tools for the analysis of pyrolysis products.

Other possible future studies could focus on the continuous development of the machine learning and artificial intelligence algorithms for the analysis of large datasets of fire debris samples and identify patterns that can help with the detection of accelerations. Another potential future investigation direction is the study of mechanistic degradation of substrates which can further enhance the library data base and provide deeper insights into the formation of accelerant-like matrix from substrates. Lastly, attempts to standardise fire debris analysis procedures with modern analytical techniques would improve the efficiency, consistency, and accuracy across different laboratories and jurisdictions.

References

- Abel, R.J. and Harynuk, J.J. (2022) 'Sensitive and representative extraction of petroleum-based ignitable liquids from fire debris for confirmatory analysis of canine-selected exhibits', *Frontiers in Analytical Science*, 2. doi:10.3389/frans.2022.857880.
- Ahmed, I.I. and Gupta, A.K. (2010) 'Pyrolysis and gasification of food waste: Syngas characteristics and char gasification kinetics', *Applied Energy*, 87(1), pp. 101–108. doi:10.1016/j.apenergy.2009.08.032.
- Ahrens, M. and Maheshwari, R. (2021) *Home Structure Fires*, *National Fire Protection Association (NFPA)*. National Fire Protection Association (NFPA). Available at: <https://www.nfpa.org/-/media/files/news-and-research/fire-statistics-and-reports/building-and-life-safety/oshomes.pdf> (Accessed: 29 March 2023).
- Akmeemana, A. (2019) *Chemometric Applications in Fire Debris Analysis: Likelihood Ratios from Naive Bayes and Frequency of Component and Pyrolysis Product Occurrence*. dissertation. STARS. Available at: <https://purls.library.ucf.edu/go/DP0023209> (Accessed: 13 April 2023).
- Aliaño-González, M. *et al.* (2018) 'Application of headspace gas chromatography-ion mobility spectrometry for the determination of ignitable liquids from fire debris', *Separations*, 5(3), p. 41. doi:10.3390/separations5030041.
- Al-Haj Ibrahim, H. (2020) 'Introductory chapter: Pyrolysis', *Recent Advances in Pyrolysis* [Preprint]. doi:10.5772/intechopen.90366.
- Almirall José R. and Furton, K.G. (2004) *Analysis and interpretation of fire scene evidence*. Boca Raton: CRC Press.
- An Garda Síochána (2023) *The garda dog unit*, *Garda*. Available at: <https://www.garda.ie/en/about-us/organised-serious-crime/operational-support-services/the-garda-dog-unit/> (Accessed: 25 November 2022).
- Anon (2019) *Metal Melting Points*, *Industrial Metal Supply Co*. Available at: <https://www.industrialmetalsupply.com/blog/melting-point-of-metals> (Accessed: 18 May 2023).

Aqel, A. *et al.* (2016) 'Determination of gasoline and diesel residues on wool, silk, polyester and cotton materials by SPME–GC–MS', *Journal of Analytical Chemistry*, 71(7), pp. 730–736. doi:10.1134/s1061934816070029.

ArrowheadForensics (2023) *Activated charcoal strips - .25" x .75" - 100 strips*, *Arrowhead Forensics*. Available at: <https://arrowheadforensics.com/a-1503-activated-charcoal-strips.html> (Accessed: 8 March 2023).

Ashenhurst, J. (2022) *Free radical reactions*, *Master Organic Chemistry*. Available at: <https://www.masterorganicchemistry.com/2013/07/30/free-radical-reactions/> (Accessed: 01 January 2023).

ASTM (2019) *ASTM E1618-19 Standard test method for ignitable liquid residues in extracts from fire debris samples by gas chromatography-mass spectrometry*, *ASTM International - Standards Worldwide*. Available at: <https://www.astm.org/e1618-19.html> (Accessed: 16 March 2023).

Baerncopf, J. (2020) "Prevalence of ignitable liquids in clothing with printing," *Forensic Science International*, 312, p. 110312. Available at: <https://doi.org/10.1016/j.forsciint.2020.110312>.

Baerncopf, J. and Hutches, K. (2020) "Evaluation of long term preservation of ignitable liquids adsorbed onto charcoal strips: 0 to 2 years," *Forensic Chemistry*, 18, p. 100234. Available at: <https://doi.org/10.1016/j.forc.2020.100234>.

Baldwin, M.D. (2015) *Practical Applications of Hydrocarbon and Photoionization Detection Units in Arson Investigations*, *Practical applications of hydrocarbon and photoionization detection units in arson investigations*. Available at: <https://www.crime-scene-investigator.net/practical-applications-of-hydrocarbon-and-photoionization-detection-units-in-arson-investigations.html> (Accessed: 19 December 2021).

Barnett, I., Bailey, F.C. and Zhang, M. (2019) "Detection and classification of ignitable liquid residues in the presence of matrix interferences by using Direct Analysis in real time mass spectrometry," *Journal of Forensic Sciences*, 64(5), pp. 1486–1494. Available at: <https://doi.org/10.1111/1556-4029.14029>.

Belcher, C.M. *et al.* (2010) "Baseline intrinsic flammability of Earth's ecosystems estimated from paleoatmospheric oxygen over the past 350 million years," *Proceedings of the National Academy of Sciences*, 107(52), pp. 22448–22453. Available at: <https://doi.org/10.1073/pnas.1011974107>.

Beyler, C.L. and Hirschler, M.M. (2002) Thermal Decomposition of Polymers. SFPE Handbook of Fire Protection Engineering 2, Section 1, Chapter 7, 111-131.

Bioinformatics for All (2021) *Tutorial 6: How to do principal component analysis (PCA) in R*, *Bioinformatics for All*. Available at: <https://bioinfo4all.wordpress.com/2021/01/31/tutorial-6-how-to-do-principal-component-analysis-pca-in-r/> (Accessed: 21 June 2023).

Boegelsack, N. *et al.* (2021a) "Development of retention time indices for comprehensive multidimensional gas chromatography and application to ignitable liquid residue mapping in wildfire investigations," *Journal of Chromatography A*, 1635, p. 461717. Available at: <https://doi.org/10.1016/j.chroma.2020.461717>.

Boegelsack, N. *et al.* (2021b) "Method development for optimizing analysis of ignitable liquid residues using flow-modulated comprehensive two-dimensional gas chromatography," *Journal of Chromatography A*, 1656, p. 462495. Available at: <https://doi.org/10.1016/j.chroma.2021.462495>.

Bogdal, C. *et al.* (2022a) "Recognition of gasoline in fire debris using machine learning: Part I, application of Random Forest, gradient boosting, support vector machine, and Naïve Bayes," *Forensic Science International*, 331, p. 111146. Available at: <https://doi.org/10.1016/j.forsciint.2021.111146>.

Bogdal, C. *et al.* (2022b) "Recognition of gasoline in fire debris using machine learning: Part II, application of a neural network," *Forensic Science International*, 332, p. 111177. Available at: <https://doi.org/10.1016/j.forsciint.2022.111177>.

Borusiewicz, R., "Fire Debris Analysis - A Survey of Techniques used for Accelerants Isolation and Concentration," *Problems of Forensic Sciences*, Vol 50, 2002, pp. 44 - 63.

Brushlinsky, N., Sokolov, S. and Wagner, P. (2022) *2022 No 27 Center of Fire Statistics World Fire Statistics*, CTIF International Association of Fire and Rescue Services. Available at:

https://ctif.org/sites/default/files/2022-08/CTIF_Report27_ESG.pdf (Accessed: 18 March 2023).

Büchler, L., Werner, D. and Delémont, O. (2021) "Detection of gasoline on suspects' hands: Study of different sampling alternatives," *Forensic Science International*, 318, p. 110590. Available at: <https://doi.org/10.1016/j.forsciint.2020.110590>.

Carmona, L. *et al.* (2021) "Activated charcoal pellets as an innovative method for forensic analysis of ignitable liquid residues from fire debris by GC-MS," *Brazilian Journal of Analytical Chemistry*. Available at: <https://doi.org/10.30744/brjac.2179-3425.ar-62-2021>.

Christy, B. *et al.* (2021) "A foundational study of fire debris interpretation using quantitative measures of chromatographic features in gasoline and the use of graphical display to demonstrate data sufficiency," *Forensic Chemistry*, 24, p. 100337. Available at: <https://doi.org/10.1016/j.forc.2021.100337>.

Churchward, D.L. *et al.* (2004) *NFPA 921, NFPA 921: Guide for Fire and Explosion Investigations*. National Fire Protection Association. Available at: <https://atapars.com/wp-content/uploads/2021/01/atapars.com-NFPA-921-2004.pdf> (Accessed: 11 April 2023).

Nic Daéid Niamh (2005) *Fire investigation*. Boca Raton, FL: CRC Press.

Dalton, L. (2017) *Forensic chemist describes the challenges of investigating a fire scene*, *Cen.acs.org*. Available at: <https://cen.acs.org/articles/95/i38/Forensic-chemist-describes-challenges-investigating.html> (Accessed: 28 November 2021).

Das, P. and Tiwari, P. (2018) 'Valorization of packaging plastic waste by slow pyrolysis', *Resources, Conservation and Recycling*, 128, pp. 69–77. doi:10.1016/j.resconrec.2017.09.025.

de Figueiredo, M. *et al.* (2019a) "Evaluation of an untargeted chemometric approach for the source inference of ignitable liquids in forensic science," *Forensic Science International*, 295, pp. 8–18. Available at: <https://doi.org/10.1016/j.forsciint.2018.11.016>.

de Figueiredo, M. *et al.* (2019b) "Exploratory study on the possibility to link gasoline samples sharing a common source after alteration by evaporation or combustion," *Forensic Science International*, 301, pp. 190–201. Available at: <https://doi.org/10.1016/j.forsciint.2019.05.032>.

DeHaan, J. and Kirk, P. (1997) *Kirk's Fire Investigation: 4th ed.* New Jersey: Prentice-Hall.

DeHaan, J.D. (2021) “Enhancing Fire Scene Investigations Through New Technologies (NCJ 302388),” *Fire and Arson Investigator Journal*, pp. 28–35.

Dhabbah, A.M. (2018) “Detection of petrol residues in natural and synthetic textiles before and after burning using SPME and GC-MS,” *Australian Journal of Forensic Sciences*, 52(2), pp. 194–207. Available at: <https://doi.org/10.1080/00450618.2018.1510029>.

EPRO (2022) *Plastics - the facts 2022*, *Plastics Europe*. Available at: <https://plasticseurope.org/knowledge-hub/plastics-the-facts-2022/> (Accessed: 28 May 2023).

Esmizadeh, E., Tzoganakis, C. and Mekonnen, T.H. (2020) ‘Degradation behavior of polypropylene during reprocessing and its biocomposites: Thermal and oxidative degradation kinetics’, *Polymers*, 12(8), p. 1627. doi:10.3390/polym12081627.

eurofins (2022) *Pyro-GC-MS*, *EAG Laboratories*. Available at: <https://www.eag.com/techniques/mass-spec/pyrolysis-gc-ms/> (Accessed: 21 June 2023).

Falatová, B. *et al.* (2019) “CHEMOMETRIC TOOLS USED IN THE PROCESS OF FIRE INVESTIGATION,” *ACTA FACULTATIS XYOLOGIAE ZVOLEN*, 61(1), pp. 111–119. Available at: <https://doi.org/10.17423/afx.2019.61.1.11>.

Ferreiro-González, M. *et al.* (2016) ‘Determination of ignitable liquids in fire debris: Direct analysis by electronic nose’, *Sensors*, 16(5), p. 695. doi:10.3390/s16050695.

Ferreiro-González, M. *et al.* (2017) ‘Validation of an HS-MS method for direct determination and classification of ignitable liquids’, *Microchemical Journal*, 132, pp. 358–364. doi:10.1016/j.microc.2017.02.022.

Fettig, I. *et al.* (2013) ‘Evaluation of a headspace solid-phase microextraction method for the analysis of ignitable liquids in fire debris’, *Journal of Forensic Sciences*, 59(3), pp. 743–749. doi:10.1111/1556-4029.12342.

Gebre, S.H., Sendeku, M.G. and Bahri, M. (2021) ‘Recent trends in the pyrolysis of non-degradable waste plastics’, *ChemistryOpen*, 10(12), pp. 1202–1226. doi:10.1002/open.202100184.

Griffin, L. (2020) *Webinar - is fluorescence an appropriate method for fire investigation?*, Foster+Freeman. Available at: <https://fosterfreeman.com/event/webinar-is-fluorescence-an-appropriate-method-for-fire-investigation/> (Accessed: 15 December 2021).

Guerrera, G. *et al.* (2019) "The potential interference of body products and substrates to the identification of ignitable liquid residues on worn clothing," *Forensic Chemistry*, 12, pp. 46–57. Available at: <https://doi.org/10.1016/j.forc.2018.11.007>.

Harries, M.E. *et al.* (2021) "Characterization of a headspace sampling method with a five-component diesel fuel surrogate," *Forensic Chemistry*, 22, p. 100301. Available at: <https://doi.org/10.1016/j.forc.2020.100301>.

Huang, J. *et al.* (2017) 'Studies on thermal decomposition behaviors of polypropylene using molecular dynamics simulation', *IOP Conference Series: Earth and Environmental Science*, 94, p. 012160. doi:10.1088/1755-1315/94/1/012160.

Huang, J.B. *et al.* (2018) 'Theoretical studies on bond dissociation enthalpies for model compounds of typical plastic polymers', *IOP Conference Series: Earth and Environmental Science*, 167, p. 012029. doi:10.1088/1755-1315/167/1/012029.

Jackson, A.R.W. and Jackson, J.M. (2011) *Forensic science*. Harlow: Prentice Hall.

Janssens, M.L. (2012) 'Material flammability', *Handbook of Environmental Degradation of Materials*, pp. 283–307. doi:10.1016/b978-1-4377-3455-3.00009-2.

Jin, J. *et al.* (2020) "Influence of thermal environment in fire on the identification of gasoline combustion residues," *Forensic Science International*, 315, p. 110430. Available at: <https://doi.org/10.1016/j.forsciint.2020.110430>.

Jin, J. *et al.* (2021) "The most remarkable interference to gasoline identification from polystyrene-co-butadiene and the corresponding cause," *Journal of Chromatography A*, 1654, p. 462462. Available at: <https://doi.org/10.1016/j.chroma.2021.462462>.

K9s4COPs (2023) *Information on K9s for Law Enforcement*, K9s4COPs. Available at: <https://k9s4cops.org/why-we-exist/> (Accessed: 25 November 2022).

Kates, L.N., Richards, P.I. and Sandau, C.D. (2020) "The application of comprehensive two-dimensional gas chromatography to the analysis of wildfire debris for ignitable liquid residue,"

Forensic Science International, 310, p. 110256. Available at: <https://doi.org/10.1016/j.forsciint.2020.110256>.

Keita, Z. (2023) *Principal Component Analysis (PCA) in R tutorial*, DataCamp. Available at: <https://www.datacamp.com/tutorial/pca-analysis-r> (Accessed: 21 June 2023).

Khan, S. (2012) *Free radical reactions (video)*, Khan Academy. Available at: <https://www.khanacademy.org/science/organic-chemistry/substitution-elimination-reactions/free-radical-reaction-alkanes/v/free-radical-reactions> (Accessed: 01 January 2023).

Kusch, P. (2012) 'Pyrolysis-gas chromatography/mass spectrometry of polymeric materials', *Advanced Gas Chromatography - Progress in Agricultural, Biomedical and Industrial Applications* [Preprint]. doi:10.5772/32323.

Lachowicz, T., Zięba-Palus, J. and Kóscielniak, P. (2012) 'Analysis of Rubber Samples by Py-GC/MS for Forensic Purposes', *Problems of Forensic Sciences*, 91, pp. 195–207.

Lancashire Constabulary (2023) *Lancashire Constabulary - Lancashire police dog training unit*, Lancashire. Available at: <https://www.lancashire.police.uk/about-us/our-organisation/dog-unit/> (Accessed: 25 November 2022).

Lee, K.-H. and Shin, D.-H. (2007) 'Characteristics of liquid product from the pyrolysis of waste plastic mixture at low and high temperatures: Influence of lapse time of reaction', *Waste Management*, 27(2), pp. 168–176. doi:10.1016/j.wasman.2005.12.017.

Lentini, J.J. (1998) 'Differentiation of asphalt and smoke condensates from liquid petroleum distillates using GC/MS', *Journal of Forensic Sciences*, 43(1). doi:10.1520/jfs16096j.

Libretexts (2022) *6.3: Radical reactions*, Chemistry LibreTexts. Available at: [https://chem.libretexts.org/Bookshelves/Organic_Chemistry/Organic_Chemistry_\(Morsch_et_al.\)/06%3A_An_Overview_of_Organic_Reactions/6.03%3A_Radical_Reactions](https://chem.libretexts.org/Bookshelves/Organic_Chemistry/Organic_Chemistry_(Morsch_et_al.)/06%3A_An_Overview_of_Organic_Reactions/6.03%3A_Radical_Reactions) (Accessed: 01 January 2023).

Liu, Z. *et al.* (2023) 'Polyvinyl chloride cooperates with biomass to assist in the directional conversion of N and CL as NH₃ and HCL to prepare clean fuel by low-temperature microwave heating', *Journal of Renewable and Sustainable Energy*, 15(1), p. 013102. doi:10.1063/5.0127158.

- Ljungkvist, E. and Thomsen, B. (2019) 'Interpretation of a fire scene with ultraviolet light', *Forensic Science International*, 297, pp. 284–292. doi:10.1016/j.forsciint.2019.02.010.
- Martín-Alberca, C., García-Ruiz, C. and Delémont, O. (2015) 'Study of acidified ignitable liquid residues in fire debris by solid-phase microextraction with gas chromatography and Mass Spectrometry', *Journal of Separation Science*, 38(18), pp. 3218–3227. doi:10.1002/jssc.201500337.
- Martin Fabritius, M. *et al.* (2018) 'Analysis of volatiles in fire debris by combination of activated charcoal strips (ACS) and automated thermal desorption–gas chromatography–mass spectrometry (ATD/GC–MS)', *Forensic Science International*, 289, pp. 232–237. doi:10.1016/j.forsciint.2018.05.048.
- Menyhárd, A., Menczel, J.D. and Abraham, T. (2020) 'Polypropylene fibers', *Thermal Analysis of Textiles and Fibers*, pp. 205–222. doi:10.1016/b978-0-08-100572-9.00012-4.
- Mesloh, C. (2006) 'Barks or bites? the impact of training on police canine force outcomes', *Police Practice and Research*, 7(4), pp. 323–335. doi:10.1080/15614260600919670.
- Moldoveanu, S.C. (1998) *Analytical pyrolysis of natural organic polymers*. Amsterdam: Elsevier.
- Mulligan, J. (2020) *Paw patrol: Revenue is training more dog detectives*, *Independent.ie*. Available at: <https://www.independent.ie/business/irish/paw-patrol-revenue-is-training-more-dog-detectives/39741495.html> (Accessed: 25 November 2022).
- Nicholas, D.J. (2008) 'FORENSIC ANALYSIS OF FIRE DEBRIS RESIDUES'. Indianapolis: INDIANAPOLIS-MARION COUNTY FORENSIC SERVICES AGENCY.
- Nisar, J. *et al.* (2022) 'Conversion of Polypropylene Waste into Value-Added Products: A Greener Approach', *molecules*, 27(9), pp. 3015–3026. doi:10.3390/molecules27093015.
- Nizio, K., Cochran, J. and Forbes, S. (2016) 'Achieving a near-theoretical maximum in peak capacity gain for the forensic analysis of ignitable liquids using GC×GC-TOFMS', *Separations*, 3(3), p. 26. doi:10.3390/separations3030026.
- O'Hagan, A. and Ellis, H. (2021) 'A critical review of canines used to detect accelerants within an arson crime scene', *Forensic Research & Criminology International Journal*, 9(2), pp.

65–72. doi:10.15406/frcij.2021.09.00342.

OSAC (2021) *OSAC 2022-S-0004 Standard Classification for Ignitable Liquids Encountered in Fire Debris Analysis*, National Institute of Standards and Technology. Organization of Scientific Area Committees for Forensic Science. Available at: https://www.nist.gov/system/files/documents/2021/10/04/OSAC%202022-S-0004%20E1618%20Std%20Classification.OPEN%20COMMENT_STRP%20VERSION.pdf (Accessed: 20 April 2023).

Pandohee, J. *et al.* (2020) “Chemical fingerprinting of petrochemicals for arson investigations using two-dimensional gas chromatography - flame ionisation detection and multivariate analysis,” *Science & Justice*, 60(4), pp. 381–387. Available at: <https://doi.org/10.1016/j.scijus.2020.04.004>.

Park, C. *et al.* (2021) “Application and evaluation of machine-learning model for fire accelerant classification from GC-MS data of fire residue,” *Analytical Science & Technology*, 34(5), pp. 231–239. Available at: <https://doi.org/https://doi.org/10.5806/AST.2021.34.5.231>.

Pawliszyn, J. (2003) ‘Solid-phase microextraction coatings and methods for their preparation’ (Accessed: 28 November 2022).

Rankin, G. and Petraco, N. (2014) *Interpretation of Ignitable Liquid Residues in Fire Debris Analysis: Effects of Competitive Adsorption, Development of an Expert System and Assessment of the False Positive/Incorrect Assignment Rate*, Office of Justice Programs. Available at: <https://www.ojp.gov/pdffiles1/nij/grants/248242.pdf>.

Roberson, Z.R. and Goodpaster, J.V. (2019) ‘Preparation and characterization of micro-bore wall-coated open-tubular capillaries with low phase ratios for fast-gas chromatography–mass spectrometry: Application to ignitable liquids and fire debris’, *Science & Justice*, 59(6), pp. 630–634. doi:10.1016/j.scijus.2019.06.009.

Ryan, H. (2019) *Melting points of common materials: Toolbox: American elements*®, *American Elements: The Materials Science Company*. Available at: <https://www.americanelements.com/meltingpoint.html> (Accessed: 28 September 2023).

Sampat, A. *et al.* (2018) ‘Detection and characterization of ignitable liquid residues in forensic fire debris samples by comprehensive two-dimensional gas chromatography’, *Separations*,

5(3), p. 43. doi:10.3390/separations5030043.

Sánchez-Jiménez, P.E. *et al.* (2010) 'A new model for the kinetic analysis of thermal degradation of polymers driven by random scission', *Polymer Degradation and Stability*, 95(5), pp. 733–739. doi:10.1016/j.polymdegradstab.2010.02.017.

Sandau, C. (2021) 'Make sure your investigation has legal chain of custody', *Chemistry Matters*. Available at: <https://blog.chemistry-matters.com/make-sure-your-investigation-has-legal-chain-of-custody> (Accessed: 11 January 2022) .

Sandercock, P.M. (2012) 'Preparation of pyrolysis reference samples: Evaluation of a standard method using a Tube Furnace', *Journal of Forensic Sciences*, 57(3), pp. 738–743. doi:10.1111/j.1556-4029.2011.02030.x.

Sandercock, P.M. (2016) 'Passive headspace extraction of ignitable liquids using activated carbon cloth', *Canadian Society of Forensic Science Journal*, 49(4), pp. 176–188. doi:10.1080/00085030.2016.1189226.

Sigman, M.E. *et al.* (2021) "Validation of ground truth fire debris classification by supervised machine learning," *Forensic Chemistry*, 26, p. 100358. Available at: <https://doi.org/10.1016/j.forc.2021.100358>.

Sisco, E. and Forbes, T.P. (2021) "Forensic applications of Dart-MS: A review of recent literature," *Forensic Chemistry*, 22, p. 100294. Available at: <https://doi.org/10.1016/j.forc.2020.100294>.

South Yorkshire Police (2017) *FOI Request Reference Number: 2017196*, *South Yorkshire Police*. Available at: <https://www.southyorks.police.uk/media/1335/police-dogs-stats-20171965.pdf> (Accessed: 22 November 2022).

Stauffer, E. (2003) "Concept of pyrolysis for fire debris analysts," *Science & Justice*, 43(1), pp. 29–40. Available at: [https://doi.org/10.1016/s1355-0306\(03\)71738-9](https://doi.org/10.1016/s1355-0306(03)71738-9).

Stauffer, E., Dolan, J.A. and Newman, R. (2008) *Fire debris analysis*. Boston, MA: Academic Press.

Swierczynski, M.J. *et al.* (2020) "Detection of gasoline residues present in household materials via headspace-solid phase microextraction and gas chromatography-mass spectrometry," *Journal of Analytical Chemistry*, 75(1), pp. 44–55. Available at: <https://doi.org/10.1134/s1061934820010153>.

Thurn, N., Williams, M. and Sigman, M. (2018) 'Application of self-organizing maps to the analysis of ignitable liquid and substrate pyrolysis samples', *Separations*, 5(4), p. 52. doi:10.3390/separations5040052.

Thurn, N.A. *et al.* (2021) "Classification of ground-truth fire debris samples using artificial neural networks," *Forensic Chemistry*, 23, p. 100313. Available at: <https://doi.org/10.1016/j.forc.2021.100313>.

Torres, M.N. and Almirall, J.R. (2022) "Evaluation of capillary microextraction of volatiles (CMV) coupled to a person-portable gas chromatograph mass spectrometer (GC–MS) for the analysis of gasoline residues," *Forensic Chemistry*, 27, p. 100397. Available at: <https://doi.org/10.1016/j.forc.2021.100397>.

Torres, M.N., Valdes, N.B. and Almirall, J.R. (2020) "Comparison of portable and benchtop GC–MS coupled to capillary microextraction of volatiles (CMV) for the extraction and analysis of ignitable liquid residues," *Forensic Chemistry*, 19, p. 100240. Available at: <https://doi.org/10.1016/j.forc.2020.100240>.

Totten, V. and Willis, J. (2020) "The use of hydrophobic pads to recover ignitable liquids from water," *Forensic Science International*, 312, p. 110309. Available at: <https://doi.org/10.1016/j.forsciint.2020.110309>.

Tsuge, S., Ohtani, H. and Watanabe, C. (2012) *Pyrolysis-GC/MS Data Book of Synthetic Polymers: Pyrograms, thermograms and MS of pyrolyzates*. Elsevier.

Vergeer, P. *et al.* (2020) "A method for forensic gasoline comparison in fire debris samples: A numerical likelihood ratio system," *Science & Justice*, 60(5), pp. 438–450. Available at: <https://doi.org/10.1016/j.scijus.2020.06.002>.

Vermesi, I. *et al.* (2016) 'Pyrolysis and ignition of a polymer by transient irradiation', *Combustion and Flame*, 163, pp. 31–41. doi:10.1016/j.combustflame.2015.08.006.

Wampler, T. (2002) *Pyrolysis/GC of Polyolefins, CDS Analytical*. Available at: https://docs.wixstatic.com/ugd/82f28b_fa3cfe6ba1de495396886b7eeb348531.pdf (Accessed: 13 July 2023).

Wampler, T.P. (2007) *Applied Pyrolysis Handbook*. Boca Raton: CRC Press/Taylor & Francis.

Wampler, T. (no date) *Polymer Degradation Mechanisms using Pyrolysis-GC/MS, PerkinElmer*. Available at: https://resources.perkinelmer.com/lab-solutions/resources/docs/far_polymer_degradation_mechanisms_using_pyrolysis_gc_ms_field_application_report.pdf (Accessed: 21 June 2023).

Wright, E. (2020) *Meet the highly trained super-security dogs that can cost as much as \$230,000, CNBC*. Available at: <https://www.cnn.com/2019/09/27/harrison-k-9s-highly-trained-security-dogs-can-cost-six-figures.html> (Accessed: 25 November 2022).

Wu, Z. *et al.* (2020) 'Development of electronic nose for qualitative and quantitative monitoring of volatile flammable liquids', *Sensors*, 20(7), p. 1817. doi:10.3390/s20071817.

Yadav, V.K. *et al.* (2021) "A forensic approach to evaluate the effect of different matrices and extraction solvents for the identification of diesel residue in simulated arson by GC–MS," *Chromatographia*, 84(5), pp. 413–423. Available at: <https://doi.org/10.1007/s10337-021-04022-1>.

Zafar, S. (2021) *Overview of biomass pyrolysis process, BioEnergy Consult*. Available at: <https://www.bioenergyconsult.com/biomass-pyrolysis/> (Accessed: 30 September 2023).

Zeng, J. *et al.* (2020) 'Complex reaction processes in combustion unraveled by neural network-based molecular dynamics simulation', *Nature Communications*, 11(1). doi:10.1038/s41467-020-19497-z.

Zhang, H.R. *et al.* (2007) "Combustion modeling and kinetic rate calculations for a stoichiometric cyclohexane flame. 1. major reaction pathways," *The Journal of Physical Chemistry A*, 111(19), pp. 4102–4115. Available at: <https://doi.org/10.1021/jp068237q>.

Zięba-Palus, J. *et al.* (2008) 'Pyrolysis-gas chromatography/mass spectrometry analysis as a useful tool in forensic examination of Automotive Paint Traces', *Journal of Chromatography A*, 1179(1), pp. 41–46. doi:10.1016/j.chroma.2007.09.044.

Appendix 1: FTIR of Selected Substrates

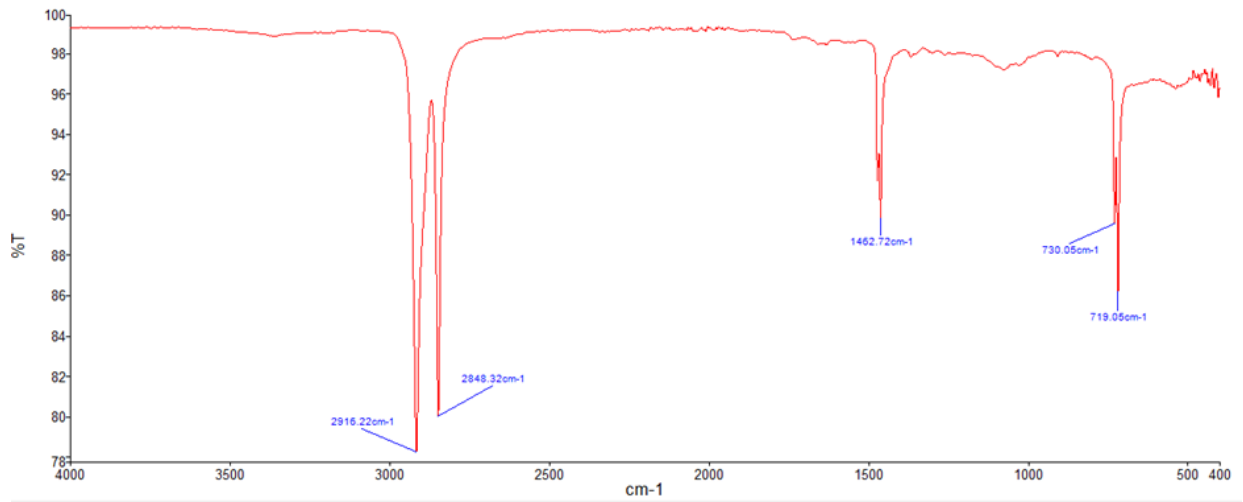


Figure 38 FTIR of HDPE sample

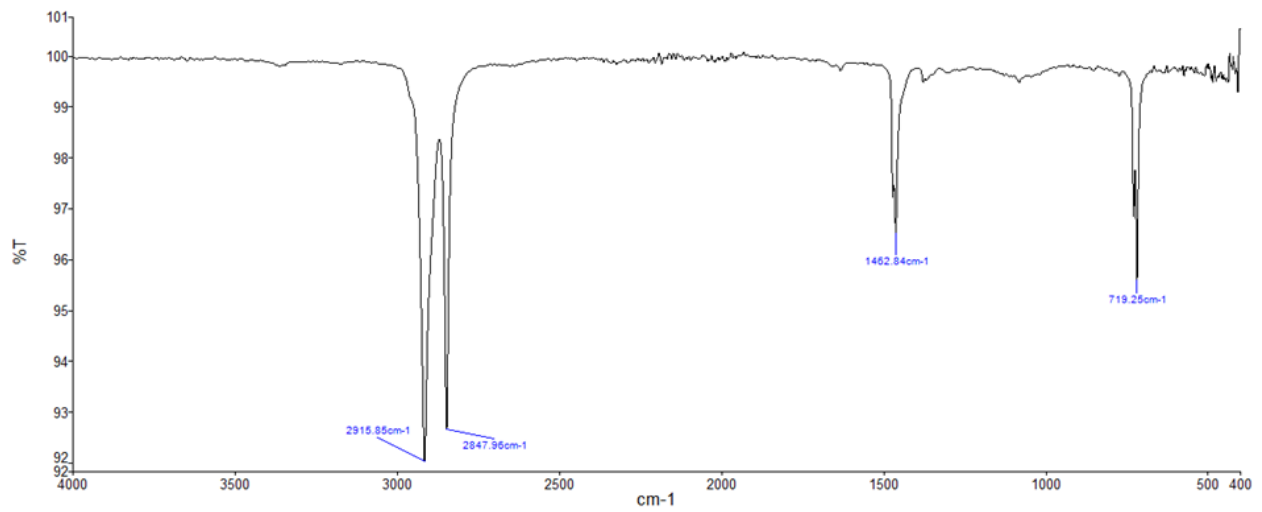


Figure 39 FTIR of LDPE sample

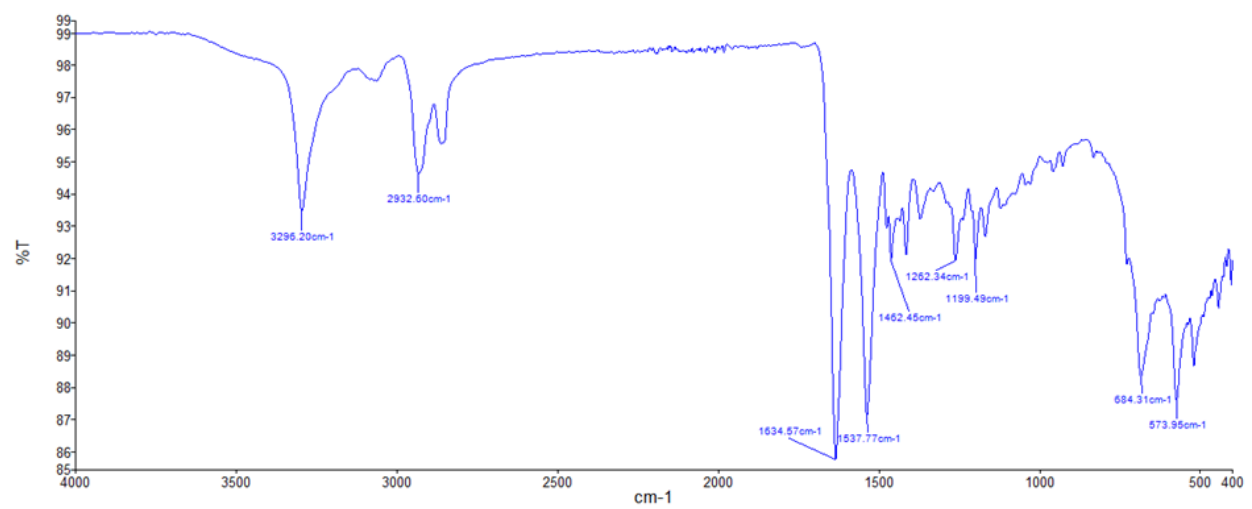


Figure 40 FTIR of nylon sample

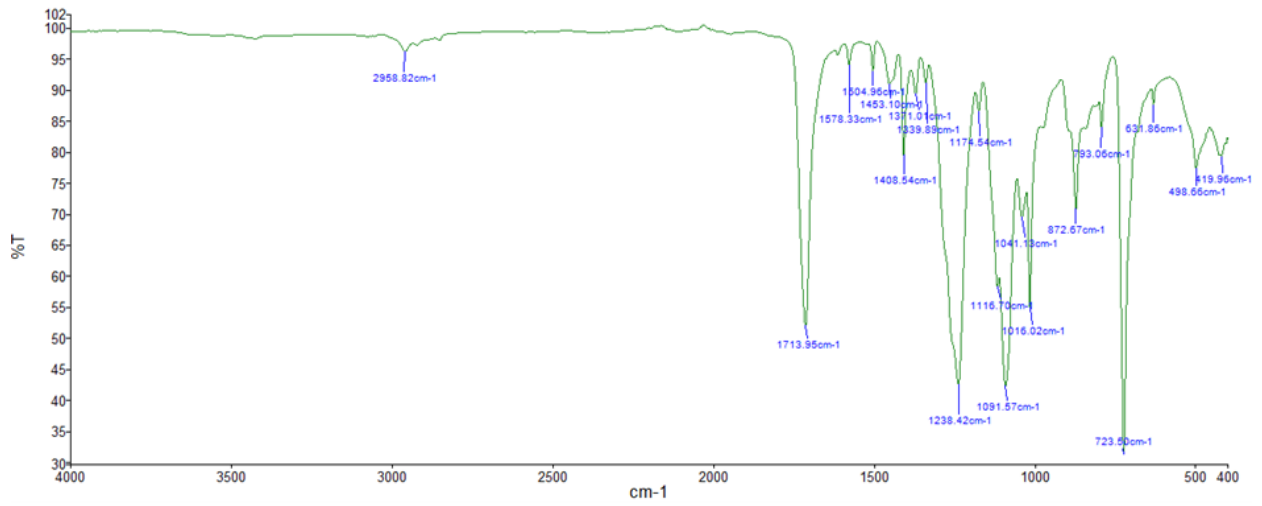


Figure 41 FTIR of PET sample

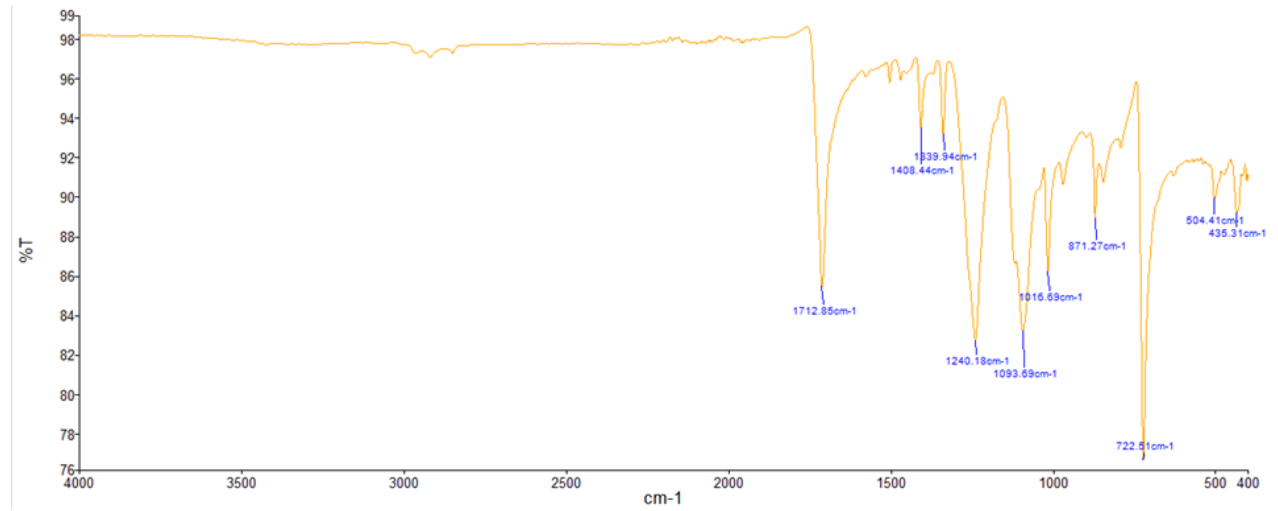


Figure 42 FTIR of PER sample

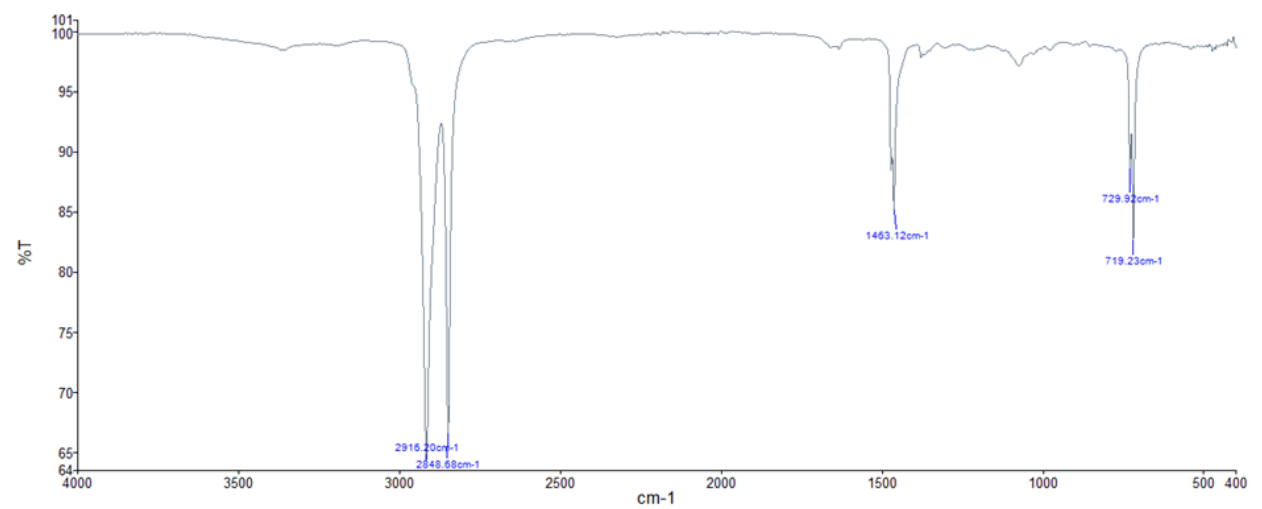


Figure 43 FTIR of PP sample

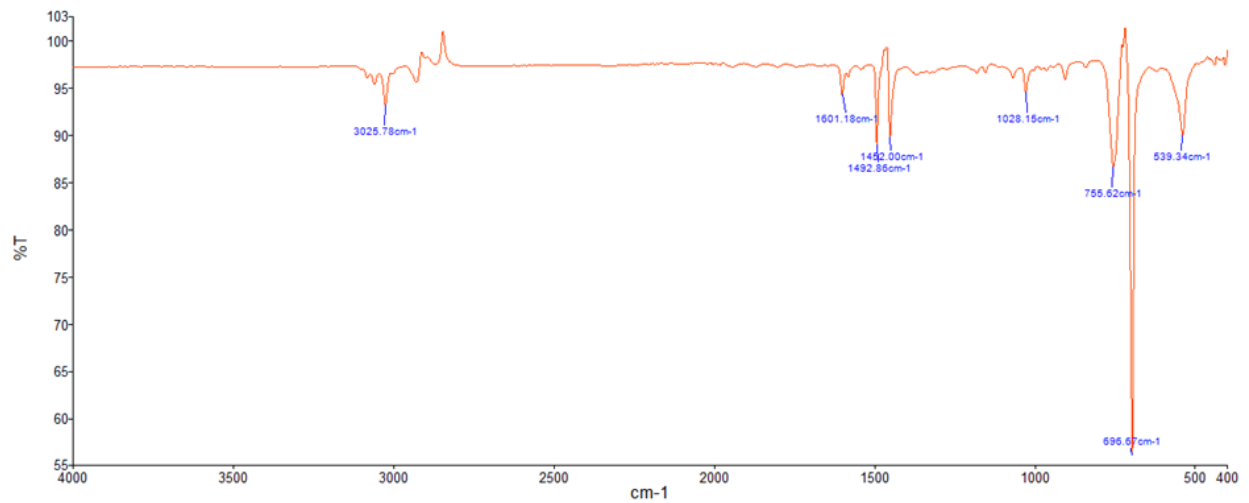


Figure 44 FTIR of PS sample

Appendix 2: RStudios Code for PCA

The following code were taken from (Keita, 2023; Bioinformatics for All, 2021) with some changes to the data set.

1. Install and load packages required to generate PCA in RStudio.

```
> install.packages("corr", "ggplot2", "ggcorrplot", "factoextra", "FactoMineR",  
"stats", "devtools", "ggpubr")  
  
> library(readr)  
  
> library(corr)  
  
> library(ggplot2)  
  
> library(ggcorrplot)  
  
> library(factoextra)  
  
> library(FactoMineR)  
  
> library(stats)  
  
> library(devtools)  
  
> library(ggpubr)
```


2. Import .csv file from locate

```
> install.packages("tidyverse")
```

```
> library(tidyverse)
```

Select "Session" > "Set Working Directory" > "Choose Directory" > select the location

```
> setwd("~/Desktop")
```

Import data.csv file from files from the lower right quarter

3. Read the .csv file

```
> data <- read_csv("data")
```

```
> view(data)
```

```
> str(data)
```

4. Check for null values

```
> colSums(is.na(data))
```

5. Normalising the data

```
> numerical_data <- data[,2:43]
```

```
> head(numerical_data)
```

```
> data_normalized <- scale(numerical_data)
```

```
> head(data_normalized)
```

6. Correlation matrix generation

```
> corr_matrix <- cor(data_normalized)
```

```
> ggcorrplot(corr_matrix)
```

7. Generate PCA summary table

```
> data.pca <- princomp(corr_matrix)
```

```
> summary(data.pca)
```

8. Scree plot generation

```
> pca.data <- PCA(data[,-1], scale.unit = TRUE, graph = FALSE)
```

```
> fviz_eig(pca.data, addlabels = TRUE, ylim = c(0,50))
```

9. Generate Cos2 plot

```
> fviz_pca_var(pca.data, col.var = "cos2", gradient.cols = c("#FFCC00", "#CC9933",  
"#660033", "#330033"), repel = TRUE)
```

10. Generate individuals - PCA

```
> pca.data <- PCA(t(library[,-1]), scale.unit = TRUE, graph = FALSE)
```

```
> fviz_pca_ind(pca.data, col.ind = "cos2", gradient.cols = c("#FFCC00", "#CC9933",  
"#660033", "#330033"), repel = TRUE)
```

11. Labelling individuals – PCA

```
> devtools::install_github("kassambara/ggpubr")
```

```
> a <- fviz_pca_ind(pca.data, col.ind = "cos2", gradient.cols = c("#FFCC00",  
"#CC9933", "#660033", "#330033"), repel = TRUE)
```

```
> ggpar(a, title = "Principal Component Analysis", xlab = "PC1", ylab = "PC2",  
legend.title = "Cos2", legend.position = "top", ggtheme = theme_minimal())
```

